A DYNAMICAL SYSTEMS APPROACH TOWARDS MODELING THE RAPID PRESSURE STRAIN CORRELATION

A Thesis

by

AASHWIN ANANDA MISHRA

Submitted to the Office of Graduate Studies of
Texas A&M University
in partial fulfillment of the requirements for the degree of

MASTER OF SCIENCE

May 2010

Major Subject: Aerospace Engineering

A Dynamical Systems Approach Towards Modeling the Rapid Pressure Strain Correlation

A DYNAMICAL SYSTEMS APPROACH TOWARDS MODELING THE RAPID PRESSURE STRAIN CORRELATION

A Thesis

by

AASHWIN ANANDA MISHRA

Submitted to the Office of Graduate Studies of
Texas A&M University
in partial fulfillment of the requirements for the degree of

MASTER OF SCIENCE

Approved by:

Chair of Committee,	Sharath Girimaji
Committee Members,	William Saric
	Hamn-Ching Chen
	Tamas Kalmar-Nagy
Head of Department,	Dimitris Lagoudas

May 2010

Major Subject: Aerospace Engineering

ABSTRACT

A Dynamical Systems Approach Towards Modeling the Rapid Pressure Strain Correlation. (May, 2010)

Aashwin Ananda Mishra, B.Tech., Indian Institute of Technology, Delhi

Chair of Advisory Committee: Dr. Sharath Girimaji

In this study, the behavior of pressure in the Rapid Distortion Limit, along with its concomitant modeling, are addressed. In the first part of the work, the role of pressure in the initiation, propagation and suppression of flow instabilities for quadratic flows is analyzed. The paradigm of analysis considers the Reynolds stress transport equations to govern the evolution of a dynamical system, in a state space composed of the Reynolds stress tensor components. This dynamical system is scrutinized via the identification of the invariant sets and the bifurcation analysis. The changing role of pressure in quadratic flows, viz. hyperbolic, shear and elliptic, is established mathematically and the underlying physics is explained. Along the maxim of "understanding before prediction", this allows for a deeper insight into the behavior of pressure, thus aiding in its modeling. The second part of this work deals with Rapid Pressure Strain Correlation modeling in earnest. Based on the comprehension developed in the preceding section, the classical pressure strain correlation modeling approaches are revisited. Their shortcomings, along with their successes, are articulated and explained, mathematically and from the viewpoint of the governing physics. Some of the salient issues addressed include, but

are not limited to, the requisite nature of the model, viz. a linear or a nonlinear structure, the success of the extant models for hyperbolic flows, their inability to capture elliptic flows and the use of RDT simulations to validate models. Through this analysis, the schism between mathematical and physical guidelines and the engineering approach, at present, is substantiated. Subsequently, a model is developed that adheres to the classical modeling framework and shows excellent agreement with the RDT simulations. The performance of this model is compared to that of other nominations prevalent in engineering simulations. The work concludes with a summary, pertinent observations and recommendations for future research in the germane field.

DEDICATION

This work is dedicated to Dr. Rama Govindarajan and Dr. Nadeem Hasan. It's not all that much, but it will have to do, for now.

TABLE OF CONTENTS

CHAPTER I

INTRODUCTION AND OVERVIEW

1. 1 Introduction

The structure and properties of fluid flows represent an omnipresent requirement to describe various phenomena, from aircraft flight to the flow of blood through the heart. In this context, most of the flows observed in nature are turbulent. In essence, turbulence is the rule and not the exception. Turbulence, described hitherto as the last unsolved problem in classical mechanics, is a manifestation of the spatio-temporal chaotic behavior of fluid flows at large values of destabilizing parameters, such as the Reynolds number. Thus, a classical turbulent flow represents a strongly nonlinear, dissipative system with an extremely large number of degrees of freedom. Some of the properties of turbulence include:

- •irregularity, intrinsic spatio-temporal randomness.
- •an extremely large range of length and time scales, which are coupled.
- •a high degree of dissipative behavior.
- •non-linearity, non-integratibility and non-locality.

This thesis follows the style of the *Journal of Fluid Mechanics*.

The final point represents the chief problem of turbulence, both from a mathematical and an engineering point of view. Despite over a century of research in this field, the prediction of turbulent flows is not viable. Some of the fields that would benefit from a theory of turbulence include Applied and Computational Physics, Engineering (Aeronautical, Hydraulic, Civil, Chemical), Meteorology, Oceanography, Geo-Astrophysical sciences, Bio-medical sciences, etc. Thus, turbulence represents a central problem in varied and various branches of physics and engineering.

The physics of turbulence can be completely described by the Navier-Stokes equations. In complex turbulent flows of engineering interest, the direct solution of the Navier-Stokes equations is unfeasible, at present and in the foreseeable future, due to the complexity of these equations and the extant state of computational capacities. Hence, all studies of turbulent flows incorporate some level of modeling. This modeling facet can be in the form of Reynolds stress models, subgrid scale models, two-point closures, etc. As a majority of practical engineering flows involve complex geometries and the presence of solid boundaries, etc, the approach for such recourses has been based on Reynolds stress modeling. The concept of Reynolds averaging was introduced by Osborne Reynolds (Reynolds(1895)) while conducting research in this field in the latter half of the nineteenth century. Dealing with the simplified case of isotropic turbulence, other investigations made fundamental contributions to the statistical theory of isotropic turbulence. Despite providing important insights regarding the physics of turbulence, the statistical approach does not provide a complete, closed form solution of practical

turbulent flows. Thus, there remains a need of Reynolds stress models to solve the Reynolds-averaged Navier-Stokes equations, which form the essence of the closure problem in turbulence. In this regard, zero-, one-, or two-equation models, second moment closures and numerically intensive tools such as Large Eddy Simulation, represent ascending tiers in the hierarchy of these approaches, arranged with respect to the computational requirements, the range of validity and the degree of information generated. In turbulent flows of engineering interest, the complex nature arises due to strong streamline curvature or body forces caused by system rotation. As the turbulent kinetic energy evolution equation is unaffected by, for instance, system rotation, the lowest level at which such complex effects are accounted, explicitly, is the second moment closure. The capabilities of second moment closures, with regard to their validity, have been extensively reported in studies such as Launder, Reece and Rodi (1975), and Launder, Tselepidakis and Younis (1987). As this approach is not as computationally expensive as the numerically intensive tools, it is widely used in engineering studies of turbulent flows.

The foundations for second order closure modeling were laid by Chou(1945) and Rotta (1951). By considering the transport equations for the individual Reynolds stress tensor components, this approach accounts for both the history and the nonlocal effects on the Reynolds stresses. This is essential as the fluctuating velocity field is a functional of the global history of the mean velocity field, albeit, with an implicit dependence on the initial and boundary conditions applied to it. Considering the Reynolds stress transport

equations, the convection and Production terms adjust themselves to such complexities via the addition of scale factors or Coriolis terms, hence this approach leads to better descriptions of complex flows. Furthermore, due to the presence of the terms representing the convection and diffusion of the Reynolds stresses, this approach is able to account for the non-local and history effects. However, due to the lack of closure in the Reynolds stress transport equations, models must be incorporated for the higher order correlations. These include the Turbulent Transport term, Pressure-Strain Correlation and Dissipation-Rate Correlation. The ability of any turbulence model, based on the exact Reynolds stress transport equations, to describe the flow physics depends on the quality of the model expressions utilized in the model. The focus of this investigation is the modeling of the Rapid Pressure Strain Correlation term. The Pressure-Strain Correlation plays a crucial role in the evolution and structure of turbulent flows. As an illustration, through its action of the redistribution, it governs the evolution of the turbulent kinetic energy production. This determines if the flow continues to remain turbulent or whether it decays to a laminar state.

The evolution of the fluctuating velocity field in an incompressible, turbulent flow is determined by the balance between inertial, pressure and viscous effects. The inertial effects deform the fluctuating velocity field without any regard to the incompressibility requirement. Subsequently, It is the function of pressure to modify this inertial deformation, so as to render the velocity field divergence free. The viscous effects are dynamically passive and do not change the dilatation state of the velocity field. The

pressure effects are manifested in the Reynolds stress transport equations as a correlation between the fluctuating velocity and the gradient of the fluctuating pressure field. Following Rotta(1951) and Chou(1945), it is a common practice to decompose the fluctuating pressure into two parts: the rapid pressure term and the slow pressure term. It is the function of the rapid pressure to impose the divergence-free condition on the fluctuating velocity produced by mean-fluctuation linear interactions. Slow pressure, on the other hand, serves to preserve the incompressibility of velocity fluctuations arising from the fluctuation-fluctuation non-linear interactions. In fulfilling its function as the enforcer of the divergence-free constraint, pressure – via the action of rapid and slow pressure-strain correlations – redistributes turbulent kinetic energy among the various Reynolds stress components. Considering the nature of this redistribution, the aforementioned decomposition affords the possibility of analyzing the action of the two components in isolation. By their very nature, the non-linear interactions are reasonably independent of the mean velocity field and therefore, the action of slow pressure-strain correlation can be considered “universal”. Consequently, It is accepted in the scientific community that the slow-pressure strain correlation tends to isotropize the fluctuating velocity field, irrespective of the mean velocity gradient. On the other hand, the action of rapid pressure – and consequently, the rapid pressure-strain correlation – is a strong function of the mean velocity field. Thus, the action of the rapid pressure strain correlation is dependent on the specific case of flow under consideration.

With exceptions, in current turbulence modeling practice, rapid pressure-strain correlations are typically developed in shear flows and used with *ad hoc* modification in other flows. This leads to inadequate performance of pressure-strain correlation closure models in rotation-dominated elliptic streamline flows. The objective of this study is to develop an improved understanding of the dependence of rapid pressure-strain behavior on different mean flow classes: strain-dominated, rotation-dominated and plane shear fields. This is utilized to consider the utility of the classical second moment closure approaches. Finally, the improved understand is used to generate a model for the Rapid Pressure Strain Correlation.

1.2 Overview

This thesis is divided into six chapters. Succeeding a brief précis of the problem in Chapter I, Chapter II presents the governing equations and the mathematical formulation. In this section, the mathematical basis for the simplification afforded by the Rapid Distortion Theory are presented and reviewed. Subsequently, the Rapid Distortion Equations and the Kelvin-Townsend set of equations are derived and discussed. In Chapter III, the underlying physics of the problem is considered. This entails a stability analysis of hyperbolic and elliptic flows in the Rapid Distortion Limit. In the analysis, the changing role of rapid pressure on the flow, with respect to the nature of the streamlines, is considered. Chapter IV addresses the issues pertaining to the modeling of the Rapid Pressure Strain Correlation. Based on the understanding developed in the prior

sections, the classical modeling approach is revisited. Its shortcomings along with its successes are articulated and explained, mathematically and from the viewpoint of the governing physics. The key issue addressed here is the engineering success of such models for open streamline flows and the lack thereof for closed streamline flows. Other issues addressed include the requisite nature of the model, namely, a linear or a nonlinear structure, the use of RDT simulations to validate models, etc. Through this analysis, the schism between mathematical and physical guidelines, and the contemporary engineering approach is substantiated. Subsequently in Chapter V, a model is developed that adheres to the classical modeling framework and shows excellent agreement with the RDT simulations. The performance of this new model is compared to that of nominations that are popular in the engineering community for the entire spectrum of flow regimes apposite to this study. Chapter VI concludes the report with a summary along with some pertinent observations, reiteration of the novel findings of this study and recommendations for future research in this field.

CHAPTER II

MATHEMATICAL FORMULATION

2.1 Rapid Distortion Theory

Rapid Distortion Theory is an essential simplification of the turbulence dynamics under specific conditions. The essential caveat pertains to a ratio of time scales, that of the mean flow in comparison to that of the fluctuating velocity field. In the rapid distortion limit, the mean flow timescale is much smaller than that of the fluctuating flow, so that the nonlinear interactions among fluctuating modes can be neglected. In this limit, the evolution equations are linear in fluctuating velocity. In the recent past, RDT analysis has been extended and applied to inhomogeneous distortions, for instance, around bluff bodies and the flow in internal combustion engines.

In inviscid, homogeneous RDT, the non-linear effects such as cascading (which consists of non-linear interactions amongst the fluctuating flow components), turbulent transport (which is absent in homogeneous turbulence) and dissipation (which is nonlinear and viscous) are absent. Hence, production (which is linear and inertial) and rapid pressure effects can be studied in relative isolation. The Rapid Pressure Strain Correlation, which represents the pressure effect in the Rapid Distortion Limit, plays a crucial role in the dynamics of complex turbulent flows. The linearity of governing equations also leads to considerable computational ease in numerically solving the evolution equations. It is

interesting to note that in the rapid distortion limit, the fluctuating velocity field exhibits elastic behavior – Reynolds stress is proportional to mean strain – instead of viscous behavior where stress is proportional to strain-rate. As has been observed in literature, this renders the turbulence-viscosity hypothesis inapplicable. Although RDT is not a theory of turbulence, it can be used in conjunction with turbulence theories as a guide to the modeling of the dynamical terms in the Reynolds stress transport equations.

2.2 The Rapid Distortion Equations

The equations governing the dynamics of incompressible fluid flow are,

$$\frac{\partial V_j}{\partial t} + V_i \frac{\partial V_j}{\partial x_i} = -\frac{1}{\rho}\frac{\partial P}{\partial x_j} + \nu \frac{\partial^2 V_j}{\partial x_i^2} \tag{2.1}$$

where, $V(\vec{x},t) and P(\vec{x},t)$ represent the instantaneous pressure and velocity fields, respectively. These are decomposed into mean and fluctuating components as follows,

$$V_i = U_i + u_i; \quad P = \bar{P} + p \tag{2.2}$$

Substituting this decomposition in the Navier-Stokes equations, we can obtain the equation that governs the fluctuating velocity field in homogeneous turbulence:

$$\frac{\partial u_j}{\partial t} + U_i \frac{\partial u_j}{\partial x_i} = \frac{\bar{D}u_j}{Dt} = -\frac{1}{\rho}\frac{\partial p}{\partial x_j} - u_i \frac{\partial u_j}{\partial x_i} - u_i \frac{\partial U_j}{\partial x_i}. \tag{2.3}$$

The fluctuating pressure (p) is governed by the Poisson equation

$$\frac{1}{\rho}\nabla^2 p = -2\frac{\partial U_i}{\partial x_j}\frac{\partial u_j}{\partial x_i} - \frac{\partial u_i}{\partial x_j}\frac{\partial u_j}{\partial x_i}. \tag{2.4}$$

Now, pressure is decomposed into two components – rapid pressure ($p^{(r)}$) and slow pressure ($p^{(s)}$) so that

$$\frac{1}{\rho}\nabla^2(p^{(r)}+p^{(s)}) = -2\frac{\partial U_i}{\partial x_j}\frac{\partial u_j}{\partial x_i} - \frac{\partial u_i}{\partial x_j}\frac{\partial u_j}{\partial x_i}. \tag{2.5}$$

The first term on the right-hand side is linear in fluctuating velocity and it accounts for the interactions between mean flow and the turbulent fluctuations whereas the second term is nonlinear and it represents the turbulence-turbulence interactions. In the RD limit, the mean flow timescale is assumed to be much shorter than the fluctuating flow timescale. Thus the fluctuation-fluctuation interactions can be neglected and equations 2.3 and 2.5 reduce to the *rapid distortion equations,*

$$\frac{\overline{D}u_j}{\overline{D}t} = -u_i\frac{\partial U_j}{\partial x_i} - \frac{1}{\rho}\frac{\partial p^{(r)}}{\partial x_j}; \tag{2.6}$$

$$\frac{1}{\rho}\nabla^2 p^{(r)} = -2\frac{\partial U_i}{\partial x_j}\frac{\partial u_j}{\partial x_i}. \tag{2.7}$$

The first term on the right-hand side of equation 2.6 represents the inertial effect and the second term refers to the pressure effect. It is noted that the equations are linear in fluctuating velocity. The incompressibility condition on the fluctuating velocity is given by $\partial u_i / \partial x_i = 0$. In the Rapid Distortion Limit, the evolution equation for Reynolds stresses can be written as:

$$\frac{d\langle u_i u_j\rangle}{dt} = P_{ij} + \Phi_{ij}^{(r)}, \tag{2.8}$$

where P_{ij} and Φ_{ij} are production and rapid pressure-strain correlation, respectively. In literature, the focus of the research is on the Reynolds stress anisotropy tensor (b_{ij}) and the turbulent kinetic energy (k): $b_{ij} = \frac{\langle u_i u_j \rangle}{2k} - \frac{1}{3}\delta_{ij}$; $k = \frac{1}{2}\langle u_l u_i \rangle$, where δ_{ij} is the *kronecker delta*.

2.3 The Kelvin-Townsend Set of Equations

The Kelvin-Townsend equations, govern the evolution of the components of the Fourier transforms of the fluctuating velocity field in the Rapid Distortion Limit. The rapid distortion equations are dealt with in Fourier space. In this approach, velocity and pressure are represented as sum of a finite number of Fourier modes:

$$u_i(\vec{x},t) = \sum_{\vec{k}} \hat{u}_i(\kappa,t) e^{i\vec{\kappa}(t)\cdot\vec{x}}, \qquad p^{(r)}(\vec{x},t) = \sum_{\vec{k}} \hat{p}(t) e^{i\vec{\kappa}(t)\cdot\vec{x}}. \tag{2.9}$$

where $\vec{\kappa}(t)$ is the wavenumber vector and $\hat{u}_i(\vec{\kappa},t)$, $\hat{p}(t)$ are the corresponding Fourier coefficients. As the equations are linear, each Fourier mode evolves independently and hence the equations can be decomposed and written for each fluctuation mode separately. The equations in Fourier space for each mode are given by,

$$\frac{d\kappa_l}{dt} = -\kappa_j \frac{\partial U_j}{\partial x_l}; \tag{2.10}$$

$$\frac{d\hat{u}_j}{dt} = -\hat{u}_k \frac{\partial U_l}{\partial x_k}\left(\delta_{jl} - 2\frac{\kappa_j \kappa_l}{\kappa^2}\right), \tag{2.11}$$

and the incompressibility constraint is given by $\hat{u}_i k_i = 0$. This indicates that the wavenumber vector $\vec{\kappa}(t)$ and velocity vector $\hat{u}_i(\vec{\kappa},t)$ are orthogonal to each other at all

times. Given the initial conditions and the mean flow gradients, the Kelvin-Townsend equations are well posed and can be solved numerically.

Three-dimensional Burgers equations are identical to the Navier-Stokes equation, except for the absence of the pressure terms. Consequently, the Burgers-RDT equations for the velocity amplitude can be written simply as

$$\frac{\overline{D}\hat{u}_j}{\overline{D}t} = -\hat{u}_k \frac{\partial U_j}{\partial x_k}; \tag{2.12}$$

The Reynolds stress evolution equation in physical space is

$$\frac{d\langle u_i u_j \rangle}{dt} = P_{ij}. \tag{2.13}$$

Thus, in the absence of pressure, wavenumber plays no role in the velocity field evolution and Reynolds stress evolution is dictated solely by production. In the same context, the incompressibility condition is not satisfied by the velocity field. The rapid distortion equations represent an excellent approximation of turbulence in the Rapid Distortion Limit. Beyond the RDL, other processes also influence turbulence. It is observed in Girimaji (2000) and Hunt and Carruthers (1990) that the rapid distortion equations still have utility beyond the RDL.

CHAPTER III

STABILITY ANALYSIS OF HYPERBOLIC AND ELLIPTIC FLOWS IN THE RAPID DISTORTION LIMIT

3.1 Introduction

In this section, the effect of pressure for flow stability of quadratic flows is considered. As has been observed in the prior sections, the action of the rapid component of the Pressure Strain Correlation is not universal, but depends on the nature of the background flow imposed. Different regimes of flow are considered and the changing behavior of the pressure terms with respect to the structure of the streamlines is analyzed. The role of pressure is isolated through the use of Burgulence. Additionally, a pertinent dynamical systems analysis is carried out for individual modes in the fluid flow to gauge the behavior of the system at a minute level. These paradigms of analysis are used to form a conclusive picture of the advent and suppression of the elliptical and hyperbolic instabilities.

It has been established in a multitude of investigations that, except for the case of pure vortical flow, all inviscid, homogeneous flows generated by Quadratic, two dimensional background flows are linearly unstable, irrespective of the closed or open nature of the streamlines. The hyperbolic instability for open streamline flows has been studied by Lagnado *et al.*(1983) and Friedlander and Vishik(1991). It has been concluded in the

aforesaid that all inviscid flows with hyperbolic stagnation points are linearly unstable. Caulfield and Kerswell(2000) have identified that almost all initial conditions for the same lead to "*transient growth*". According to Caulfield and Kerswell, this mechanism corresponds to the streamwise vortex stretching along the extensional strain. The set of zero measure leading to unbounded growth was ascertained by the same and it was thus shown that the perturbation kinetic energy could reach arbitrarily large values. This set was expanded upon by Craik and Criminale(1986). Pierrehumbert(1986) and Bayly(1986) have established the instability in the analogous case of closed streamline flows. This has been identified as the elliptic instability resulting from parametric resonance. Waleffe(1990) and Kerswell(2002) have established the corresponding mechanism to be vortex stretching which actualizes three dimensional instabilities in rotating flows via the transfer of energy from an elliptical eddy to a propagating Kelvin wave. Hence, it is observed that in spite of the fundamental differences in the characteristics and the disposition of the instabilities manifested in the aforementioned classes of flows, the underlying physical mechanism is accepted to be the same, viz. vortex stretching.

As stated earlier, the objective of this section is to explicate this physical mechanism via the role of pressure in the initiation, protraction and suppression of the corresponding instabilities. With this aim, the Kelvin-Townsend set of equations are studied. These are derived from the incompressible, inviscid form of the Navier Stokes equations expressed in Fourier space under the Rapid Distortion Limit. Salhi et al. (1997) have demonstrated

the equivalence of such a homogeneous RDT based analysis with respect to the corresponding linear stability analysis. For the specific case of the two dimensional mean gradient fields considered in this study, the structure of the Kelvin-Townsend set is as follows,

$$\begin{aligned}
\frac{de_1}{dt} &= ae_1^3 - ae_1(1+e_2^2) - be_2 \\
\frac{de_2}{dt} &= -ae_2^3 + ae_2(1+e_1^2) + be_1 \\
\frac{de_3}{dt} &= ae_3(e_1^2 - e_2^2) \\
\frac{du_1}{dt} &= (2ae_1^2 + 2be_1e_2 - a)u_1 - (2be_1^2 + 2ae_1e_2 - b)u_2 \\
\frac{du_2}{dt} &= (2be_2^2 + 2ae_1e_2 - b)u_1 - (2ae_2^2 + 2be_1e_2 - a)u_2 \\
\frac{du_3}{dt} &= 2e_3(ae_1 + be_2)u_1 - 2e_3(ae_2 + be_1)u_2
\end{aligned} \tag{3.1}$$

where,

$$\beta = \frac{W_{ij}W_{ij}}{W_{ij}W_{ij} + S_{ij}S_{ij}}$$

$$[S_{ij} = \frac{1}{2}(\frac{\partial U_i}{\partial x_j} + \frac{\partial U_j}{\partial x_i}), W_{ij} = \frac{1}{2}(\frac{\partial U_i}{\partial x_j} - \frac{\partial U_j}{\partial x_i})]$$

and,

$$a = \sqrt{\frac{1-\beta}{2}}, b = \sqrt{\frac{\beta}{2}}$$

This represents a six-dimensional, non-linear differential equation governing the evolution of the Fourier velocity coefficients (u_1, u_3, u_3) and the unit wavenumber vector (e_1, e_2, e_3), $e_i = \frac{\kappa_i}{|\kappa|}$. With the imposed background velocity gradient field expressed as a function of the ratio of the magnitude of the rate of rotation tensor to the sum of the

magnitude of the rate of strain and rate of rotation, β, this forms a single parameter system. With the desideratum of *isolating* the action of pressure, the behavior of the Navier-Stokes equations (referred to as RDT-NS) is contrasted to its pressure-released analogue, the Burgers' equations (referred to as RDT-B). RDT-B corresponds to the "pressureless modes" referred to in literature. The specific form of the Kelvin-Townsend set for the Burgers' equation is as follows,

$$\begin{aligned}
\frac{de_1}{dt} &= ae_1^3 - ae_1(1+e_2^2) - be_2 \\
\frac{de_2}{dt} &= -ae_2^3 + ae_2(1+e_1^2) + be_1 \\
\frac{de_3}{dt} &= ae_3(e_1^2 - e_2^2) \\
\frac{du_1}{dt} &= -au_1 + bu_2 \\
\frac{du_2}{dt} &= -bu_1 + au_2 \\
\frac{du_3}{dt} &= 0
\end{aligned} \tag{3.2}$$

In the following analysis, the present investigation considers both the evolution of the ensemble of initial conditions via the statistical treatment entrenched in the RDT analysis, along with the behavior of specific modes, in isolation. The latter paradigm of analysis corresponds to the "classical" Hydrodynamic stability analysis. The former represents the approach based on RDT. The correspondence between the two has been established in literature and for details, the reader is referred to Salhi et al(1997).

3.2 Comparison of Navier-Stokes to Burgers Behavior

The evolution of the perturbation kinetic energy (for an ensemble of realizations) for the Navier-Stokes and the Burgers' systems are exhibited in figure 1. Figure 1 (a) shows the evolution for a representative hyperbolic flow case. As can be observed, in the absence of pressure (RDT-B), the kinetic energy continues to grow exponentially and the consonant flow is unstable. In the case of the dynamics which are affected by the action of pressure (RDT-NS), the kinetic energy grows, exponentially, to a high value where it settles down. Thus, the corresponding flow is linearly unstable, but supercritically stable. Figure 1 (b) displays the kinetic energy evolution for a representative elliptic flow case. In this case, for RDT-NS, the perturbation kinetic energy has no upper bound and keeps increasing even for the long time spans simulated in this study. In contrast, for RDT-B, the kinetic energy is in a bounded, oscillatory state which has a constant amplitude and frequency of oscillation. Figure 1 (c) exhibits the evolution of the kinetic energy for the case of a Homogeneous shear flow, which acts as the transition between the hyperbolic and the elliptic flow regimes. As can be observed, the behavior of both RDT-NS and RDT-B is very similar. The kinetic energy evolution exhibited in this figure represents an algebraic (as opposed to exponential) growth in the energy. Thus, it is observed that the effect of pressure on the evolution of turbulent kinetic energy is diametric for hyperbolic flows and elliptic flows. For the case of open streamline flows, pressure causes the suppression of the hyperbolic instability. Contradistinctly, for the case of closed streamline flows, pressure acts so as to initiate the elliptic instability. At the point of

transition between these flow regimes, i.e., homogeneous shear, pressure has a minimal effect and does not alter the *nature* of flow stability.

It is accepted in the scientific community that the central role of pressure for incompressible flows is the imposition of the incompressibility constraint, rendering the velocity field solenoidal. With regard to the action of pressure, the present investigation, under the aegis of the Rapid Distortion Limit, considers the role of the "rapid" pressure. It is the function of rapid pressure to impose the divergence-free condition on the fluctuating velocity field produced by linear interactions between the perturbation velocities and the background flow. On the other hand, slow pressure acts to conserve the incompressibility of the velocity fluctuations due to the nonlinear interactions in the fluctuating velocity field. In fulfilling this role, pressure, through its rapid and slow components, redistributes the perturbation kinetic energy amongst the components. This redistribution of the kinetic energy is the *action* of pressure and is the agency through which it fulfills its *role* of maintaining continuity. This has been referred to by diverse cognomen, such as Intercomponent Energy Transfer, redistribution, realignment of the Reynolds stress tensor, etc; and represents a key towards understanding the role of pressure in this stability problem. The phenomenon of Intercomponent Energy Transfer is a subject of considerable importance and ongoing research. Brasseur and Lee,(1987) and (1988), have studied the same in physical space and have tried to correlate it to vorticity distribution. Hallback et al.(1993), studied the same for the case of the "slow" pressure strain correlation. A large section of the prior studies into this aspect have

emphasized on the Intercomponent Energy Tansfer and its modeling, vis a vis second moment closures. The present investigation seeks to consider the physics underlying this phenomenon and its ancillary ramifications to flow stability. Along this paradigm, this work employs a phenomenological approach to study the nature of this redistribution for different classes of flows. The evolution of the anisotropy of the covariance of the perturbation velocities is exhibited in Figure 2. For the case of hyperbolic flows, represented in Figure 2 (a), it is observed that for RDT-B, the perturbation kinetic energy is predominantly contained in u_2. For the case of RDT-NS, it is observed that the kinetic energy is transferred from u_1 and u_2 to u_3. It is reiterated that the Burgers' velocity field develops due to the exclusive effects of production while the Navier Stokes velocity field is affected by the dual effects of production and rapid pressure. Additionally, invoking the inherent linearity of the governing equations, the difference between the two fields is solely due to the action of pressure, explicitly the intercomponent redistribution of perturbation kinetic energy. Furthermore, referring to Figure 1 (a), it is observed that this transfer corresponds to the juncture where the perturbation kinetic energy ceases its exponential growth and becomes bounded. As stated earlier, the transfer of energy amongst the perturbation velocity components constitutes the action of pressure. From the observations made above, the mien of the Intercomponent Energy Transfer and its effects on the evolution of the perturbation kinetic energy are established for hyperbolic flows. For the elliptic flows, represented in Figure 2 (b), RDT-B suggests that the perturbation kinetic energy is contained in u_1 and u_2. For the case of RDT-NS, the kinetic energy is accommodated in u_2 and u_3, while u_1 has a very small fraction of the

same. Thus, for elliptic flows the Intercomponent Energy Transfer causes the cumulative difference between the energy contained in u_2 and u_1 to be significant. The ramifications of this effect will be commented upon in succeeding sections. For the case of pure shear flows, it is observed that the evolution of the anisotropies is very similar for both RDT-NS and RDT-B. In this case, the effect of the Intercomponent Energy Transfer is not significant. At this juncture, the characteristics of the action of pressure have been established phenomenologically. Forthwith, the investigation addresses the mathematical relevance of the same, apropos the issue of flow stability.

3.3 Mathematical Properties of the Governing Equations

To understand the nature of this redistribution, the mathematical properties of the governing equations are exploited to simplify the numerical formulation. The key difference between the velocities generated by the Kelvin-Townsend set (1) and its Burgers' analogue is the solenoidal nature of the velocity field generated by the former. Furthermore, the governing equations, under the Rapid Distortion assumption are linear, thus affording the use of the principle of superposition. In the light of these arguments, an abridged, discretized, linear model for (1) is proposed, viz. the "Corrected" Burgers' equations. The velocity vector and the wave number vector evolve independently, governed by the pressure released form of (1). After every discrete step, the orthogonality of the wavenumber and the velocity vector is reemployed. This is done in

a manner so that the magnitude of the velocity vector does not change as the pressure terms have no direct effect on the turbulent kinetic energy. This corresponds to the projection of the velocity vector to the solenoidal plane, perpendicular to the wavenumber vector. This projection constitutes the discrete analogue of the Intercomponent Energy Transfer and offers a simplified mathematical expression for the same, which is much more amenable to analysis. In mathematical terms, this is synonymous to a realignment of the perturbation velocity covariance matrix while maintaining its invariants. Using power series expansions, the energy transfer to the dimension "α" for each discrete step is,

$$\Delta k_\alpha = \frac{1}{2}\{x u_\alpha^2 + y^2 \kappa_\alpha^2 - 2 y u_\alpha \kappa_\alpha\}$$

where,

$$x = \frac{(u.\kappa)^2}{(u.u)(\kappa.\kappa)}, y = \frac{(u.\kappa)}{(\kappa.\kappa)}$$

$$k = \frac{(u_1^2 + u_2^2 + u_3^2)}{2} \textit{ and}$$

$$k_\alpha = \frac{u_\alpha^2}{2} \qquad (3.3)$$

In the limit of infinitesimally small time steps, considering the orthogonality of the wavenumber and velocity vectors at the beginning of each iteration in the model, the first 2 terms in the expression for Δk_α are negligible, with respect to the third. Hence,

$$\Delta k_\alpha \approx -y u_\alpha \kappa_\alpha \qquad (3.4)$$

From the analysis of the Poisson equation governing pressure, the role of pressure is to prevent temporal change in the velocity gradients (i.e., to ensure that $\frac{\partial}{\partial t}\left(\frac{\partial u_i}{\partial x_i}\right) = 0$). The

expression (4) manifests the mechanism of the action of pressure while fulfilling this role of enforcing incompressibility. This action is to transfer energy to the dimension where the velocity gradient, $\frac{\partial u_\alpha}{\partial x_\alpha}$, has the opposite sign with respect to $\frac{\partial u_i}{\partial x_i}$. (In the given expressions, the summation convention is not applied to the Greek indices.)

3.4 A Dynamical Systems Analysis of the Kelvin-Townsend Set

The set of equations (3.1) form a system of six-dimensional, non-linear differential equations governing the evolution of the Fourier velocity coefficients and the unit wave number vector. With the imposed mean gradient field expressed as the ratio of the magnitude of the rate of rotation tensor to the sum of the magnitude of the rate of strain and rate of rotation, β, these form a single parameter system. It must be emphasized that the three dimensional system governing the evolution of the unit wavenumber vector, can be decoupled from the original set. Additionally, the Fourier coefficients evolve via an equation that is linear with respect to them and where the terms involving the wavenumber vector act as equation coefficients. This role of the wave number vector components is pivotal towards understanding the dynamics of the Fourier coefficients and concordantly, that of the fluctuating velocity field in the Rapid Distortion Limit.

At the outset, the analysis commences with a scrutiny of the set of equations governing the evolution of the unit wave number vector, reproduced below,

$$\frac{de_1}{dt} = ae_1^3 - ae_1(1+e_2^2) - be_2$$
$$\frac{de_2}{dt} = -ae_2^3 + ae_2(1+e_1^2) + be_1 \qquad (3.5)$$
$$\frac{de_3}{dt} = ae_3(e_1^2 - e_2^2)$$

The emphasis is on the structure and properties of the equations, along with its dynamics subsuming the requisite invariant sets, bifurcations etc.

The attributes of the action of pressure are entrenched in the dynamics of the unit wavenumber vector in Fourier space, (e_1, e_2, e_3). By definition, a first integral can be obtained, of the form of $\frac{d(e_1^2 + e_2^2 + e_3^2)}{dt} = 0$. Hence, the phase space for the dynamics of this equation is a smooth, bounded and compact manifold, representing the surface of a unit sphere in three dimensions. The interaction between the effects of the rate of strain tensor, S_{ij}, and the rate of rotation tensor, W_{ij}, determines the nature of the solution for the wavenumber vector on this surface. The fundamental difference between the action of these tensors is the spatial dependence of the action of the rate of strain, while the dynamics governed by the rate of rotation are spatially independent. For hyperbolic streamline flows, the magnitude of S_{ij} is more than that of W_{ij}. Thus, the wavenumber vector exhibits stationary solutions for this class of flows. In contrast, for elliptic flows, the magnitude of W_{ij} is greater than S_{ij}. Consequently, the wavenumber vector manifests periodic solutions in this regime.

Herewith, the analysis of the dynamics of the unit wave number vector for strain dominated or hyperbolic flows is carried out. Initially, the discussion will entail the invariant sets and the evolution of the trajectories. Thenceforth, the scrutiny will turn to the changes in the aforementioned as the parameter β is increased, leading to the bifurcations exhibited by the system and their ramifications.

For strain dominated flows, the phase space has six discrete fixed points, two attractor-repeller pairs stationed on the "equator" and a saddle point on each "pole" of the spherical manifold. The structure of this distribution, along with representative trajectories, is exhibited in figure 3, for the case of plane strain (β=0). As can be observed, for this case, each attractor, repeller and saddle point is situated diametrically opposite to its counterpart. The basins of attraction for the attractors are demarcated by the attracting manifolds of the saddle points. The corresponding separatrices are marked in the figure. At this juncture, the evolution of the trajectories on the phase space is considered. As the basins of attraction form a cover for the entire phase space, omitting a set of measure zero, i.e. the seperatrices, for almost all initial conditions, the unit wavenumber vectors converge, exponentially, to either one of the attractors. Thus, in finite time, the state of almost all wave number vectors can be approximated by the attracting fixed points. Furthermore, this time span is very brief due to the exponential nature of this convergence. This behavior leads to the success of Classical pressure-strain correlation models for hyperbolic flows. The rationale behind this claim will be addressed in the sections pertaining to modeling. Presently, the topology of the phase

space is correlated to the underlying physics. The attracting fixed points for the hyperbolic flows represent the solutions where $\kappa_1 and \kappa_2$ grow exponentially. Thus, for non-zero values of $u_1 and u_2$, these correspond to the velocity gradient along the 1 and 2 directions, reaching arbitrarily large values. Physically, this represents a stretching of the Lagrangian fluid particle along these directions. This is observed for the Burgers' RDT solutions, where the velocity field is not required to be solenoidal. In the incompressible Navier Stokes RDT, such growth in velocity gradients would cause a violation of the continuity equation. Concordantly, in the incompressible case, the kinetic energy from these dimensions is transferred to the dimension aligned with the system's rotation, i.e., 3, thus maintaining the solenoidal velocity field. As there is no shear and hence, no production along this dimension, this transfer of energy causes the suppression of the instability. This Intercomponent Energy Transfer is governed by (4). Hence, for the case of hyperbolic flows, the incompressibility constraint causes the flow to become supercritically stable. Additionally, the set of zero measure leading to unbounded growth, corresponds to the seperatrix, along with the saddle points. This set represents the alignments of the unit wavenumber vector for perturbations which can grow without violating the continuity condition.

Forthwith, the evolution of the phase space with change in the value of the parameter, β, is considered. As has been mentioned earlier, for plane strain, each attractor, repeller and saddle point is situated diametrically opposite to its counterpart. As the parameter, β, is increased from 0 to 0.5, the attractor-repeller pairs migrate towards each other, along the

equator. This is exhibited in the series of figures 4, (a) to (c). This migration leads to the first of the two simultaneous bifurcations that occur in the system. In the limit of the shift from strain dominated to rotation dominated flows, at the parameter value of 0.5, the two attractor-repeller pairs collide and mutually annihilate. This constitutes the Saddle-node or the blue-sky bifurcation manifested in the system. This is one of the most basic mechanisms for the creation and destruction of fixed points and is found in a variety of nonlinear systems such as models for autocatalytic reactions, the synchronous flashing in herds of fireflies and others. The repercussions of this specific bifurcation occurring in the system are manifold and shall be discussed in the succeeding sections. The other bifurcation present in the system materializes at the saddle points located at the poles. These undergo a saddle-center bifurcation at the same parameter value of 0.5. It must be reiterated that this value corresponds to the case of Homogeneous shear flow. The bifurcation transmutes the saddles into centers which has concomitant effects in the invariant sets found in the phase space for elliptic flows. Once again, correlating the dynamical system analysis to the physics, as the parameter, β, is incremented, the relative magnitude of the rate of rotation tensor increases, vis a vis the rate of strain. This causes a shift in the principal axes of the mean gradient field. Thus, the respective attractor-repeller pairs migrate towards their counterparts. In the critical case of $\beta=0.5$, corresponding to Homogeneous shear flow, these collide and cause the bifurcation. As this parameter value represents the critical value for the system, it is helpful to apply appropriate coordinate transformations and analyze the equations in the principal coordinate system. In these coordinates, the mean flow reduces to a case of pure linear

shear. Landahl, (1975) and (1980), has studied the stability of such inviscid parallel shear flows, observing algebraic, non-modal growth in the perturbation kinetic energy, as observed in the prior sections. This is caused by the generation of vorticity perturbations by the "lift-up" of fluid elements in the presence of mean shear. The present work has observed that, based on the numerical evidence, the application of continuity (videlicet, the role of pressure) does not affect the nature of the stability problem for quadratic flows. Mathematically, this is valid as the pressure term enters the stability equation via the second gradient of the mean velocity field, which for quadratic flows is zero. This is further bolstered by the observations of Hanifi and Hennignson(1998), who have studied the compressible pure linear shear flow and have found the mechanism of the transient growth to be the same as the incompressible counterpart. The case of Homogeneous shear represents the transition between hyperbolic flows and elliptic flows. It has been proved in the preceding section that pressure does not affect the nature of the stability problem for this case. Thus, this represents the transition point for the effect of pressure, from the suppression of flow instability to being the cause of the instability.

Before considering the regime of elliptic flows, this work seeks to discuss a salient behavior exhibited by this system for hyperbolic flows. As has been mentioned, all the wave vectors that lie in the basin of attraction of one of the 2 fixed points, converge exponentially to the corresponding attractor. The remaining set of this phase space is constituted of the seperatrix and the 2 saddle points. Any unit wavenumber vector that lies on the seperatrix, lies on an attracting manifold for the saddle point. It is trivial to

prove that the set of equations (1) is Lipschitz continuous. Thus, these trajectories will never approach the attracting fixed points. Explicitly, these will lie on the seperatrix for any time span. This set of initial conditions for the wavenumber vector has been analyzed, from the paradigm of stability, in Caufield and Kerswell (2000). These eddies (or coherent motions of a specific physical scale) exhibit behavior that is different from that which has been observed in the sets of figures (1) and (2). The turbulent kinetic energy of these eddies would exhibit unbounded, exponential growth in an inviscid flow. Further, for small spanwise wavenumbers, this instability would persist in viscous flows. The behavior of eddies with initial conditions in the proximity of this set is similar. Thus, given any arbitrarily large time span, an open set can be found such that the eddies with initial conditions inside this set, would exhibit growth in turbulent kinetic energy for this time span. Hence, the turbulent kinetic energy, vis a vis its temporal growth and its eventual stationary value, is not just a function of the parameter β, but also of the initial conditions of the flow. Thus, in any numerical simulation, the evolution of the kinetic energy represents that for only the very specific set of parameter value and initial conditions. In essence, this discussion questions the concept of modal independence for such a simulation. The behavior of the ensemble of modes is dependent on the modes with the highest growth rate and growth time span, that is, the modes closest to or on the seperatrix. Consequently, the behavior of any pair of starting conditions, with the same parameter value, will be different based on the relative density of the Fourier modes in the vicinity of the seperatrix. Using this behavior to validate models or tailor their coefficients is mathematically erroneous as these models are purportedly mimicking the

behavior of any such system, irrespective of its initial conditions. Besides questioning the methodology of the development of these models, the aforesaid observations question the inherent assumption of the Classical Reynolds stress modeling. The assumption entrenched in the Classical approach states that the Reynolds stresses represent an adequate basis to model their evolution. This ignores the initial conditions of the velocity field as an input to the model. In terms of Fourier space representation, the set of Fourier velocity coefficients is made available to the model while the information in wavenumber space, e.g. the set of unit wavenumber vectors is not. As the preceding discussion establishes, this set represents information that is essential to predicting the evolution of the system.

Considering the regime of elliptic flows, i.e. for β values between 0.5 and 1.0, the consequences of the bifurcations on the structure of the phase space is established. As had been stated, the attractor-repeller pairs are not extant for this regime and the saddle points have been transformed into centers. Additionally, the phase space is closed, bounded and compact manifold. Thus, applying the Poincare-Bendixson theorem for the compact phase space, all the wave number trajectories must approach closed orbits. Presently, the scrutiny turns to a key feature of the saddle-node bifurcation, the square-root scaling law caused by the saddle-node remnant, also termed as the “ghost” region. A general feature of most systems, just after the manifestation of a saddle-node bifurcation, is the occurrence of a region in phase space where the trajectories are attracted to and retained in, before they leave this open neighborhood. This contains the

location of the collision of the attractor-repeller involved in the bifurcation and is termed as the saddle-node remnant. Despite the fact that this region has no attractors, *per se*, it pulls any proximate trajectory to itself. Thus, it is referred to as a "ghost" region. The invariant sets just after the occurrence of the bifurcation are shown in figure 5, for a representative case. As can be observed, the closed orbits are highly distorted in the aforementioned ghost region. In absence of the same, they would have been simple closed circles, akin to those observed for vortical flow. Instead of circular paths, the closed orbits are elongated ellipses on the sphere. Mathematically, this is a consequence of the fact that the solutions for the unit wavenumber vector are elliptic integrals, albeit complete.

Additionally, the presence of the ghost region introduces new time scales into the problem. After the bifurcation, there are two time scales that are present in the system. They correspond to the time for which the trajectories are slowed down and retained in the ghost region, τ_g, and secondly, to the time for which the trajectories move, much faster, in the rest of the phase space, τ_f. Just after the bifurcation, the discrepancy in the two scales is most evident and they are different by orders of magnitude. This can be seen in figure 6, where the time history of a representative trajectory is plotted, close to the parameter value for the bifurcation. This retention of the trajectories leads to the characteristic scaling law for the saddle-node bifurcation. The time spent by the trajectories in the ghost region, increases as $(\mu-\mu_c)^{-1/2}$, where μ is the control parameter and μ_c is the critical parameter value corresponding to the bifurcation. As indicated

earlier, near the bifurcation, $\tau_g \approx \tau_f$. Concordantly, the time scale for the orbit of the trajectories is almost equal to τ_g. Thus, the period of the orbits scales with $(\mu-\mu_c)^{-1/2}$.

Considering the phase space and the evolution of the trajectories for elliptic flows, a waning of the extent of this distortion is observed with an increase in the parameter value. This leads to a reduction in the extent of the distortion of the closed orbits, corresponding to their attraction to the same. The series of figures 7, (a) to (c), exhibit this change for archetypal cases. As can be seen, the distortion of the orbits from closed circular paths diminishes as β is increased. In the limit of pure vortical flow, corresponding to a parameter value of unity, the orbits are simple circular paths. For vortical flow, there is no evolution of the turbulent kinetic energy. This is due to the fact that the ghost region, that is the deviation of the orbits from purely circular paths, does not exist for the vertical flow case.

Presently, the problem concerning the additional vector required to form a basis for the formulation of the Pressure Strain Correlation tensor is considered. A closed from solution of the wavenumber vector would mitigate this, partially. Nonlinear differential equations are notoriously difficult to solve in an analytical form. Considering the first integral available (regarding the magnitude of the wave number vector being constant.) as a lemma, an analytical solution of the same can be formulated in terms of elliptic functions in a spherical coordinate frame. The solution is of the form,

$$f(t) = \frac{\gamma \tan(\gamma(t + c_1)) - a}{b}$$
$$\theta = \tan^{-1}(f(t))$$
$$\phi = \cot^{-1}[c_2(1 + \frac{2\lambda f(t)}{1 + f^2(t)})^{1/2}]$$
, where
$$\gamma = \sqrt{b^2 - a^2} \tag{3.6}$$
$$\lambda = \frac{a}{b}$$
c_1, c_2 : arbitrary
and
$e_1 = \cos\theta \sin\phi$
$e_2 = \sin\theta \sin\phi$

3.5 The Role of Pressure in the Elliptic Instability

For elliptic flows, the magnitude of the magnitude of W_{ij} is greater than S_{ij}. In absence of any fixed points or attracting sets in the phase space, the unit wavenumber vector has periodic solutions in the form of closed orbits. It has been observed in prior investigations that the wavenumber vector exhibits periodic behavior for elliptic flows. This fact is conspicuous and can be established via analytic solutions, as in Craik and Criminale (1986) or by utilizing the Poincare-Bendixson theorem for the compact phase space. It is proposed that it is not the nature of these trajectories in wavenumber space, but their geometrical shape, that holds the key to the instability and its mechanism. The periodicity of the wavenumber solutions is a reflection of the fact that the background

flow is a closed streamline flow. As can be observed in Figure 6, the trajectories in wavenumber space are not simple closed circles on the sphere but distorted ellipses. Mathematically, this is a consequence of the fact that the solutions for the unit wavenumber vector are complete elliptic integrals as exhibited in (6). Physically, this distortion occurs due to the interaction of the principal axes of the rate of strain and the rate of rotation tensors. As the magnitude of W_{ij} is greater than S_{ij}, the background strain field is not able to offset the effects of the background rotation field, completely. In the region with the distortion, it is able to counteract the effects of rotation to the highest degree.

At the onset of this section of analysis, the behavior of a hypothetical fluid particle governed by the Burgers' equations is considered. In Fourier space, the wavenumber components and the velocity coefficients of the same undergo linear oscillations, with a constant phase difference and amplitude. Considering the spatial gradients of the perturbation velocity in physical space, correlated via

$$F\{\frac{\partial U_i}{\partial x_j}\} = -iu_i\kappa_j \tag{3.7}$$

(here the operator F{ }, denotes the Fourier transform and U represents the perturbation velocity vector in physical space.) It is observed that the consequent velocity gradients are in a state of linear oscillation. Thus, the aforementioned particle, in physical space, is stretched and compressed, periodically, along the dimensions 1 and 2 (To reiterate, these 2 dimensions represent the plane of the background flow, which is a plane, quadratic

flow.). At this juncture, a norm of the perturbation velocities is introduced. This is equivalent to the kinetic energy of a mode in Fourier space. This is similar to that used in Caulfield and Kerswell(2000).

$$k = \frac{(u_1^2 + u_2^2 + u_3^2)}{2},$$
$$\frac{dk}{dt} = a(u_2^2 - u_1^2) \tag{3.8}$$

As can be observed from the form of the evolution of the kinetic energy for a mode, the instability will grow when the magnitude of u_2 is higher than that of u_1. For the Burgers' particle, the integral of $(u_2^2 - u_1^2)$, over a time period of oscillation is zero, as both the velocity coefficients are in linear oscillation with equal amplitudes. Thus, the flow governed by the Burgers' equations is in a state of neutral stability. There is a cyclic exchange of energy to and from the external source, representing negative and positive production, respectively. This is exhibited, schematically, in Figure 8 (c). Forthwith, envisaging the behavior of a synonymous fluid particle governed by the Navier-Stokes equations, it is observed that the evolution is affected by an additional term, that due to pressure. As has been observed in numerous investigations, additional terms can have mercurial effects on the stability of a system. For instance, as reported by Becker and McKinley(2000), viscous heating destabilizes the viscoelastic Poiseuille flow modes with long wavelengths, but stabilizes the modes with short wavelengths. In a similar vein, with reference to the present investigation, the addition of the pressure terms may

stabilize the modes, destabilize them or not affect their stability characteristics at all. As will be proved, all three of these effects are manifested by the system on the inclusion of the pressure term. In the cited work, the effect on the nature of stability of specific modes was dependent on their wavelength. Under the auspices of the Rapid Distortion Theory and its concomitant assumptions, it is known that the evolution of the velocity is independent of the wavelength. For this problem, the nature of modal stability depends on the alignment of the mode, that is, the coefficients of the unit wavenumber vector, $[e_1, e_2, e_3]$. The unit wavenumber vector subsumes the information regarding the alignment of the "eddy" (or the coherent motion of a specific physical scale) with the principal axes of the background flow. Additionally, with reference to Waleffe (1990), the wavenumber vector contains the information regarding the relative length scale of the Lagrangian particle along the coordinate axes. Presently, the evolution of a specific mode that is destabilized via the action of pressure is considered, to glean the mechanism of the instability. The rationale underlying the choice of this specific mode and that of the variable effect of pressure on modal stability will be addressed subsequently. Observing the perturbation kinetic evolution of this representative unstable mode, exhibited in Figure 9 (a), it is noted that while the averaged growth of kinetic energy is exponential, there is a cyclic variation in this evolution, where a half of the cycle has "sub-exponential" growth and the other half consists of "super-exponential growth". The corresponding pressure strain correlation terms are illustrated in Figure 9 (b), for one such cycle. These can be analytically expressed for a single mode. As can be observed, for a part of the cycle the pressure strain correlation transfers energy to u_3^2 and from

u_2^2 (approximately during 11.5-14 St units, with reference to the figure). While for the rest of the cycle, pressure strain correlation transfers energy to u_2^2 from u_3^2 and u_1^2 (approximately 9.5-11.5 St and 14-15.5 St). This needs to be correlated to the inherent tendency of the Burgers system, ensconced in the Production mechanism. The evolution of the production term, for the corresponding duration, is exhibited in Figure 9 (c). From the illustrations of the Figure 9 (b) and (c), it is noted that the pressure strain correlation term transfers energy to u_2^2, from u_1^2 and u_3^2 when P_{11} is more than P_{22}. Furthermore, when P_{22} is more than P_{11}, the pressure strain correlation transfers energy from u_2^2 to u_3^2. With reference to (8), this ensures that the consequent evolution of kinetic energy is positive through the aforementioned cycle, thereupon engendering the instability. Continuing along the same paradigm, having identified the action causing the instability, this study seeks the reasons underlying this action, i.e., the physical mechanism. For incompressible flows, the evolution of the pressure field is governed by a Poisson equation. From the analysis of the same, the role of pressure is to prevent temporal change in the velocity gradients (i.e., to ensure $\frac{\partial}{\partial t}\left(\frac{\partial u_i}{\partial x_i}\right)=0$). Expressing this condition in Fourier space,

$$\begin{aligned}&\frac{\partial}{\partial t}(e_1R_{11}+e_2R_{22}+e_3R_{33})=0\\&\Rightarrow \dot{e}_1R_{11}+e_1\dot{R}_{11}+\dot{e}_2R_{22}+e_2\dot{R}_{22}+\dot{e}_3R_{33}+e_3\dot{R}_{33}=0\end{aligned} \tag{3.9}$$

(in (9), $R_{\alpha\alpha}$ denotes the product $u_\alpha\, u_\alpha$, and the overdot represents differentiation with respect to time.) Considering a representative section of the aforementioned cycle, St

ϵ(9.5,11.5), it is observed that for this duration, $\dot{e}_i > 0; e_1, e_3 > 0; e_2 < 0$. The tendency of the production term would lead to $\dot{R}_{11} > \dot{R}_{22} > 0$, thus violating (9). Thus, the Intercomponent energy transfer endeavors to reduce $\dot{R}_{11}$ while increasing $\dot{R}_{22}$. Additionally, as energy is transferred from R_{33} to R_{22}, pressure causes $\dot{R}_{33}$ to be negative. This ensures that (9) is satisfied. In terms of the fluid particle in physical space during this time (considering this scale of motion, in isolation.), the particle has a tendency to be stretched along 1 and contracted along 2. The pressure strain term mitigates the rates for the same while causing the particle to contract along 3, so as to ensure that the continuity condition is met.

At this juncture, this investigation seeks to explain the physical reasons intrinsic to the manifestation of the elliptical instability in wavenumber space. It has been observed in the Floquet analysis conducted during prior research in this field, such as Pierrehumbert (1986) and Bayly(1986), that the elliptical instability has a “banded” appearance in wavenumber space, vis a vis the alignment of the unstable modes. This peculiar form has been attributed to the phenomenon of Parametric resonance by Sagaut and Cambon(2008). Parametric resonance causes the instability to manifest itself in bands in wavenumber space instead of discrete modes of instability, as would be expected in the case of other generic forms of resonance. As observed in Kerswell(2002), parametric resonance is a “generic” mechanism. The physical mechanism cardinal to this peculiar feature of the instability is to be observed in the Intercomponent energy transfer; its

magnitude, direction and temporal variations. At the outset, this study considers the direction of the Intercomponent energy transfer. At a fixed value of the parameter, β (0.75 for the germane figures in this section.), the time period of the oscillation of each mode is the same, (say) T, and is analytically determinable. Based on Floquet theory, the temporal variation in the Intercomponent energy transfer is restricted to a periodic solution with a time period 2T. The scaled integrals of the pressure strain correlation terms for each of the dimensions, over this period give the comprehensive direction of the Intercomponent Energy Transfer, to or from the specific dimension, depending on the sign of this integral. Figure 10 (a) exhibits this integral for both φ_{11} and φ_{22}, for the entire set of alignments of the unit wavenumber vector. Based on a simplistic view of the action of the Intercomponent energy transfer, it would be expected that the direction of energy transfer would be directly correlated to the inception of the instability. Thus, with reference to (8), modes for which energy is transferred to u_2^2 and from u_1^2, would be expected to be unstable. As can be observed from Figure 10 (a), this is not the case, for a considerable region of wavenumber space, the pressure strain correlation transfers energy to u_1^2 and from u_2^2, yet the representative mode is unstable. The reasons for the same are to be found in the nature of the Production term, i.e. the interaction between the background flow and the perturbation velocity field.

$$\begin{aligned} P_{11} &= -2(ar_{11} - br_{12}) \\ P_{22} &= -2(-ar_{22} + br_{12}) \end{aligned} \tag{3.10}$$

As can be observed from (10), the evolution of u_1^2 involves negative production. Hence, while transferring energy to u_1^2, the pressure strain correlation is constraining the growth

of u_1^2 by influencing the Production term for the same. The onset of stability, in wavenumber space, occurs due to a similar argument. Beyond the most unstable mode (denoted by θ_c), the magnitude of the production is more than that of the pressure strain correlation for u_1^2, as shown in Figure 10 (b). Thus, over a time period, the magnitude of u_1^2 increases. When this (averaged) rate of growth of u_1^2 becomes more than that of u_2^2, the mode is stabilized according to (8).

Thus, it is observed that, for elliptic flows, the unit wavenumber vector exhibits periodic solutions. However, due to the nature of these solutions, the Intercomponent Energy Transfer is variable, dependent on the alignment of the unit wavenumber vector. Further, due to the magnitude of the same and its interaction with the Production term, the stability of the specific mode is determined. Hence, in unit wavenumber space, there exist bands of stable and unstable modes. These are demarcated by periodic solutions (denoted by θ_1 and θ_2 in Figure 10), where the (averaged) magnitude of the pressure strain correlation and the Production terms is equal. The key qualifier to note here is that the stability of the system is completely determined by the most unstable node. Further, the kinetic energy of perturbation is determined by the evolution of this mode, along with that of the modes in its vicinity, if any such modes are present. This was the mode whose evolution was analyzed and explained in the preceding section.

In conclusion, this report seeks to make a few pertinent observations regarding the stability of a given plane, quadratic flow. As has been observed, the stability of the flow

depends on the alignment of the "eddies" with the background velocity field. Additionally, the instability is manifested for a small band of wavenumbers. This band depends on the parameter β. For strongly elliptic flows, this band is very narrow. Thus, a representative flow can be envisioned which has no eddies with their alignments in this band. Consequently, the specific flow under consideration will be stable. In coda, this reiterates the fact that the stability of a plane, quadratic, closed streamline flow is not just a function of the background strain and rotation fields, but of the alignment of the eddies in the flow. An argument along similar lines may be considered for the reciprocal case of open streamline flows. From the analysis, these are supercritically stable. However, there exists a set in the unit wavenumber space, for which the specific mode would be unstable. The key argument to consider here is the fact that this set of unstable alignments has zero measure. Thus, this is of only academic import with respect to the modeling and simulations of such flows. In the case of the elliptic flow, the corresponding set can be arbitrarily small, yet finite, hence leading to the ambiguity in flow stability.

Before concluding this section, certain questions concerning the validity of the application of Rapid Distortion Theory and its concomitant numerical simulation, for modeling purposes are articulated. This is analogous to the questions addressed for hyperbolic flows, and will be discussed at length in the sections pertaining to modeling. A preamble to this issue is placed here due to its close association with the issue of flow stability and the preceding dynamical system analysis. As has been established in the

preceding analysis and re-iterated in the aforementioned discussion on the flow stability for elliptic flows, the perturbation kinetic energy, its evolution and specifically, it's rate of growth, are dependent on the initial alignment of the "eddies" with the plane of shear. Furthermore, due to the periodic, closed orbit behavior of the alignment vector, the nature of this distribution persists in its temporal evolution. This is in contrast to the case of hyperbolic flows where almost all initial conditions of the alignment vector converge towards the attracting fixed point. Further, due to the banded nature of the instability in wavenumber space, there is a small proportion of the modes that will have growing kinetic energy. In this band too, there will be modes for which this growth is faster. This is exhibited in figure 11, showing the integral of the perturbation kinetic energy over a time period of oscillation for a distribution of azimuthal alignments of the eddies. Thus, the kinetic energy evolution is highly dependent on the initial alignment of the eddies. In the modeling procedures, utilized at present, the simulations are conducted for generic initial conditions and thus, the kinetic energy evolution is taken to be a function of the parameter and not of the initial conditions. This represents a flaw in the modeling methodology. Additionally, in the Classical Pressure Strain Correlation modeling formulations, the initial conditions of the perturbation (or fluctuating) velocity field are not considered. As can be deduced from this discussion, such an approach is incorrect as it does not acknowledge the complete set of basis tensors required to model the pressure strain correlation. The Classical modeling approaches consider only the Reynolds stress tensor as the basis (or in Fourier space, the set of Fourier velocity amplitudes). The complete set would also include the initial conditions of the velocity field (or the set of

unit wavenumber vectors). In summation, due to the banded nature of the instability, the concept of modal independence does not exist for elliptic flow simulations. Moreover, due to the same reasons, Classical modeling formulations are incorrect for these cases, as they attempt to recreate the evolution of the velocity field with an insufficient basis of tensors.

CHAPTER IV

RAPID PRESSURE STRAIN CORRELATION MODELING

4.1 Introduction

In the context of second moment closure approach to turbulence modeling, the development of a pressure-strain correlation model that is *accurate and universal* on one hand and *computationally simple* on the other is of paramount importance. The foundations for second moment closures were established in landmark papers by Chou (1945) and Rotta (1951). The second moment closures are tailored for practical applications requiring higher degree of physical fidelity than two-equation closures at a much reduced computationally expense than approaches such as Large Eddy Simulation (LES) or Direct Numerical Simulation (DNS). Various pressure strain correlation models have been developed till date. Some of the notable examples include those by Launder, Reece and Rodi (1975), Speziale, Sarkar and Gatski (1991), Shih and Lumley (1985), Johansson and Hallback (1994), Sjogren and Johansson (2000), Girimaji (2000) and Ristorcelli et al (1995). These models attempt to express the pressure strain correlation as a function of the Reynolds stress anositropy and the mean strain tensors and thus, are categorized as classical models. In the aforementioned, two of the key kinematic and mathematical assumptions are:

(i) the Reynolds stress and the mean gradient tensors form an adequate and complete basis for closure.

(ii) the closure expression should be linear in the Reynolds stress and the mean gradient tensor components to reflect the properties of pressure strain correlation (Pope (2000)).

While these models have achieved notable success, they remain deficient in many flows and are far from universal in their applicability. In particular, in elliptic streamline flows, the classical pressure-strain correlation models have been found wanting. The predicted behavior is, even qualitatively, different from that seen, for instance in the Direct Numerical Simulations of Blaisdell and Shariff (1996). Kassinos and Reynolds (1994) developed the Structure-based closure that includes other basis tensors beyond Reynolds stress and mean velocity gradients for improving the accuracy of second moment closures. Van Slooten and Pope (1997) derived a Langevin-particle equivalent of the same. However, these closures are not widely used due to the increased computational burden. Similarly, there have been some works that advocate the pressure-strain correlation closures that are non-linear in Reynolds stress to improve the model's adherence to real world phenomena, viz. realizability. However, non-linear rapid pressure-strain correlation models do not satisfy the essential linear super-position requirement. The general objective of this article is to examine the tensor bases and linearity topics in the context of two-dimensional homogeneous mean flows at the rapid distortion limit of turbulence and propose avenues for closure model improvement.

4.1.1 Pressure-Strain Correlation Physics

Bradshaw ((1972), (1997)) argues that, in order to institute improved prediction of turbulent flows, one needs to increase the level of physical understanding of the underlying process. Thus, it is important to first establish the general role of pressure-strain correlation in the Reynolds stress evolution.

From the perspective of turbulence physics, the evolution of the fluctuating velocity field is determined by the interplay between inertial, pressure and viscous effects. Inertial effects deform the velocity field without regard to the incompressibility requirement. Viscous effects are dynamically passive and thus, do not significantly affect the dilatation state of the velocity field. It is then the function of pressure to modify this inertial deformation, rendering the velocity field divergence free. From a mathematical standpoint, in incompressible flows, the pressure term acts as a Lagrange multiplier to enforce the divergence-free constraint on the velocity field. With regard to its action, it is pertinent to divide the fluctuating pressure into two components, viz. rapid and slow components. The terms “rapid” and “slow” refer to the components of pressure arising respectively from the linear and non-linear parts of the source term in the Poisson equation for pressure. The slow component acts to conserve the incompressibility of the velocity field generated by the nonlinear interactions among velocity fluctuations. It is the function of rapid pressure to impose the divergence free condition on the fluctuating velocity field produced by linear interactions between the mean and fluctuating fields. By their very nature, the non-linear interactions are reasonably independent of the mean

velocity field and the action of slow pressure-strain correlation can be considered "universal". It is generally accepted that slow-pressure strain correlation tends to isotropize the fluctuating velocity field, irrespective of the mean velocity gradient. In contrast to the slow pressure, the action of rapid pressure – and consequently rapid pressure-strain correlation – is a strong function of the mean velocity field. Despite the apparent simplification afforded by linearity, the action of rapid pressure is not straightforward. Depending on the nature of the mean velocity field and initial conditions of the flow field, the effect of the rapid pressure-strain correlation can be diametric.

A key tool used to investigate rapid pressure-strain correlation physics is the Rapid Distortion Theory (RDT) introduced by Batchelor and Proudman (1954) In the rapid distortion limit, the mean flow timescale is much smaller than that of the fluctuating flow, so that the nonlinear interactions amongst fluctuating modes can be neglected. Thus, the evolution equations are linear in fluctuating velocity. This affords a degree of simplification in the analysis of the resulting equations. Under the auspices of RDT, the physics of rapid pressure can be investigated in isolation without the complicating presence of non-linear and viscous processes. It must be pointed out that these linear equations still have utility beyond the rapid distortion limit even when other processes also influence turbulence (Girimaji (2000) , Hunt and Carruthers (1994)). Consequently, it is reasonable to demand, even in the presence of non-linear processes, that the rapid pressure-strain correlation closure physics be consistent with RDT.

4.1.2 Objectives and Overview

The categorical objectives of this section of the thesis are:

1. To collate and characterize the RDT dynamical system behavior in two-dimensional mean flows.

2. To examine the classical rapid pressure-strain closure modeling tenets in light of dynamical properties of RDT equations and identify possible inconsistencies.

3. To develop a clear closure methodology that leads to improved consistency with the Navier-Stokes equation in the rapid distortion limit.

4.2 Properties of the Equations

In this section, the segment of the Kelvin-Townsend equations governing the evolution of the velocity vector is investigated. The nature of the equations and their concomitant effects on the dynamics of the variables is addressed originally. Thereupon, the behavior of the phase space of the velocity vector components is analyzed. Additionally, the scrutiny of the stability of this set of equations is undertaken. This is correlated to observations made in Chapter II regarding the evolution of the turbulent kinetic energy for elliptic flows in the Rapid Distortion Limit, which are associated to observations made in prior investigations. The structure of the equations governing the evolution of the velocity vector is abridged in light of the analysis of Section 4.3. The simplified form of the equations is as follows,

$$\frac{d}{dt}\begin{bmatrix} u_1 \\ u_2 \\ u_3 \end{bmatrix} = \begin{pmatrix} C(t) & D(t) & 0 \\ E(t) & F(t) & 0 \\ G(t) & H(t) & 0 \end{pmatrix}\begin{bmatrix} u_1 \\ u_2 \\ u_3 \end{bmatrix}$$

where,

$$\begin{aligned} C(t) &= 2ae_1^2 + 2be_1e_2 - a \\ D(t) &= -2be_1^2 - 2ae_1e_2 + b \\ E(t) &= 2be_2^2 + 2ae_1e_2 - b \\ F(t) &= -2ae_2^2 - 2be_1e_2 + a \\ G(t) &= 2e_3(ae_1 + be_2) \\ H(t) &= -2e_3(ae_2 + be_1) \end{aligned} \tag{4.1}$$

As can be observed, the evolution of the Fourier velocity coefficients is governed by equations linear in the components of the vector. The covariance of the Fourier coefficients, conditioned on a given wavenumber is given by,

$$\hat{R}_{ij}(\vec{e},t) = \left\langle u_i(\vec{e},t)u_j(\vec{e},t)\right\rangle \tag{4.2}$$

The import of this quantity is manifested while recreating the Reynolds stress tensor in physical space. The germane equation for the same is given by,

$$R_{ij} = \Sigma\hat{R}_{ij}(\vec{e},t) \tag{4.3}$$

An essential mathematical caveat from an ideal model for the rapid pressure strain correlation, is its linearity in the components of the Reynolds stress tensor. In the light of equations (4.1), (4.2) and (4.3), it is trivial to prove that the evolution of the components of the Reynolds stress tensor is governed by differential equations that are linear in the tensor components. The fundamental issue concerns the nature of the coefficients in this equation for the evolution of the Reynolds stress tensor components, in physical space.

As observed in the preceding section, the coefficients are periodic functions of time. Thus, the ideal equation for the Reynolds stress evolution, in the Rapid Distortion Limit, should be a linear, non-stationary differential equation. Such equations are often referred to as time-varying differential equations, the addendum referring to the nature of the equation coefficients. The primary step in the analysis of a set of differential equations is the identification of the invariant sets and their stability, Guckenheimer and Holmes (1983), Chow and Hale (1982). For autonomous systems, these are compact, invariant, attracting or repelling subsets of the phase space and determine the dynamics at asymptotic time spans. Vis a vis the non-autonomous case, this line of inquiry is not feasible as the invariant sets are not stationary by themselves having transient basins of attraction or repulsion. Such analysis has been considered by prior investigations such as Langa et al. (2002), Soliman (1995) besides others. In the context of fixed points, the linearity of the equation set (4.1) affords a unique level of simplification. In a linear, homogeneous system, the only fixed point is the origin of the phase space, representing the trivial solution. Concordantly, the analysis of the stationary solutions is equivalent to the analysis of the stability of the fixed point at the origin. In the analysis of preceding sections of this chapter, the key issues to be investigated from the paradigm of physics were the oscillatory behavior of the Reynolds stress anisotropies and the growth in turbulent kinetic energy for elliptic flows. The former has been resolved via the dynamics in the unit wavenumber space. The latter corresponds to the stability of the fixed point at the origin. If the origin was an asymptotic attractor for the set of equations (4.1), turbulence would decay and eventually die out as the Reynolds stresses would

approach values of zero. In the other case, if the origin was a linear center, i.e. there were stable periodic trajectories, we would observe a similar behavior (that is, linear oscillations bounded from above) in the evolution of the turbulent kinetic energy, corresponding to a periodic oscillation in its value. In Chapter III, this was the exact behavior shown by the turbulent kinetic energy governed by the Burgers' equations in the case of elliptic flows. Finally, if the origin was a global repeller, the value of the turbulent kinetic energy would diverge, exponentially, to infinity, which is the behavior observed for NS-RDT in Chapter III. Thus, it is expected that the origin represents a global repeller for the set of equations (4.1). With detailed analysis, the scenario is found to be more intricate than what such a naïve analysis suggests. It is observed that the eventual behavior of the Fourier velocity coefficients is dependent on the initial conditions attributed to the wave number vector. This is in addition to the obvious dependence on the value of the parameter, β. There exists a thin "band" of initial alignments of the wavenumber vector on the spherical phase space which lead to divergent solutions for the velocity vector. For any other initial value of the wavenumber vector, the magnitude of the velocity vector approaches zero. Additionally, this band is dynamic, vis a vis its extent with respect to the parameter value. This was exhibited in figure 11, which shows the integral of the magnitude of the velocity vector with respect to the initial alignment with the axis of rotation. This analysis underscores the importance of the information corresponding to the wavenumber vector with respect to the formulation of the pressure strain correlation model. This banded instability corresponds to the elliptic instability identified in flows with curved stream lines

(Kerswell (2002)). It has been established in prior literature that a general analysis based on Rapid Distortion Theory is equivalent to a linear stability analysis for homogeneous flows (Salhi et al. (1996)). This and similar approaches have been utilized by Cambon and others to identify the elliptical instability in elliptic flows in the Rapid Distortion Limit (Bayly (1986), Waleffe (1990), Cambon and Scott (1999), Cambon et al. (1994)). Waleffe (1990) has claimed the mechanism of this instability to be vortex stretching in physical space. Cambon et al. (1994) and Sagaut and Cambon (2008) have analyzed the instability from the paradigm of mathematics and have claimed that this occurs due to parametric resonance, thus leading to the banded nature of the same as opposed to a discrete instability that might be expected from other forms of resonance.

In this regard, the stability of the solutions of equations (4.1) is investigated using Floquet analysis, Floquet (1883), which deals with equations of the form $\dot{u}(t) = A(t)u(t)$ where A(t) is a continuous, periodic matrix with period T. The Floquet stability of the system for a representative case is exhibited in figure 13. For the purposes of generation of this plot, the radial angle of the initial conditions in unit wavenumber space was fixed at a constant value, while the azimutal angle and the parameter, β, were varied. The shaded regions in the figure correspond to decaying solutions of the velocity vector. The non-shaded regions correspond to divergent solutions. These are separated by the solutions corresponding to the boundary of the shaded regions, which represent the periodic solutions of the velocity vector.

At this juncture, a parallelism is drawn between an analysis based on Floquet theory and Liapunov stability. Considering a generic system, whose form is similar to the Hill's equations,

$$y(x)'' + G(x).y(x) = 0, x \in \square \quad (4.4)$$

The Floquet-Liapunov theorem states that,

a) v is a Floquet exponent of (4.4) if and only if exp(iTv) is an eigenvalue of Y(T).

b) There exists a T -periodic solution of (4.4) if and only if, v = 0 or v = $\frac{\pi}{T}$

c) All solutions of (4.4) are bounded if and only if the following condition holds: All Floquet exponents are real and for every eigenvalue of y(T), the algebraic and geometric multiplicities are equal. Thus, the real part of the Floquet exponent corresponds to the Liapunov exponent of the set of equations. According to Liapunov stability theory, the zero solution is stable if all Liapunov exponents are negative or non-positive and unstable if any of the Liapunov exponents are positive. In Floquet theory, the Floquet exponent v, leads to a characteristic multiplier for the system of the form of exp(iTv). Thus, vis a vis the stability analysis for the system of equations (4.1), Floquet stability is equivalent to Liapunov stability.

Presently, the evolution of volumes in the phase space is addressed. It is reiterated that this phase space is denoted by the Fourier velocity components, $[u_1, u_2, u_3]$. Considering

the linear system with 1-periodic coefficients, if u(t) is any fundamental matrix solution of the equation set (4.1), expressed as

$$\dot{u}(t) = A(t)u(t)$$

then,

$$\det(u(t)) = \det(u_0(t)) \exp\{\int_{t_o}^{t} trA(s)ds\} \tag{4.5}$$

where tr[A(s)], signifies the trace of the matrix of coefficients. This constitutes the Liouville's formula for phase spaces governed by sets of differential equations with periodic coefficients, Hale and Kocak (1991), Ott (1993), and relates an invariant of the coefficient matrix to the evolution of a volume in phase space. Due to the similarity of the matrix to its Jordan form, this is equivalent to the sum of the eigenvalues of the coefficient matrix. For the specific set of equations (4.1), the requisite trace is given by

$$C(t) + F(t) = 2a(e_1^2 - e_2^2) \tag{4.6}$$

Over a time period of oscillation of the coefficients, using the analytical form from the set of equations, this is evaluated as zero. This can be analytically derived, as the solutions of $e_1 and e_2$ are symmetric elliptic integrals. This is a seminal result as it signifies that the volumes in phase space are constant over an oscillation period. This would be contrary to what would be expected. Considering the dynamics in Fourier velocity coefficient space, it is acknowledged that due to the instability, almost all sets of initial conditions (which define the volume under consideration) would have points

which would have a growing L_2 norm, that is, their kinetic energy. Thus, the trajectories of these points would evolve so that their distance from the origin (defined under the Cartesian metric function) would increase exponentially. Yet, according to the proof above, the volume defined by these staring conditions would be constant over a time period. Thus the generic shape formed by these conditions, along with its evolution is interesting from the viewpoint of physics.

Before considering the evolution of such volumes for elliptic flows, we consider the evolution of similar volumes for hyperbolic flows. The series of figures 14, (a) to (d), exhibit this for the parameter value of $\beta=0$, that is the case of plane strain. Initially, the starting conditions were distributed over a unit sphere. For hyperbolic flows, almost all of these initial conditions exhibit "transient growth". (The initial conditions with the unit wavenumber vector aligned in the plane of shear form the only exception to this phenomenon of transient growth.) Thus, due to the transfer of energy from the applied mean gradient field to the turbulent velocity field, the dimension of this sphere starts to increase along the plane of shear. Additionally, due to the redistributive role of the rapid pressure strain correlation, the dimension of the sphere along the unit vector perpendicular to the plane of shear increases. By definition, this redistribution is conservative, thus during this process, the L_2 norm of each trajectory is conserved. By extension of this argument, the kinetic energy of the ensemble of eddies is conserved too. The key issue lies in the fact that the ensemble kinetic energy of these eddies is not equal to the magnitude of the volume defined by them. In the asymptotic limit, the

pressure strain correlation transfers all the energy from the dimensions 1 and 2 (that is, the unit vectors lying in the plane of shear.) to the dimension 3 (that is, the unit vector lying perpendicular to the plane of shear). Thus, initially the volume formed by the set of initial conditions is a unit sphere. Due to Production, this volume increases. For hyperbolic flows, the bias of the Intercomponent energy transfer has been established in the last chapter, that is, to transfer energy from R_{11} and R_{22} to R_{33}. This causes the volume to reduce, in the asymptotic limit, to a surface. Thus, the stabilizing effect of pressure leads to a reduction of phase volumes.

At this juncture, the evolution of a similar volume for elliptic flows is considered. The series of figures 15, (a) to (e), exhibit the same over 2 time periods of oscillation of the unit wavenumber vector at the parameter value of β=0.75. The set of initial conditions lie on a unit sphere, as in the prior case. Further, this set spans the entire range of unit wavenumber vector alignments. Thus, the set of initial conditions consists of eddies with exponentially growing kinetic energy, eddies with decaying kinetic energy and eddies for which the kinetic energy evolution would be bounded and periodic. For the purposes of the numerical simulation, the final category is not observed as it forms a set of zero measure. The evolution of the decaying modes is such that they move closer to the origin. It is the evolution of the unstable modes that exhibits singular behavior. All the unstable modes lie on a geometric entity that can be approximated as a symmetrical manifold. Additionally, it was found that (if the manifold is considered to be an open set. This is correct as every differentiable manifold forms an open set, relative to itself, if the

ambient space is ignored.) this manifold was robust and not sensitive to the set of initial conditions that were chosen. Thus, for the case of the hyperbolic flows, a geometrical entity of zero volume lead to supercritical stability. Contradistinctly, for elliptic flows, a set of zero volume lead to instability. The authors are not aware of any other, non-trivial system that shows instability along with such volume conservation.

4.3 Characteristics of the RDT System of Equations

It has been established in prior literature that a general analysis based on Rapid Distortion Theory is equivalent to a linear stability analysis for homogeneous flows (Salhi et al. (1997)). This and similar approaches have been utilized by Cambon and others to identify the elliptical instability in the Rapid Distortion Limit (Waleffe (1990), Cambon and Scott (1999)). Waleffe has claimed the mechanism of this instability to be vortex stretching in physical space. Sagaut and Cambon (2008) have analyzed the instability from the paradigm of mathematics and have claimed that this occurs due to parametric resonance, thus leading to the banded nature of the same as opposed to a discrete instability, which might be expected from other forms of resonance. This banded instability has also been identified in flows with curved stream lines (Kerswell (2002), Girimaji et al.(2003)). In this section, we summarize the findings from the succeeding chapters to characterize the rapid distortion flow physics relevant to closure model development in different regimes. In the following discussion, we focus on the evolution of:

(i) the wave-vector,

(ii) the Fourier amplitude vector and

(iii) the statistical quantities, such as the Reynolds stress anisotropy tensor components.

The first two items pertain to individual modes or eddies and the third is a ensemble average of several modes, which are distributed isotropically, initially.

The Kelvin-Townsend set governs the evolution of the unit wavenumber vector and the Fourier velocity coefficients in the RDT limit. As can be observed, this system of equations can be decoupled and the unit wavenumber vector evolution is not dependent on the velocity field. In physical space, the evolution of the unit wavenumber represents the evolvement of the alignment of the "eddies" (the motion associated with each wave-vector can be identified as an eddy) in the turbulent flow. Due to the linear nature of the problem, each eddy motion evolves in isolation. Moreover, the evolution of the turbulent kinetic energy contained in such an eddy is dependent upon, besides other factors, the alignment of the eddy.

4.3.1 Hyperbolic Flows

For hyperbolic flows, the effect of the applied mean gradient field has a "stretching" and a "squeezing" component. In mathematical terms, the mean gradient matrix has an extensional and a compressional principal direction, in physical space, associated with these effects. Furthermore, for hyperbolic flows, that is $\beta \in [0, 0.5)$, these directions are real and distinct. This leads to the characteristic hyperbolic shape of the streamlines for these flows.

4.3.1.1 Wavenumber Vector Dynamics

In a dynamical systems analysis, the emphasis is on the evolution of quantities, in a phase space. In this regard, we commence this with the identification of "fixed points", which are the roots of the evolution equation. The fixed points in wavenumber space are located at,

$$P_1 = [\sqrt{\frac{1+\sqrt{1-c^2}}{2}}, \sqrt{\frac{1-\sqrt{1-c^2}}{2}}, 0], \quad P_2 = [-\sqrt{\frac{1+\sqrt{1-c^2}}{2}}, -\sqrt{\frac{1-\sqrt{1-c^2}}{2}}, 0]$$
$$P_3 = [-\sqrt{\frac{1+\sqrt{1-c^2}}{2}}, \sqrt{\frac{1-\sqrt{1-c^2}}{2}}, 0], P_4 = [\sqrt{\frac{1+\sqrt{1-c^2}}{2}}, -\sqrt{\frac{1-\sqrt{1-c^2}}{2}}, 0] \quad (4.7)$$
and
$$P_5, P_6 = [0, 0, \pm 1]$$

As can be gleaned, there are six fixed points. Four of these, namely, P_1 to P_4 lie on the plane of applied shear and their location is dependent on the parameter value. P_5 and P_6 lie on the poles of the phase space and their location is not affected by the parameter value.

The requisite Jacobian matrix for the wavenumber evolution, is given by,

$$J = \begin{bmatrix} 3ae_1^2 - a(1+e_2^2) & -2ae_1e_2 - b & 0 \\ 2ae_1e_2 + b & -3ae_2^2 + a(1+e_1^2) & 0 \\ 2ae_1e_3 & -2ae_2e_3 & a(e_1^2 - e_2^2) \end{bmatrix} \tag{4.8}$$

Using this, for the fixed points located at the "poles" of the phase space, that is, P_5 and P_6, the eigenvalues are given by, $\lambda = \pm\sqrt{a^2 - b^2}$. Thus, these are classified as saddle points.

Further, for the other points, P_1 to P_4, applying the general from of,

$[e_1, e_2, e_3] = [\sin\theta, \cos\theta, 0]$, the Jacobian matrix reduces to its diagonal form,

explicitly,

$$J_\theta = a\begin{bmatrix} 2\cos(2\theta) & 0 & 0 \\ 0 & 2\cos(2\theta) & 0 \\ 0 & 0 & \cos(2\theta) \end{bmatrix} \tag{4.9}$$

Applying (4.7) to (4.9), we observe that, P_1 and P_2 represent a pair of attractors and P_3 and P_4 represent a pair of repellers. The topology of the phase space is exhibited in figure 16 (a). Figure 16 (b), exhibits trajectories and their evolution in phase space. As can be seen, eddies in the flow tend to align with the attracting fixed points.

The attracting fixed points. The attractors in the phase space, referred to as P_1 and P_2 in equation (4.7) , are located along the compressional principal axis of the mean gradient. These represent stationary states for the unit wavenumber vector. At these states, the

eddies in the flow obtain a temporally constant state of alignment. As per dynamical systems theory, each attractor has a "basin of attraction". Trajectories lying in this basin would, eventually, end up at the corresponding attractor. For hyperbolic flows, the basins of attraction for the two attracting states cover the entire phase space, omitting a set of measure zero, i.e. the separatrices. Thus, with reference to the physics, all eddies in the flow have a tendency to align themselves with the compressive direction of the mean gradient field.

The repelling fixed points. The repellers in phase space, referred to as P_3 and P_4 in equation (4.7), are located along the extensional principal axis. They represent highly unstable alignments for the eddies in the flow. As can be inferred, eddies aligned along the extensional direction are in an unstable state of alignment. Thus, eddies aligned with this tend to "veer off" this state, which is manifested as the repulsion in the dynamical systems analysis.

The saddle points. As can be seen in the figure 16 (a), the basins of attraction for the stationary states are demarcated by the attracting manifolds of the saddle points, namely the seperatrices. In physical terms, the seperatrices in the $[e_1, e_2, e_3]$ space represent the extensional direction of the applied mean gradient field in physical space. The presence of the seperatrices is indicative of the fact that eddies that are perfectly aligned with the extensional direction tend to align themselves perpendicular to the plane of applied strain. The saddle points, located at the "poles" of this phase space, represent states where the eddy is aligned perpendicular to the plane of mean gradient. As can be

inferred, this state of perpendicular alignment is unstable. However, eddies that are *perfectly* aligned with the extensional direction, will require a perturbation to force them off this alignment.

Classification of states. From the topology of the phase space, it can be inferred, *for almost all initial conditions* of the unit wavenumber vectors, each trajectory consummates, eventually, at either one of the stationary states. However, in the initial few time units, the trajectories are of two disparate categories:

a. the initial conditions that are initially attracted to the saddle point.
b. those that are initially attracted to one of the fixed points.

For instance, the initial conditions lying very close to the attracting manifold of the saddle will be attracted to the saddle for a considerable period. This demarcation is important, as it shall be seen that the evolution of the Fourier velocity coefficients is very different for the two cases. This classification can be mathematically expressed as,

$$\begin{aligned} &for\ |e_1| > |e_2| : the\ trajectory\ is\ attracted\ to\ the\ saddle. \\ &for\ |e_1| < |e_2| : the\ trajectory\ is\ attracted\ to\ one\ of\ the\ stationary\ states. \end{aligned}$$

In summary, the wave-vector behavior for all hyperbolic flows can be summarized as follows:

1) The unit wave-number vectors from nearly all initial conditions evolve toward attracting fixed points. This represents that fact that for hyperbolic flows, all eddies, eventually, have to align themselves with the compressional direction of the mean gradient field.

2) Wave-vectors whose components initially satisfy which $|e_1| < |e_2|$ are rapidly attracted to the fixed point. They are rendered dynamically insignificant immediately thereafter.

3) Those wave-vectors with $|e_1| > |e_2|$ experience a two-stage evolution. First, they move in phase-space toward the saddle and eventually they are attracted to the fixed point. The closer a wave-vector is to the separatrix, the longer it will be attracted toward the saddle. These wave-vectors will be dynamically active over a longer period of time. With respect to the physical space, these represent eddies in the flow that have a preponderance to align themselves perpendicular to the plane of applied shear. The degree to which these eddies are able to attain this state, depends on their initial alignment with reference to the extensional principal direction. Furthermore, as this state of alignment is unstable, minor perturbations or non-linear effects cause these to align themselves with the extensional principal direction.

4.3.1.2 Evolution of the Fourier Velocity Coefficients

The evolution of the velocity field associated with an eddy in the flow is dependent on its state of alignment with the applied mean gradient field. Based on the two types of wave-vector behavior described above, we have two categories of Fourier amplitude behavior. In figure 17 (a), the amplitude evolutions of several wave-vectors are shown

for the plane-strain mean flow. The two categories of amplitude growth are immediately evident.

1) The Fourier amplitude of wave-vectors that go directly to the fixed point (for these eddies, initially, $|e_1| < |e_2|$) experience very little growth. These are attracted to the compressive direction of the mean gradient field. Furthermore, at this state, the Fourier amplitude vector aligns itself perpendicular to the plane of applied shear, causing the Production to cease.
2) The wave-vectors that initially move toward the saddle ($|e_1| > |e_2|$) grow relatively more rapidly. These tend towards an alignment with the extensional direction, causing the aforementioned growth. As mentioned, this state of alignment would be unstable and these would be forced off such a state by perturbations. Thence, they tend towards one of the attracting stationary states.

4.3.1.3 Evolution of the Flow Statistics

In an RDT analysis, the flow field is considered in a holistic sense. Consequently, the flow statistics reflect the collective behavior of the modes, via an ensemble average. As shall be observed, the three stage evolution of the individual modes, coupled with the ensemble averaging procedure, leads to a four stage behavior for the flow statistics. Furthermore, it must be reiterated that the averaging procedure associates a weighing factor based on the kinetic energy pertaining to a single eddy. Thus, modes with high

associated kinetic energy tend to affect the flow statistics to a higher degree. As mentioned in the prior section, in a numerical simulation, all modes will end up at a stationary state wherein all of the turbulent kinetic energy is contained, solely, in the R_{33} component. This final stage is evident in figure 18 (a), where eventually, the b_{33} component goes to the requisite value. The three stages preceding this are shown in detail in figures 19, (a) and (b):

1) The first stage is a short transient, highly dependent on the set of initial conditions chosen for the study. In figure 4 (b), this would correspond to the time span: $0 < St < 2$.
2) The second stage occurs in the time period $2 < St < 8$ for the case considered in figure 19 (b). In this stage the turbulent kinetic energy is contained chiefly in R_{22} and R_{33}. This behavior can be attributed to the combined effects of the two types of modes identified in the prior sections. The R_{22} content is due to the wave-vectors moving toward the saddle and R_{33} is due to those modes being attracted to the fixed-points. Towards the end of this stage, all the modes attracted to the fixed points cease to be dynamically active as the amplitude vector is completely aligned along the 3-direction. On the other hand, those modes attracted to the saddle gain strength and begin to dominate the dynamics.
3) Stage three is onset at about $St \sim 8 - 10$ (Fig. 19 a and 19 b). The statistics are completely dominated by a few modes that are still being attracted to the saddle and hence a large fraction of the energy is resident in R_{22}.

4) When the last of wave-vectors starts its move toward the attracting fixed point, the fourth stage commences -- *St = 50* in Figure 18 (a). In order to satisfy the continuity constraint, the pressure term transfers all of the R_{22} energy into R_{33} as shown by the dominance of b_{33} beyond *St = 50*.

This four stage behavior can be seen clearly in the evolution of the turbulent kinetic energy of the flow. In figures 19, (c) and (d), the evolution of k and $\frac{dk}{dt}$ is exhibited, for the case of β=0.19. The correspondence to figure 19 (b) and the stages evidenced therein is evident. For instance, in figure 19 (d), the initial transient (0-2 St units), the second stage (2-10 St units) and the third stage (10-onwards) are clearly discernable.

4.3.2 Homogeneous Shear Flow and the Bifurcations in the System

4.3.2.1 Wavenumber Vector Dynamics

As the parameter, β, is increased from 0 towards 0.5, the attractor-repeller pairs migrate towards each other, along the equator. In the limit of the homogeneous shear flow, this migration leads to the first of the two simultaneous bifurcations that occur in the system. In the limit of the shift from strain dominated to rotation dominated flows, at the parameter value of 0.5 (or a homogeneous shear flow), the two attractor-repeller pairs collide and mutually annihilate. This constitutes the Saddle-node bifurcation manifested

in the system. This is one of the most basic mechanisms for the creation and destruction of fixed points and is found in a variety of nonlinear systems such as models for autocatalytic reactions, the synchronous flashing in herds of fireflies and others. The repercussions of this specific bifurcation occurring in the system are many-fold but only the salient features shall be highlighted in the discussion on elliptic flows. The other bifurcation present in the system materializes at the saddle points located at the poles. These undergo a saddle-center bifurcation at the same parameter value. For this case, the evolution of the unit wavenumber vector is still that of attraction to an asymptotic state of $[\pm\frac{1}{\sqrt{2}}, \mp\frac{1}{\sqrt{2}}, 0]$. However, for the case of homogeneous shear the approach to this "stationary" state is linear, and not exponential. This causes a marked change in the evolution of the dependent variables.

4.3.2.2 Evolution of the Fourier Velocity Coefficients

The evolution of the Fourier velocity coefficients for the Homogeneous shear case is markedly different from the generic hyperbolic flows. Despite the fact that for all these flows, the kinetic energy is growing (i.e., the flow is unstable), the growth in the homogeneous shear case is a non-modal growth. Explicitly, the modal kinetic energy exhibits polynomial and not exponential growth. Figure 20 (a) shows this non-modal growth for a specific mode in such a flow.

4.3.2.3 Evolution of the Flow Statistics

As in other cases discussed till now, the ensemble kinetic energy reflects the behavior of the individual modes and exhibits growth, albeit, non-exponential. This is exhibited in figure 20 (b). As can be observed, the growth in the turbulent kinetic energy is non-exponential and is almost linear, except for a brief transient.

Vis a vis the Reynolds stress anisotropies, the set $\{b_{11}, b_{22}, b_{33}\}$ approaches the asymptotic state of $[b_{11}, b_{22}, b_{33}]_{asymptotic} = [\frac{1}{6}, \frac{1}{6}, -\frac{1}{3}]$ at a much slower time scale, as seen in figure 20 (b). In case of the generic hyperbolic flow, we had observed stationary states for the anisotropy tensor. However, for the homogeneous shear flow, the flow statistics never reach a stationary state. This asymptotic approach is due to the fact that the equation set is Lipchitz continuous and furthermore, the attraction for the wavenumber vector is linear and not exponential. The shift in the asymptotic state of the Reynolds stress anisotropies and the turbulent kinetic energy of the flow is due to the change in the mechanism of flow instability.

4.3.3 Elliptic Flows

4.3.3.1 Wavenumber Vector Dynamics

Considering the regime of elliptic flows, i.e. for β values between 0.5 and 1.0, the phase space for the unit wavenumber vector, a compact manifold, is devoid of any attractors or repellers. *Thus, applying the Poincare-Bendixson theorem, all the wave number trajectories must approach closed orbits.* Consequently, in elliptic flows, wavenumber vectors in the system exhibit periodic oscillations.

The invariant sets just after the occurrence of the bifurcation are shown in figure 20 (a), for the representative case of β=0.51. As can be observed, the closed orbits are highly distorted in the region of the saddle-node remnant. In absence of this distortion, they would have been simple closed circles, akin to those observed for vortical flow. Thus, instead of elementary circular paths, the closed orbits are elongated ellipses on the sphere. Mathematically, this is a consequence of the fact that the solutions for the unit wavenumber vector are elliptic integrals, albeit complete. As the parameter β is increased to unity (representing a state of pure rotation), the distortion in the closed orbits wanes and they approach closed, circular paths, as seen in figures 20, (a) to (c).

4.3.3.2 Evolution of the Fourier Velocity Coefficients

The banded nature of the elliptic instability has been mentioned at the beginning of this section and has been extensively discussed in the germane references contained herein. The result of this phenomenon is a diametric difference of the energy of a specific mode based on its initial alignment. Such phenomena are amenable to Floquet analysis and a corresponding Floquet stability diagram is presented in figure (21), for a specific set of conditions. Effectively, if the initial alignment of the eddy lies in the unstable region (in the figure, the shaded region), its kinetic energy grows. Else the kinetic energy shows quasiperiodic behavior and remains bounded.

4.3.3.3 Evolution of the Flow Variables

Due to the growth in the kinetic energy of select modes, the turbulent kinetic of the elliptic flow grows, if the flow has any modes with their initial alignments in the band of instability. Further, due to the periodic nature of the coefficients in equation (4.1), the evolution of the Reynolds stress anisotropies has an oscillatory character. This is exhibited in figure 18 (c). As can be observed, the evolution of the Reynolds stress anisotropies is best characterized as a two-stage process: an initial stage of attraction towards a finite mean value, followed by the second stage of oscillation about this mean. With regard to the behavior of the Fourier velocity coefficients, the first stage represents the development of the dominance of the unstable modes on the flow statistics, over the

effect of the bounded modes. Once this is established, the second stage represents the sustention of this dominance.

4.4 Dynamical Properties versus Modeling Tenets

Classical approaches use the Reynolds stress and mean-velocity gradient field as the basis for representing rapid pressure-strain correlation. This is due to the lack of easy availability of wave vector information. The classical representation is thus :

$$\frac{1}{k}\Pi_{ij}^{(r)} = S_{pq}[Q_1\delta_{ip}\delta_{jq} + Q_2(b_{ip}\delta_{jq} + b_{jp}\delta_{iq} - \frac{2}{3}b_{pq}\delta_{ij}) + Q_3 b_{pq}b_{ij} + Q_4(b_{iq}b_{jp} - \frac{1}{3}b_{pk}b_{kq}\delta_{ij})$$
$$+Q_5 b_{pk}b_{kq}b_{ij} + (Q_5 b_{pq} + Q_6 b_{pl}b_{lq})(b_{ik}b_{kj} - \frac{1}{3}II_a\delta_{ij})]$$
$$+\Omega_{pq}[Q_7(b_{ip}\delta_{jq} + b_{jp}\delta_{iq}) + Q_8 b_{pk}(b_{jk}\delta_{iq} + b_{ik}\delta_{jq}) + Q_9 b_{pk}(b_{jk}b_{iq} + b_{ik}b_{jq})] \tag{4.10}$$

, here, Q_i are scalar functions of the invariants of the imposed strain and rotation rates along with those of the Reynolds stress anisotropy tensor. Except for a few notable exceptions, such as Ristorcelli et al. (1995) and Girimaji (2000), these are considered constants, whose values are assigned from algebraic relations and numerical simulations. Thus, the Reynolds stress transport equations, under the auspices of classical closure schemes, represent a dynamical system in a state space composed of the Reynolds stress tensor components. In this section, we present the various challenges posed by elliptic flows to classical tenets of rapid pressure-strain correlation modeling.

4.4.1 The Requirement for Additional Tensors

In their paradigm of research, Reynolds, Kassinos and co-workers (Reynolds (1989), Kassinos et al. (2001), Kassinos and Reynolds (1994))have claimed that the Reynolds stress tensor components do not form an adequate basis for one point second moment closures. Their assertion is based on the incorrect behavior predicted by the classical models for rapid rotation and additionally, the requirement for material indifference to mean rotation about the axis of independence of two-dimensional turbulence. For a complete basis, additional tensors such as Dimensionality, Stropholysis and Circulicity would be required for describing the structure of the turbulent flow field. The requirement for these tensors, though mathematically rigorous, is impracticable, from an engineering perspective. These tensors cannot be measured in experiments and thus, do not from a part of the data set that might be possibly available for engineering purposes.

With reference to the present investigation, the aforementioned tensors consist of second and higher order correlations between the $\{e_i\}$ *and* $\{\hat{u}_i\}$ vectors. With regard to the *requirement for these tensors for closure modeling*, the dynamics of the wavenumber play an essential role in the fidelity of the classical models and, synchronically, that of the assumptions of the classical modeling framework.

For hyperbolic flows, it has been observed in Section III, that almost all wavenumbers are exponentially attracted to a stationary state. The set of initial conditions which is not

in accord with this behavior is inconsequential, both numerically and physically. In simulations, the numerical error would force the trajectory off this set. In real world flows, the same would be done by the non-linear effects. Thus, within a very short span of time, irrespective of initial conditions, the state of all unit wavenumber vectors can be approximated by a stationary value. The coefficients Q_i in the model expression (4.7) subsume this wavenumber state information. Due to the stationarity in the wavenumber behavior, all unit wavenumber vectors reach an identical value and thus, the Reynolds stress tensor *emerges* as an adequate basis for modeling. With respect to the extant modeling practice, the "tuning" of the coefficients is tantamount to approximating this stationary value of the wavenumber vector.

In summation, for hyperbolic flows, the structure of turbulence evolves in a manner so as to make information regarding the turbulence structure (or dimensionality) non-essential for modeling purposes. This causes the ostensible success of classical modeling approaches for hyperbolic flows.

As the mean flow changes from hyperbolic to elliptic, there is a marked change in the action of pressure, manifested in the nature of flow stability. This shift represents a bifurcation in the Reynolds stress transport equations. To ensure concurrence between the system's behavior and the model's predictions, RPSC models would need to capture the *location* and the *nature* of this bifurcation. With regard to this, the location of the bifurcation is discussed first. It has been shown that popular models are unable to predict

the occurrence of this shift at the point of homogeneous shear flow. As has been proved in this study, the bifurcation occurs in the equations governing the wavenumber evolution. The basis utilized in the classical second moment closure framework does not include any information from this set. Consequently, models under the aegis of the classical framework cannot capture the location of this shift in behavior. To discuss this nuance in the paradigm of Reynolds, Kassinos and coworkers, we take cognizance of the structure of the turbulent flow field. The classical framework heeds information about the turbulent velocity components (componentality) and not the structure of the turbulent flow field (dimensionality). In the passage from hyperbolic flows to elliptic, the response of the coherent motions in the flow to the applied strain field changes. For hyperbolic flows, the eddies in the flow align themselves with the compressional principal axis. However, for elliptic flows, the eddies in the flow exhibit periodic motion along complicated elliptical paths. Bereft of the information concerning turbulent structure, the classical models are oblivious to this fundamental change in the behavior of the flow structure and are thus, unable to mimic it. The nature of this bifurcation and its consequences will be discussed with respect to the linearity requirement, in the next section.

4.4.2 Linear Dependence of RPSC on Reynolds Stress

In the Rapid Distortion Limit, the pressure strain correlation is completely determined by the fourth order tensor, M_{ijkl}. Thus, the expression for the rapid pressure strain correlation must be linear in the Reynolds stresses, as the tensor M is linear in the spectrum. Reynolds has argued in favor of linearity observing that a field that is the sum of two uncorrelated fields should give a pressure stain correlation that is equal to the sum of the pressure strain correlation of the respective fields. As has been observed earlier, these arguments are offset by the need for the Reynolds stress tensor to satisfy realizability which requires a non-linear expression.

Furthermore, elliptic flows pose a challenge to the linearity requirement. Considering the anisotropy evolution for elliptic flows, exhibited in figure 18 (c), it is observed that the behavior of the Reynolds stress anisotropies for RDT-B is perfectly oscillatory right from the initiation of the simulation. In dynamical systems theory, such behavior would be classified as linear oscillations (referring to the linearity of the governing equations). In contrast, the evolution of the anisotropies for RDT-NS has an initial transient followed by oscillatory behavior. In the transient, the values of the anisotropies approach the mean value about which they oscillate. This difference in the dynamics of RDT-B and RDT-NS for elliptic flows is of crucial importance. The nature of behavior observed in RDT-NS is indicative of the presence of an attracting limit cycle. Therein lays another

fundamental direction from dynamical systems theory which states that limit cycles can only be observed in systems governed by nonlinear differential equations. Thus, for rotation dominated flows, the behavior of the Reynolds stress anisotropies is of a nature that cannot be replicated using linear equations for their evolution. Additionally, it is the role of rapid pressure to cause the aforementioned nonlinear, limit cycle behavior. Thus, in the preceding steps, the analysis has identified the need for nonlinearity and also the location of the term that contains it. This requirement for non-linear terms arises due to the nonlinearity of the equations governing the behavior of the unit wavenumber vector. After the saddle-node bifurcation in the same, the characteristic time-scaling of the oscillations occurs. Regarding the Reynolds stress tensor as a complete basis, this would be perceived as an Infinite period bifurcation in the same and mimicking this would require an expression that is nonlinear in the Reynolds stress tensor components. According to Pope, the *ideal* model for pressure strain correlation should be linear in the components of the Reynolds stress and mean gradient tensors. This schism between the mathematical guidelines and engineering needs arises due to the lack of wavenumber information in the classical modeling framework.

In summary, under the assumptions of Classical Reynolds stress closure schemes, the correct behavior of the Reynolds stress tensor in elliptic flows obligates a rapid pressure stain model that is nonlinear in the Reynolds stress anisotropy components.

4.4.3 The Constraint of Constant Coefficient Models

In the classical second moment closure framework, the model coefficients Q_i are scalar functions of the invariants of the Reynolds stress anisotropy tensor. With few exceptions, these are assigned constant values based on numerical simulations, the Crow's constraint etc. As has been mentioned by the authors and is evident from the equations (4.1), (4.2) and (4.3), these incorporate the information regarding the ensemble behavior of the second and higher order correlation between the $\{e_i\}\, and\, \{\hat{u}_i\}$ vectors. In elliptic flows, the wavenumber vector and consequently, the Fourier amplitude vector have oscillatory solutions. Thus, the model coefficients should reflect this and exhibit periodic behavior. Therefore, constant coefficient models, dictated by practice and not physics, are deficient for elliptic flows.

However, a solution for this deficiency is not facile. Considering solely the information in wavenumber space included in the coefficients, to completely characterize a state of oscillation, of the generic form $x = A\sin(\omega t + \sigma)$, one requires three functions, namely amplitude, frequency and phase. The frequency of oscillation is an explicit function of the parameter, β. However, the determination of the amplitude and the phase require the knowledge of the initial conditions of the turbulent flow field. Thus, to approximate the oscillatory behavior shown in elliptic flows, the wavenumber space information needs to be a part of the basis utilized in the model.

In summation, due to the lack of wavenumber space information in the basis, constant coefficient models are deficient for modeling purposes, especially for elliptic flows.

CHAPTER V

TOWARDS A UNIVERSAL RPSC MODEL

5.1 Introduction

In addition to the engineering requirement for accuracy in its predictions, there are other guidelines decreed on a pressure strain correlation model, via mathematics, physics and convention. At this juncture, we commence by enumerating the same. According to established mathematical theory, the *ideal* RPSC model would be (Pope (2000)):

a) linear in the mean velocity gradients.

b) linear in the Reynolds stresses.

c) satisfying material frame indifference in the limit of two dimensional turbulence.

d) realizable, for all times and for different imposed flows.

e) determined by the tensor M_{ijkl}.

Additionally, under the auspices of the classical second moment closure framework,

f) the RPSC should be completely described in terms of the Reynolds stress and the mean gradient tensors.

As has been proved in this communication and argued in prior investigations, the classical framework puts an exorbitant constraint on the modeling procedure, insisting

that the task of modeling be carried out with an incomplete basis. Due to this conflict, the complete set of properties of an ideal model, (a) to (e), cannot be satisfied for a model adhering to the classical framework, i.e., (f), for all regimes of flows. In hyperbolic flows, wherein the RDT system goes to a fixed point and the basin of attraction includes nearly all initial wave-vectors, the classical RSPC modeling premises are adequate. However, as has been shown, elliptic flows do pose three important challenges to classical modeling principles:

(i) the non-stationary nature of the wavenumber vector solutions cause the need for the coefficients, Q_i, to be periodic functions as well. Constant coefficient models cannot simulate the dynamics of elliptic flows. Further, replication of these functions, Q_i, requires the dimensionality tensor to be an explicit part of the basis.

(ii) due to the flow instability manifested by the system, the unstable modes are the ones that determine the system's behavior. However, due to the "banded" nature of the elliptic instability, the wavenumber space information (or the initial conditions of the flow field) needs to be integrated into the model.

(iii) the oscillatory behavior exhibited by the Reynolds stress anisotropies is of a nature that cannot be replicated via simple linear expressions, leading to a disagreement between physical guidelines and engineering needs.

These present important conflicts between model capability in elliptic flows, on one hand, and reasonable closure premises on the other. To find a physically adequate and practically viable resolution of this conflict, we propose the following compromise.

It is first noted from DNS studies as well as RDT results that the amplitude of the elliptic flow limit cycle oscillations is somewhat small compared to the absolute value of its mean value. Therefore, it may be reasonable to approximate the RDT elliptic behavior to that of a fixed point located at the center. This is schematically displayed in figure 22, where such a mean value prediction is fitted to the data of Blaisdell and Shariff (1996). This approximate physics can be duplicated by a RPSC closure which is linear in Reynolds stress. Further, the dimensionality information of this center-tuned fixed point can be used for model closure, alleviating the need for precise wave-vector information for description of the banded instability.

Additionally, vide Chapter IV, the evolution of flow statistics follows distinct stages. For hyperbolic flows, this is a three stage process. Out of the three stages, the brief initial stage is highly dependent on the alignment of the modes in the flow. Without the information of the structure of the turbulent flow, replicating this transient is not possible. Furthermore, in the third stage, vide figure 18 (a), the energy is transferred to the u_3 component. Capturing these sudden shifts, with a high degree of accuracy, is still not possible within the classical second order closure modeling framework. Instead, this investigation focuses on the early evolution of the Reynolds stress anisotropy tensor, specifically till the vicinity of twenty non-dimensional time steps. This represents the

duration with a high relevance, as accurate predictions are sought in the same for engineering purposes. Additionally, beyond this duration, the validity of the assumptions of RDT is questionable, owing to the flow instability. For elliptic flows, the very short, initial transient is still not captured due to the same reasons as above.

5.2 Formulation

Forthwith, we initiate the development of such an RPSC model. The model development can by no means be regarded as complete. The main purpose is to demonstrate that the compromise proposed in the previous section can lead to improved behavior in elliptic flows. Validation over a wide range of flows must be conducted before the model developed here can be used in engineering computations.

We consider classical quasi-linear pressure strain correlation model of the form:

$$\Pi_{ij} = C_1 P b_{ij} + C_2 k S_{ij} + C_3 k (b_{ik} S_{kj} + b_{jk} S_{ki} - \frac{2}{3} b_{mn} S_{mn} \delta_{ij}) + C_4 k (b_{ik} W_{kj} + b_{jk} W_{ki}) \quad (5.1)$$

The model coefficients C_i, have to be determined. The conclusions of this study have established that a constant coefficient model cannot replicate the dynamics of elliptic flows. Thus, for the purposes of this investigation, the model coefficients are assumed to be variable. Based on equation (4.8), the anisotropy evolution equation can be derived from the corresponding Reynolds stress equation as,

$$\frac{db_{ij}}{dt} = L_1 b_{ij} b_{mn} S_{mn} + L_2 S_{ij} + L_3 (b_{ik} S_{kj} + b_{jk} S_{ki} - \frac{2}{3} b_{mn} S_{mn} \delta ij) + L_4 (b_{ik} W_{kj} + b_{jk} W_{ki})$$

where, (5.2)

$$L_1 = C_1 + 2,\ L_2 = \frac{C_2}{2} - \frac{2}{3},\ L_3 = \frac{C_3}{2} - 1,\ L_4 = \frac{C_4}{2} - 1.$$

Based on representation theory, the comprehensive and physically correct polynomial form of the Reynolds stress anisotropy, for two-dimensional mean flows, is (Girimaji (2000)),

$$b_{ij} = G_1 S_{ij} + G_2 (S_{ik} W_{kj} - W_{ik} S_{kj}) + G_3 [S_{ik} S_{kj} - \frac{1}{3}(1-\beta)\delta_{ij}] \quad (5.3)$$

In this approach, the value of the parameter L_1 is fixed at two. This is in line with the fundamental assumptions of RDT and further, agrees with the values in the LRR model. The coefficients L_2, L_3 *and* L_4 are allowed to vary.

Based on the equations (5.3) and (5.2), there is a non-invertible mapping from the set $\{G_i\}$ to the set $\{L_i\}$, at any equilibrium value of b_{ij}, where it achieves a stationary state. This is defined as,

$$\begin{aligned} L_2 &= -2(1-\beta)G_1^2 - 4\beta(1-\beta)G_2^2 + \frac{(1-\beta)^2}{3} G_3^2 \\ L_3 &= -(1-\beta)G_3 \\ L_4 &= 2(1-\beta)G_2 \end{aligned} \quad (5.4)$$

This map is defined in a unique manner everywhere, except for the case of a pure rotational flow. Additionally, at every fixed point of the anisotropy, there is a one-to-one

transformation between the set $\{G_i\}$ and the basis $\{b_{11}, b_{22}, b_{12}\}$ for the Reynolds stress anisotropy tensor. This is defined as,

$$
\begin{aligned}
b_{11} &= aG_1 + [a^2 - \frac{(1-\beta)}{3}]G_3 \\
b_{22} &= -aG_1 + [a^2 - \frac{(1-\beta)}{3}]G_3 \\
b_{12} &= -2abG_2 \qquad\qquad (5.5)
\end{aligned}
$$

where,

$$a = \sqrt{\frac{1-\beta}{2}}, b = \sqrt{\frac{\beta}{2}}$$

On defining the inverse transform, at each stationary state,

$$
\begin{aligned}
G_1 &= \frac{b_{11} - b_{22}}{2a} \\
G_2 &= \frac{-b_{12}}{2ab} \qquad\qquad (5.6) \\
G_3 &= \frac{b_{11} + b_{22}}{2[a^2 - \frac{(1-\beta)}{3}]}
\end{aligned}
$$

The inverse map is ill defined for the cases of plane strain and pure rotation. For these flows, the transform defines an indeterminable form.

This investigation has laid out the methodology for locating stationary states corresponding to the mean of the Reynolds stress anisotropy evolution for elliptic flows. After the fixed point values are determined for the Reynolds stress anisotropy tensor, the corresponding $\{G_i\}$ values are calculated at these stationary states using equation(5.5).

These are used to compute the values of $\{L_i\}$ using the relation expressed in equation(5.6).

The results of this exercise are exhibited in the figures 23, (a) to (c). The computed $\{L_i\}$ for different values of the ellipticity parameter, β, are plotted against the corresponding values of popular linear and quasi-linear models such as that of LLR and SSG, respectively. For the parameter $\{L_4\}$, the corresponding curve for the variable SSG model, envisaged in Girimaji (2000) are plotted as well. As can be observed from the aforementioned figures, the $\{L_i\}$ values indicated by RDT appear to be very amenable to approximation via smooth functions of the ellipticity parameter. Furthermore, the $\{L_i\}$ curves, thus conceptualized, represent minor corrections to the magnitude of the coefficients of the popular models, at any β value. The departure from the convention of constant coefficient models to such an engineered variable coefficient model, harbors the possibility to afford better RPSC models (vis a vis their fidelity) while still adhering to the classical second moment closure framework. Videlicet the guidelines, (a) to (f), enumerated at the beginning of this section, such a model would conform to (f), by definition, while still abiding by a maximal set of properties of an ideal model. Thus, it would represent a close conception of an ideal model, within the classical modeling framework.

As has been mentioned, to ensure concurrence between the system's behavior and the model's predictions, RPSC models would need to capture the *location* and the *nature* of the bifurcation in the transition from hyperbolic to elliptic flows. The requisite bifurcation diagram is presented as figure 25. Addressing the dynamics of the b_{22} and b_{12} components of the anisotropy tensor, the diagram represents fixed point behavior by a solid line and oscillatory behaviors by a dashed line, along the mean of the oscillations. Within the proposed modeling framework, the present model always exhibits stationary, fixed point behavior. As is exhibited in figure 26, the predictions of this model are within engineering accuracy. With respect to the LRR model's dynamics, the bifurcation is predicted to occur at β=0.75. Thus, LRR is unable to capture even the location of this bifurcation. Similarly, the SSG model predicts the location of the bifurcation at β=0.65. Thus, it is observed that these popular models are unable to capture location of the transition of the behavior of the system correctly. As the incipience of the bifurcation is in wavenumber space which is not part of the constituent basis under the classical modeling framework, the nature of the bifurcation can not be predicted by such models. Thus, it is observed that the lack of success of the models for elliptic flows is due to the flaws in the classical modeling framework. Both LRR and SSG, after their respective bifurcations, predict linear oscillations, as seen in figures 26, (a) and (b). The bifurcation behavior of these models is analyzed in Girimaji (2000) and the interested reader is referred to the same. The present model retains a fixed point attractor and allows the location of the same to be a function of the parameter value. This enables it to match the behavior of the RDT data for both hyperbolic and elliptic flow regimes.

5.3 Concluding Remarks

The aim of this facet of the present investigation is to revisit the classical pressure strain correlation modeling framework in the context of elliptic flows. Restricting the scope of the study to the rapid part of the pressure strain correlation for two-dimensional mean gradient fields, exigent questions regarding the structure of the models are addressed.

The paradigm of analysis considers the Reynolds stress transport equations to govern the evolution of a dynamical system, in a state space composed of the Reynolds stress tensor components. This dynamical system is scrutinized via the identification of the invariant sets and the bifurcation analysis. Along the maxim of "understanding before prediction", this allows for a deeper insight into the behavior of pressure, thus aiding in its modeling. Based on the comprehension developed in the preceding section, the classical pressure strain correlation modeling approaches are revisited. Their shortcomings along with their successes are articulated and explained, mathematically and from the viewpoint of the governing physics. Some of the salient issues addressed include, but are not limited to, the requisite nature of the model, viz. a linear or a nonlinear structure, the success of the extant models for hyperbolic flows, their inability to capture elliptic flows, etc. Through this analysis, the schism between mathematical and physical guidelines and the engineering approach, at present, is substantiated. It is explained that this disagreement is due to the fact that Reynolds stress do not form an adequate basis for representing the rapid pressure strain physics in elliptic flows.

Based on the conclusions of this analysis, this investigation outlines the methodology to

develop a model for the RPSC that is universal and accurate, as well as computationally simple. This represents the best conception of an ideal model, abiding by the classical modeling framework. The relevant mathematical equations for the same are illustrated and applied, to endorse the verity of this approach.

CHAPTER VI

CONCLUSIONS

This investigation was aimed at the development of a model for the Rapid Pressure Strain Correlation of turbulence. The intent was to institute a model that is applicable to both the hyperbolic, as well as the elliptic flow regimes. Additionally, to have a tangible contribution, the model had to be of a form that would be applicable for engineering purposes. These represented constraints on the complexity of the model and the physical variables that could be inducted into the framework of the same.

Before delving into the modeling facet, the study aimed at developing an improved understanding of the role of pressure in the specific flow regimes. To this end, the behavior of plane, quadratic flows was analyzed, from the paradigm of linear hydrodynamic stability theory. In the stability analysis, the role of pressure in the initiation, suppression and protraction of flow instabilities was identified and explained. This was shown that the redistribution of the turbulent kinetic energy, based on the fulfillment of the continuity condition, led to a state of supercritical stability for hyperbolic flows, while the same action by pressure caused a secondary instability in elliptic flows. Starting with these observations, it was proved that pressure suppresses the hyperbolic instability and initiates the elliptic instability. For the case of homogeneous shear flow, pressure does not affect the nature of the stability problem, which is a case of algebraic, non-modal instability. The relevant governing equations for

the problem were derived, in physical and Fourier space, and the concomitant dynamical systems analysis was performed. It was shown that the fundamental difference between the behavior of hyperbolic and elliptic flows arises due to a Saddle-node bifurcation occurring in the system at the point where the flow is in a state of homogeneous shear. This was correlated to the underlying physics of the problem, wherein it was shown that the bifurcation arises due to the relative interaction between the rate of rotation and the rate of strain tensors. Explicitly, for elliptic flows, this interaction causes the eddies in the flow field to be in a state of rotation, along distorted paths. The dynamics and the ramifications of this behavior were established and the mechanism, that is, the Intercomponent Energy Transfer was explained.

With regard to Rapid Pressure Strain Correlation modeling, it was proved that many of the assumptions inherent to the classical modeling approach were incorrect. It has been known amongst the practitioners in this field that the second moment framework has flaws and is an engineering tool. In this study, these shortcomings were addressed, sequentially, and the rationale responsible for their performance, or the lack thereof, was explained, mathematically. It is shown that within the aegis of this classical closure scheme, the prediction of elliptic flows is highly unfeasible, from a mathematical perspective. In summary, some of the key issues addressed include the requisite nature of the model, viz. a linear or a nonlinear structure, the success of the extant models for hyperbolic flows, their inability to capture elliptic flows and the use of RDT simulations to validate models. Through this analysis, the schism between mathematical and physical

guidelines and the engineering approach, at present, is substantiated. As can be observed, besides addressing the framework of the classical modeling approaches, the investigation questions the methodology adopted to validate the same.

Beyond this, a rapid pressure strain correlation model was developed. This adheres to the classical framework and yet offers excellent prediction of the evolution of the Reynolds stress anisotropies. Additionally, the complexity of this model is not more than the nominations being used at present in the engineering community. The performance of the same was compared against other nominations for the entire spectrum of flows that are germane for this research.

REFERENCES

Bayly, B.J., 1986 Three-dimensional instability of elliptical flow. *Phys. Rev. Letters,* **57**(17), 2160-2163.

Becker, L.E. & McKinley, G.H., 2000 The stability of viscoelastic creeping plane shear flows with viscous heating. *J. Non-Newt. Fluid Mech.* **92**, 109-133.

Blaisdell, G. A. & Shariff, K. 1996 Simulation and modelling of elliptic streamline flow. Center for Turbulence Research, Proc. Summer Program 1996.

Bradshaw, B., 1972 The understanding and prediction of turbulent flow. *Aeronaut. J.* **76**, 403-418.

Bradshaw, B., 1997 The understanding and prediction of turbulent flow-1996. *Int. J. Heat Fluid Flow,* **18**, 45-54.

Brasseur, J.G. & Lee, M.J. 1987 Local structure of intercomponent energy transfer in homogeneous turbulent shear flow. Proc. 1987 Summer Program**,** Center for Turbulence Research Report.

Brasseur, J.G. & Lee, M.J. 1988 Pressure-strain-rate events in homogeneous turbulent shear flow. Proc. 1988 Summer Program**,** Center for Turbulence Research Report.

Cambon,C., Benoit, J.P., Shao, L. & Jacquin,L. 1994 Stability analysis and large-eddy simulation of rotating turbulence with organized eddies. *Journal of Fluid Mechanics,* **278**, 175-200.

Cambon, C., & Scott, J.F., 1999 Linear and nonlinear models of anisotropic turbulence. *Ann. Rev. Fluid Mech*. **31**, 1-53.

Caulfield, C.P. & Kerswell, R.R., 2000 The non-linear development of three-dimensional disturbances at hyperbolic stagnation points: A model of the braid region in mixing layers. *Phys. Fluids* **12**(5), 1032-1043.

Choi, H. & Lumley, J. 2001 The return of isotropy of homogeneous turbulence. *J. Fluid Mech*. **436**, 59-84.

Chou, P.Y., 1945 On velocity correlations and the solutions of the equations of turbulent fluctuation. *Quart. Appl. Math*. **3**, 31-44.

Craik, A.D.D. & Criminale, W.O., 1986 Evolution of Wavelike Disturbances in Shear Flows: A Class of Exact Solutions of the Navier-Stokes. *Proc. R. Soc. London* A **406** , 13-26.

Crow, S. C., 1968 Viscoelastic properties of fine-grained incompressible turbulence. *J. Fluid Mech*. **33**, 1-20.

Friedlander, S. & Vishik, M.M., 1991 Instability criteria for the flow of an inviscid incompressible fluid. *Phys. Rev. Letters*, **66**(17), 2004-2206.

Girimaji, S.S., 2000 Pressure strain correlation modeling of complex turbulent flows. *J. Fluid Mech.* **422**, 91-122.

Girimaji, S.S., Jeong, E. & Poroseva, S.V. 2003 Pressure-strain correlation in homogeneous anisotropic turbulence subject to rapid strain-dominated distortion. *Phys. Fluids* **15**, 3209-3222.

Girimaji, S.S., O'Neil, J.R. & Yu,D., 2006 Rapid distortion analysis of homogeneous turbulence subjected to rotating shear. *Phys. Fluids* **18**, (085102) 1-13.

Hallback, M., Sjogren, T. & Johansson,A.V. 1993 Modelling of intercomponent transfer in Reynolds stress closures. *Turbulent Shear Flows IX*.

Hanifi, A. & Henningson, D.S., 1998 The compressible inviscid algebraic instability for streamwise independent disturbances. *Phys. Fluids* **10**(8), 1784-1786.

Hunt, J.C.R & Carruthers, D.J., 1990 Rapid distortion theory and the 'problems' of turbulence. *J. Fluid Mech*. **212**, 497-532.

Johansson, A.V. & Hallback,M. 1994 Modelling of rapid pressure-strain in Reynolds-stress closures. *J. Fluid Mech*. **269,** 59-90.

Kassinos, S.C., Reynolds, W.C. & Rogers, M.M., 2001 One-point turbulence structure tensors. *J Fluid Mech.,* **428**, 213-248.

Kerswell, R.R., 2002 Elliptical instability. *Ann. Rev. Fluid Mech*. **34**, 83-113.

Kassinos, S.C. & Reynolds, W.C., 1994 A structure based model for the rapid distortion of homogeneous turbulence. Stanford University Technical Report No. TF-61.

Lagnado, R.R., Phan-Thien, N. & Leal, L.G., 1983 The stability of two-dimensional linear flows. *Phys. Fluids* **27**(5), 1094-1101.

Landahl, M.T., 1980 A note on an algebraic instability of inviscid parallel shear flows. *J. Fluid Mech.*, **98**(2), 243-251.

Launder, B.E., Reece, G. & Rodi, W., 1975 Progress in the development of a Reynolds stress turbulence closure. *J. Fluid Mech*. **68**, 537-566.

Launder B. E., Tselepidakis, D.P. & Younis, B.A., 1987 A second-moment closure study of rotating channel flow. *J. Fluid Mech.,* **183**, 63-75.

Lumley, J. 1978 Computational modelling of turbulent flows. *Adv. Appl.Mech*. **18**, 124-176.

S. B. Pope, 2000 *Turbulent Flows.* Cambridge University Press.

Pierrehumbert, R.T., 1986 Universal short-wave instability of two-dimensional eddies in an inviscid fluid. *Phys. Rev. Letters*, **57**(17), 2157-2159.

Reynolds, W. C. & Kassinos, S. C., 1995 A one-point model for the evolution of the Reynolds stress and structure tensors in rapidly deformed homogeneous turbulence. *Proc. R. Soc. Lond. A* **451**, 87-104.

Reynolds, W.C., 1989 Effects of rotation on homogeneous turbulence. *10th Australasian Fluid Mechanics Conference.*

Reynolds O., 1895, On the dynamical theory of incompressible viscous fluids and the determination of the criterion. *Philos. Trans. R. Soc*. **186**, 123-164.

Ristorcelli, J.R., Lumley, J.L. & Abid, R., 1995 A rapid pressure covariance representation consistent with the Taylor-Proudman theorem materially frame indifferent in the two-dimensional limit. *J. Fluid Mech*. **292** (1995), 211-248.

Rotta, J., 1951 Statistische theorie nichthomogener turbulenz. *Z. Phys*. **129** (1951), 547-560.

Sagaut, P. & Cambon, C. 2008 *Homogeneous Turbulence Dynamics.* Cambridge University Press.

Salhi, A., Cambon, C. & Speziale, C.G., 1997 Linear stability analysis of plane quadratic flows in a rotating frame with applications to modeling. *Phys. Fluids* **9**(8), 2300-2309.

Sjogren, T., Johansson, A.V., 2000 Development and calibration of algebraic nonlinear models for terms in the Reynolds stress transport equations. *Phys. Fluids* **12** (6), 1554-1572.

Speziale, C.G., Sarkar, S. & Gatski, T.B. 1991. Modelling the pressure–strain correlation of turbulence: An invariant dynamical systems approach. *J. Fluid Mech,* **227**, 245-272.

S. Strogatz, 1994, *Nonlinear Dynamics and Chaos: With Applications to Physics, Biology, Chemistry and* Engineering. Addison-Wesley, Reading, MA.

Van Slooten, P.R., Pope, S.B., 1997 PDF modeling for inhomogeneous turbulence with exact representation of rapid distortions. *Phys. Fluids* **9**, 1085-1105.

Waleffe, F., 1990 On the three-dimensional instability of strained vortices. *Phys. Fluids* A, **2**(1), 76-80.

APPENDIX A

FIGURES

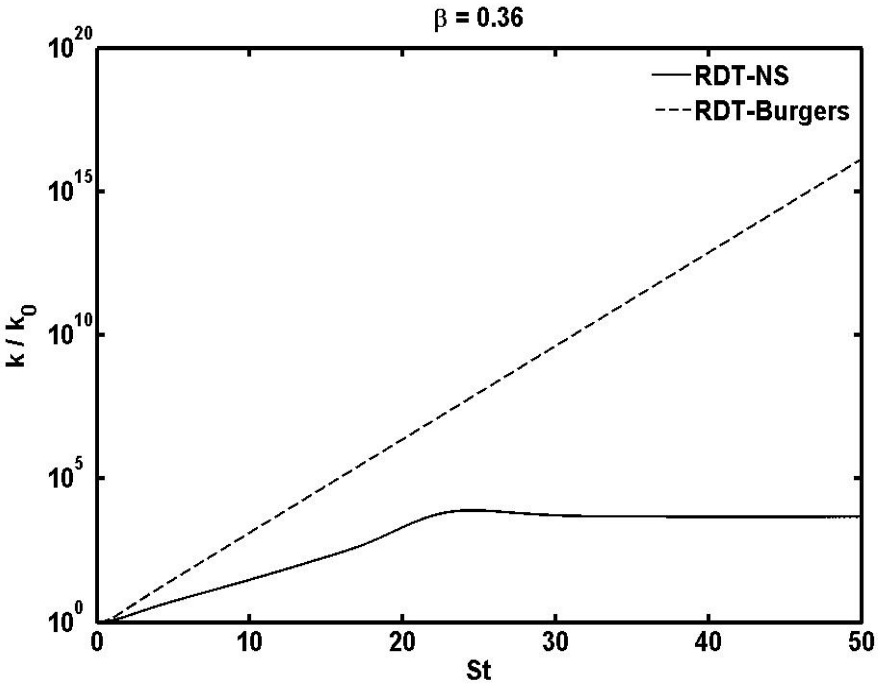

Figure 1 (a) Evolution of kinetic energy for a representative hyperbolic flow.

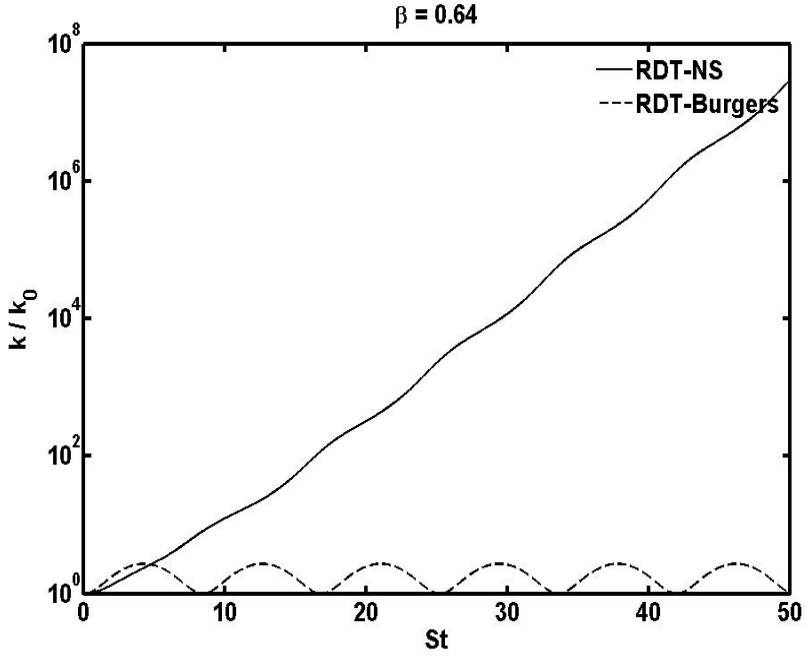

Figure 1 (b) Evolution of kinetic energy for a representative elliptic flow.

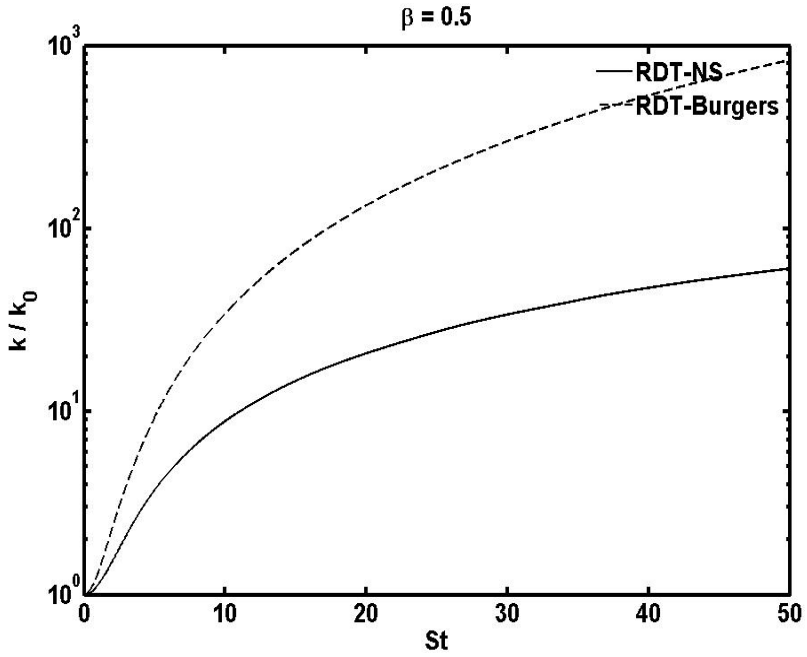

Figure 1 (c) Evolution of kinetic energy for the homogeneous shear flow.

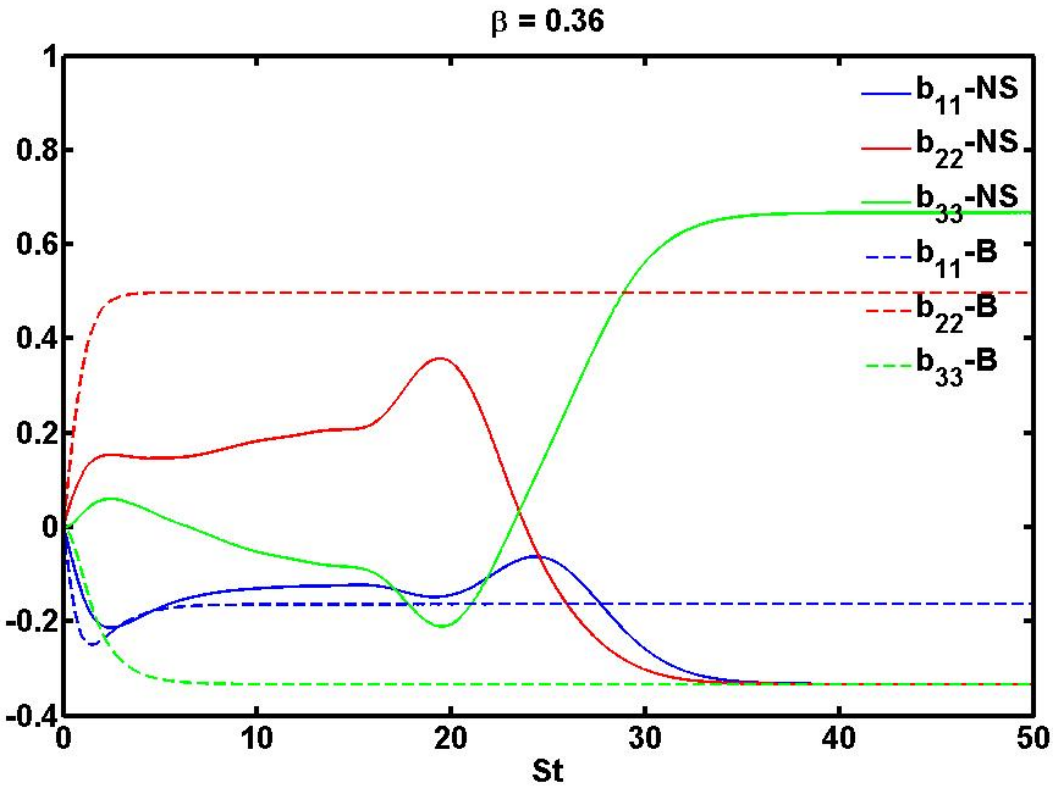

Figure 2 (a) Evolution of the anisotropy of the covariance of the perturbation velocities for a representative hyperbolic flow.

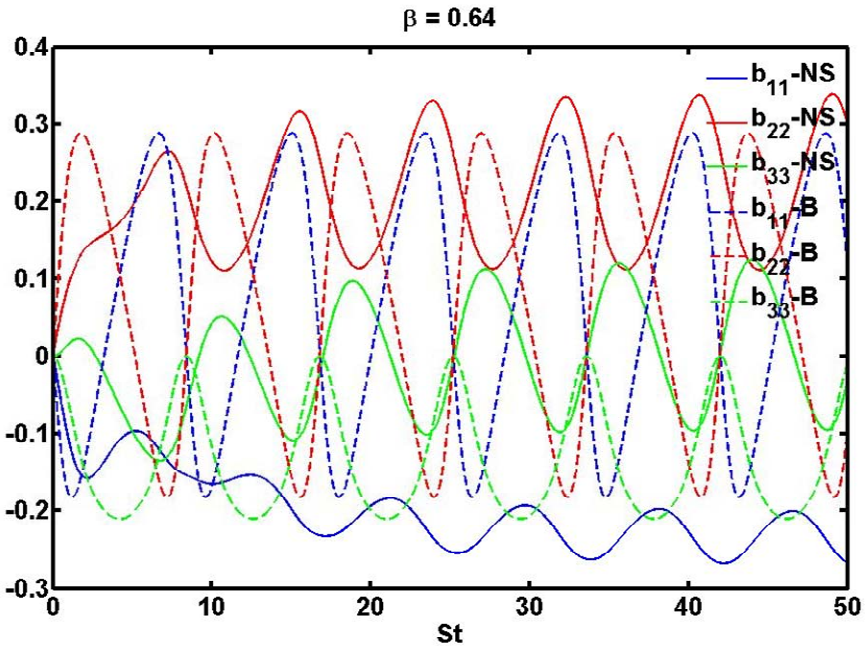

Figure 2 (b) Evolution of the anisotropy of the covariance of the perturbation velocities for a representative elliptic flow.

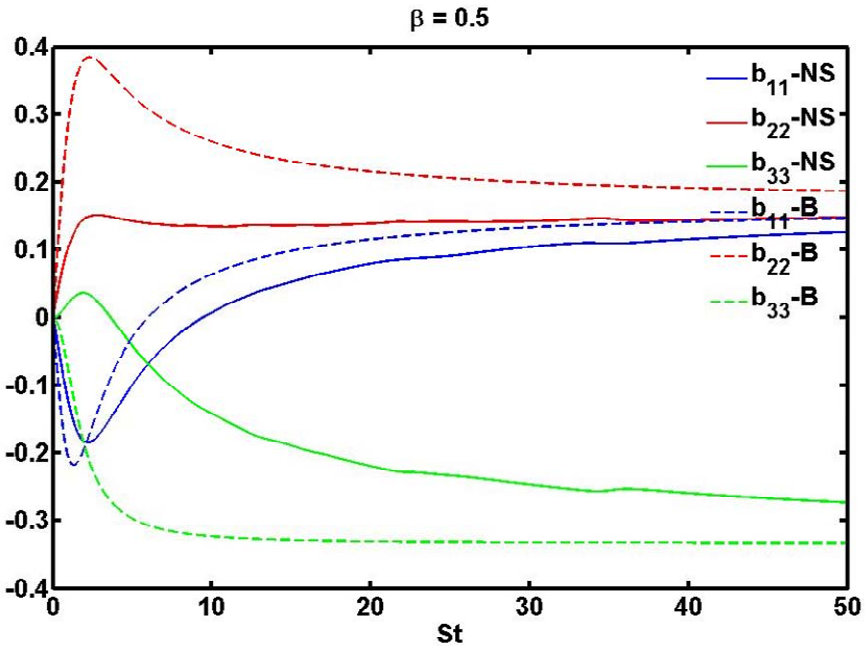

Figure 2 (c) Evolution of the anisotropy of the covariance of the perturbation velocities for homogeneous shear.

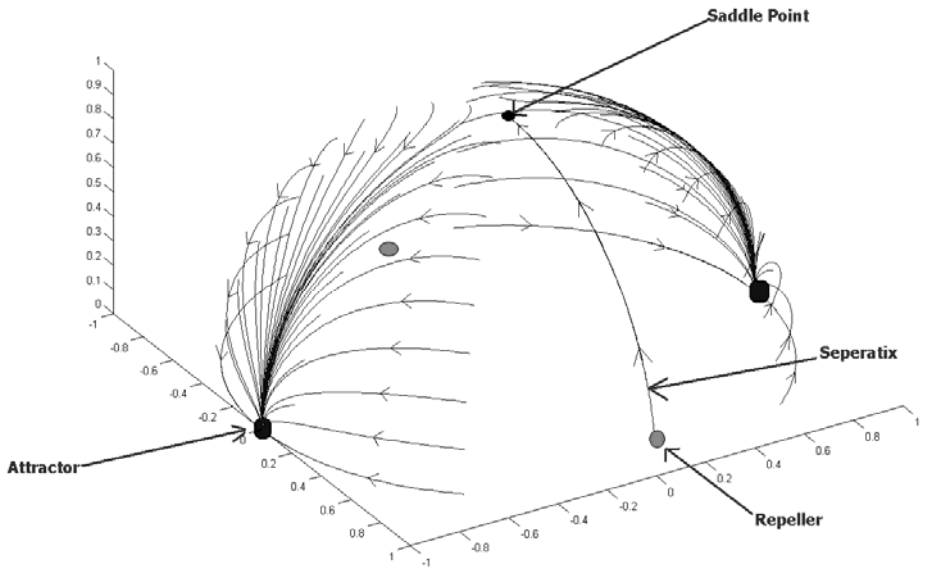

Figure 3 Dynamics in unit wavenumber space for a representative hyperbolic flow.

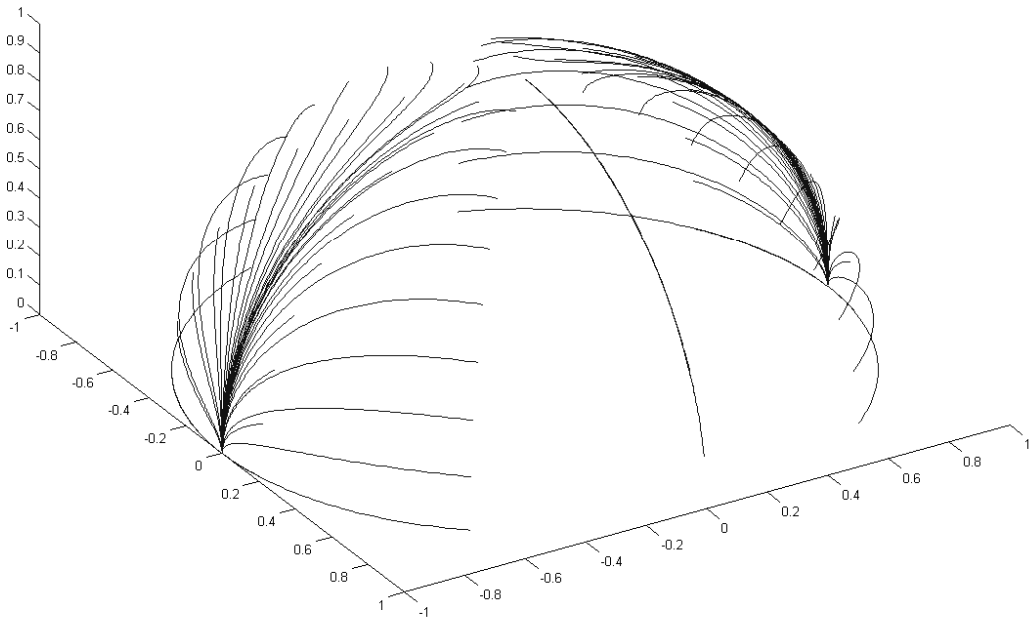

Figure 4 (a) Trajectories on the sphere for parameter value 0.

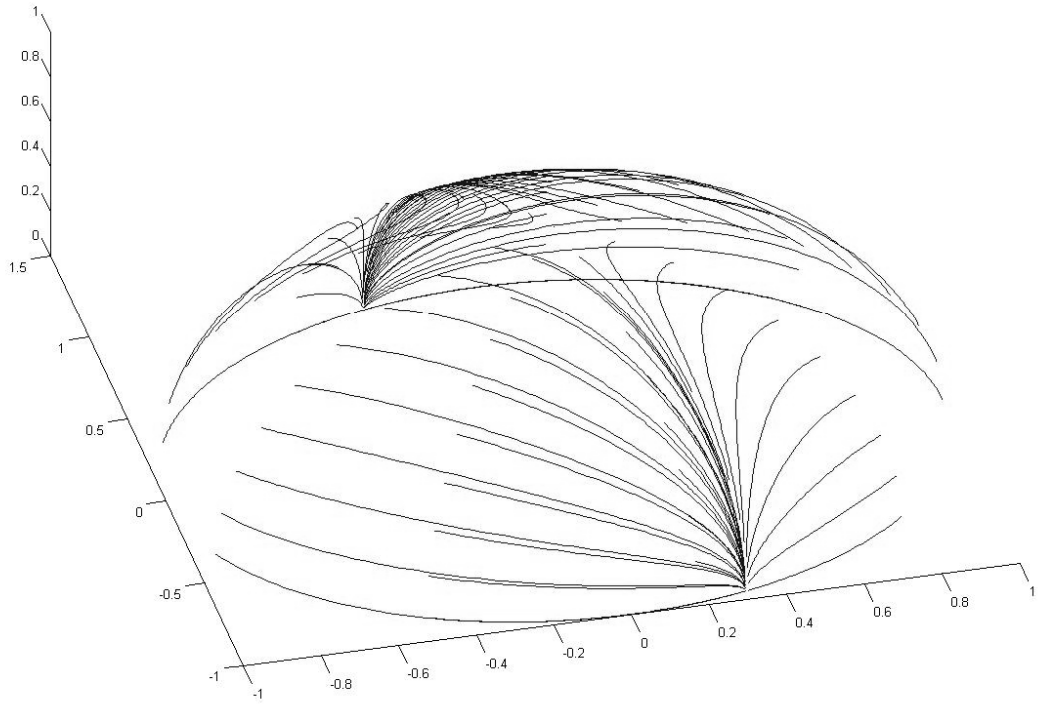

Figure 4 (b) Trajectories on the sphere for parameter value 0.25.

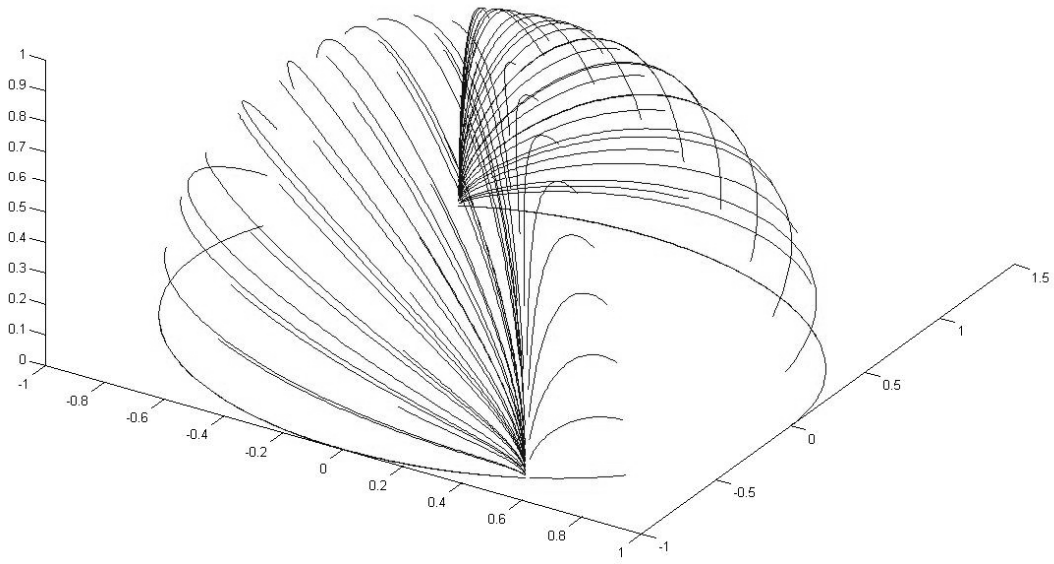

Figure 4 (c) Trajectories on the sphere for parameter value 0.45.

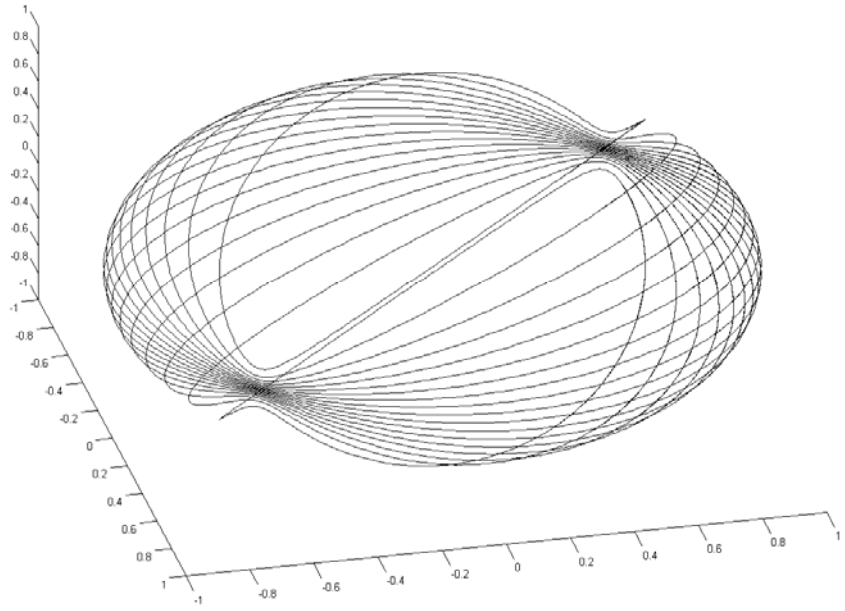

Figure 5 Dynamics in unit wavenumber space for a representative elliptic flow.

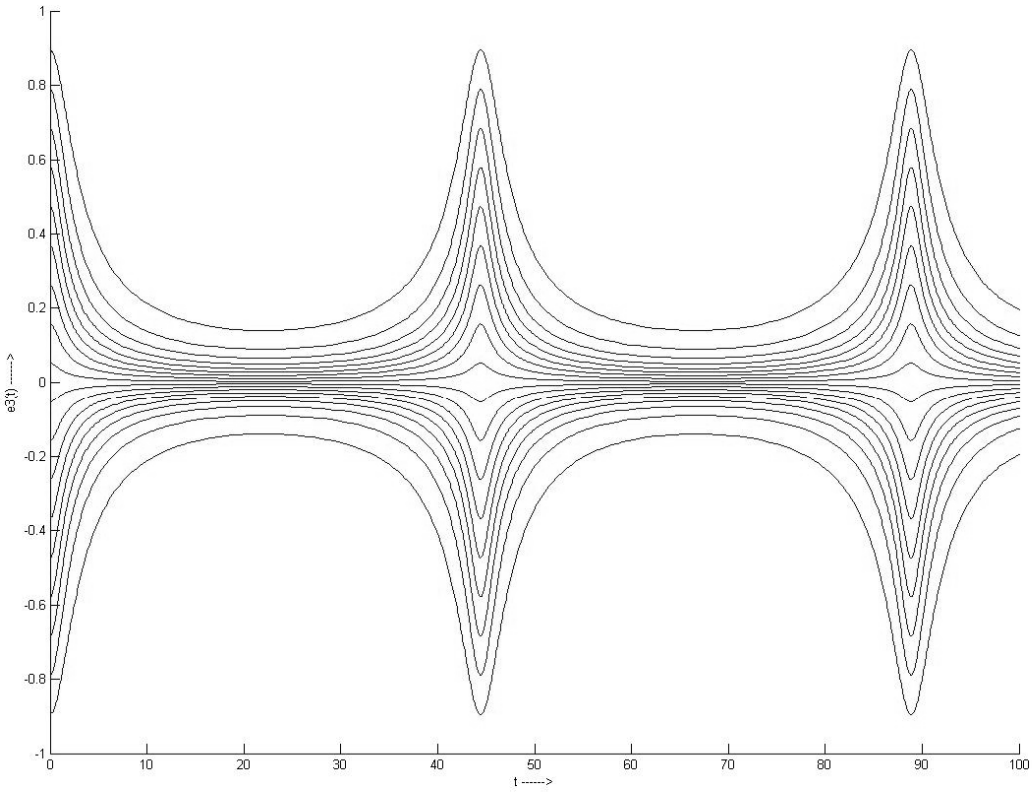

Figure 6 The different time scales evident in the evolution of the wavenumber vector, at a parameter value of β=0.501.

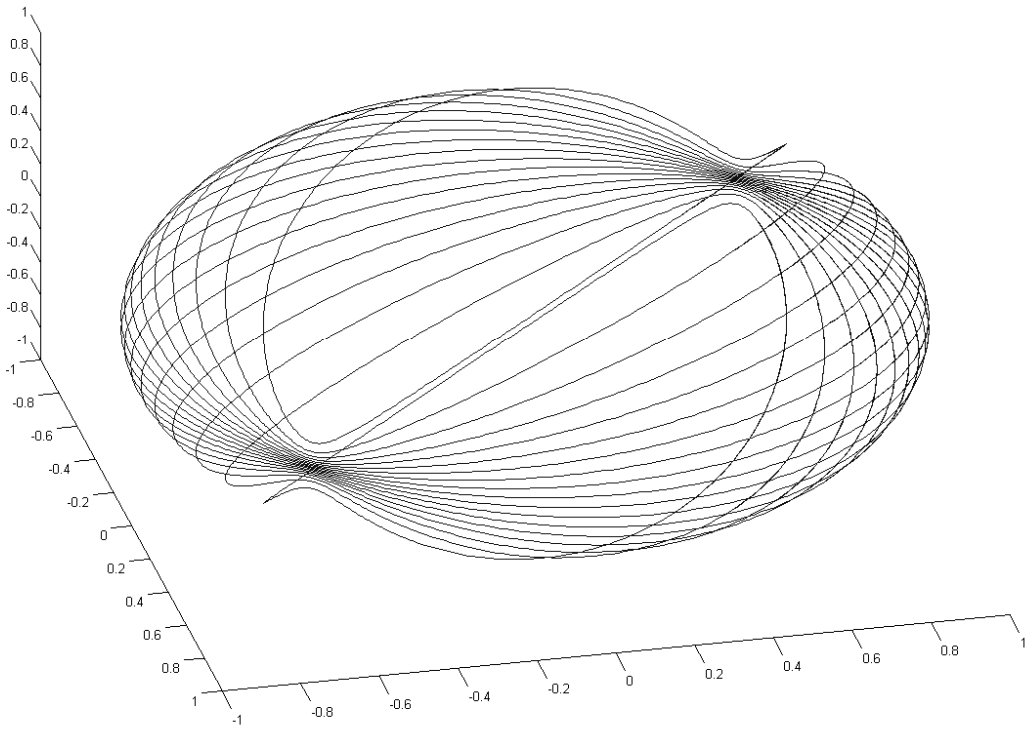

Figure 7 (a). The closed orbits on the sphere, at a parameter value of β=0.501.

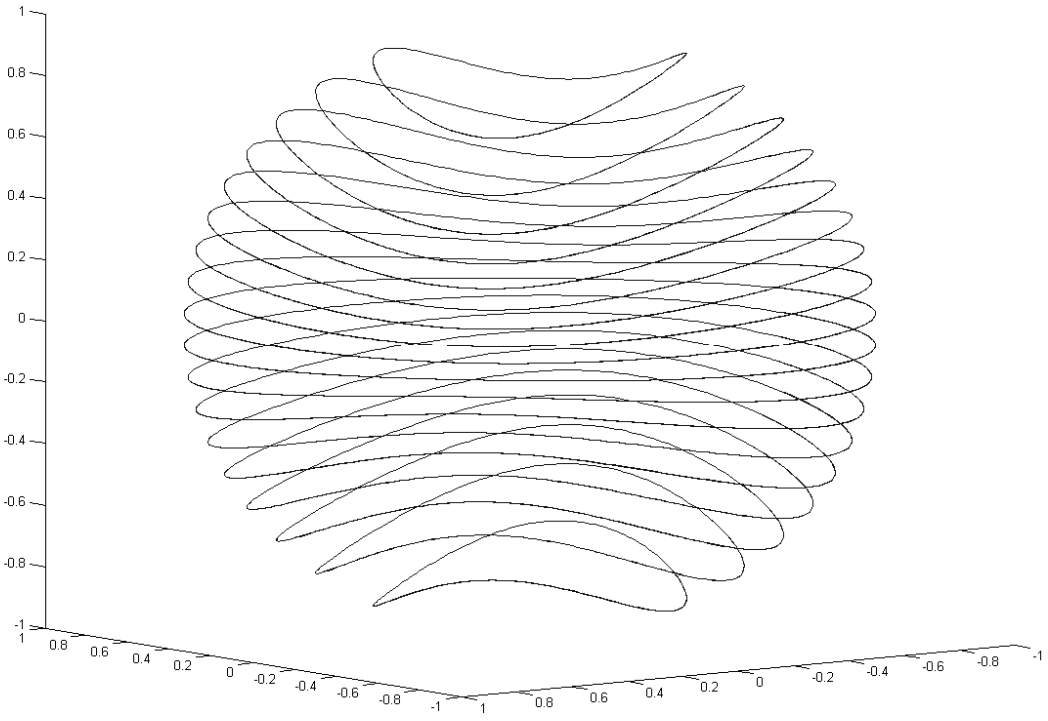

Figure 7 (b). The closed orbits on the sphere, at a parameter value of β=0.75.

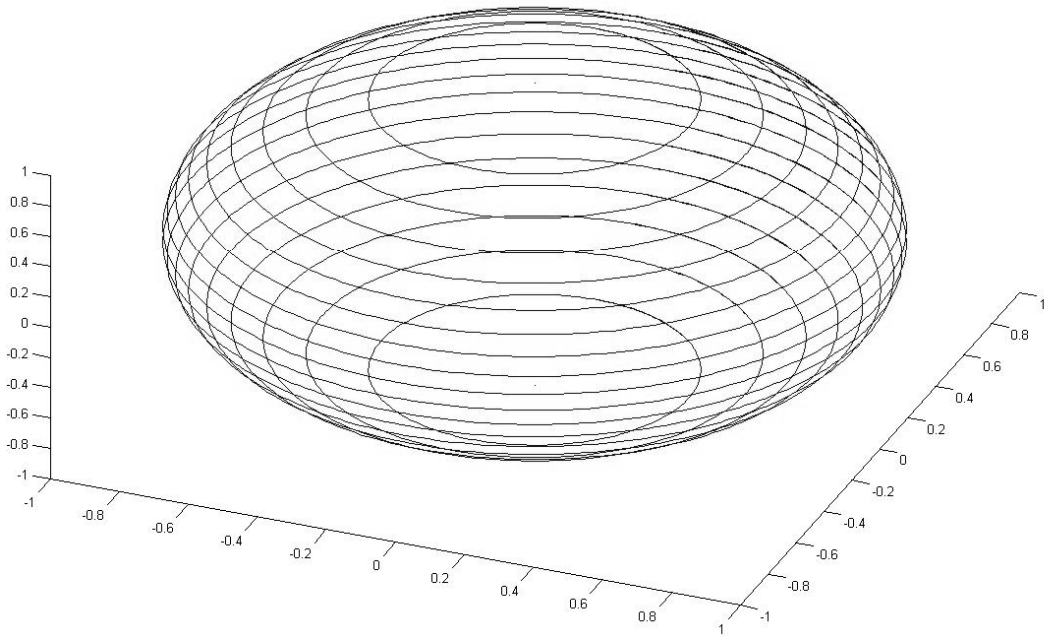

Figure 7 (c). The closed orbits on the sphere, at a parameter value of β=1.0.

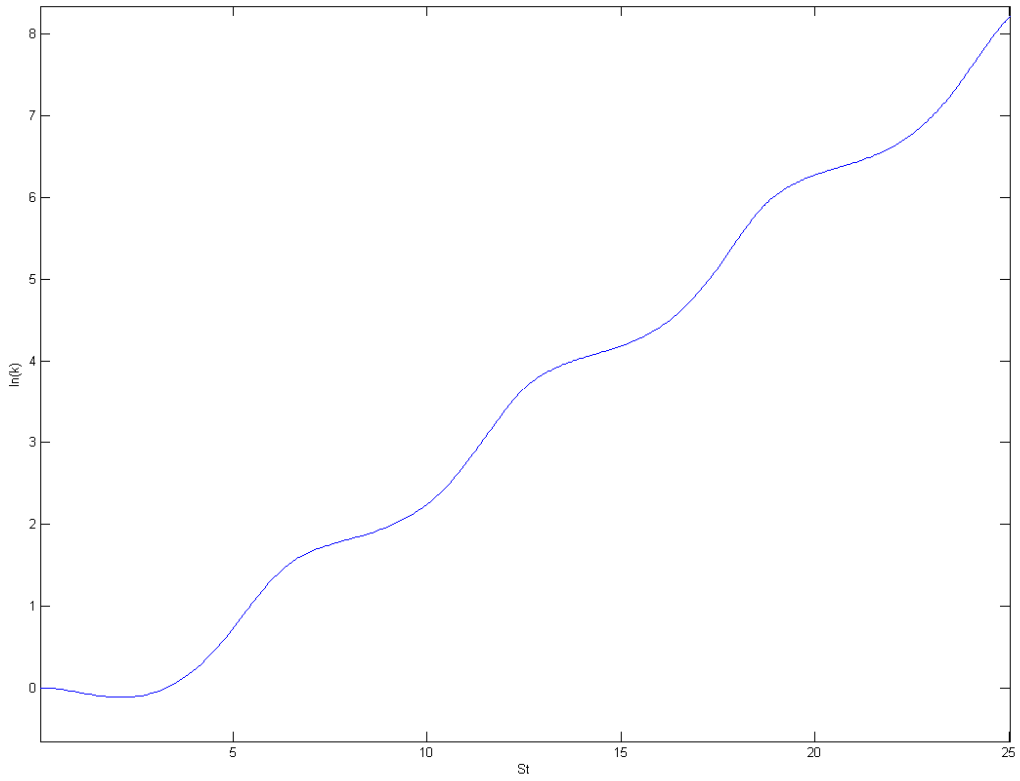

Figure 8 (a) Evolution of perturbation kinetic energy for the specific mode.

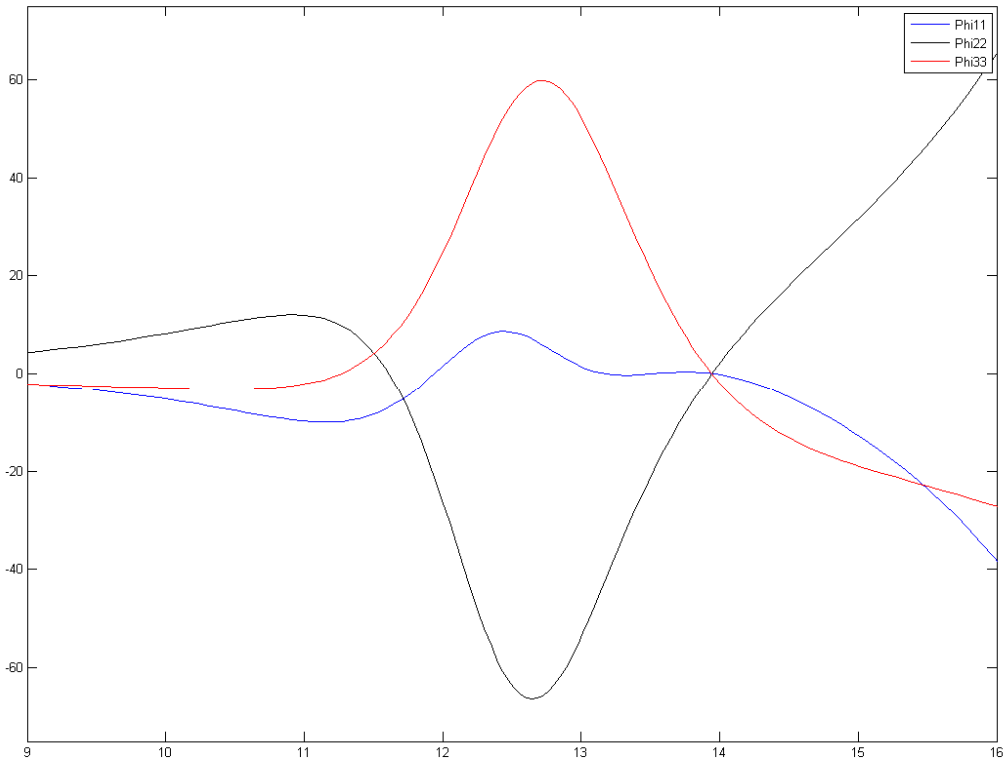

Figure 8 (b) Evolution of the pressure terms for the specific mode.

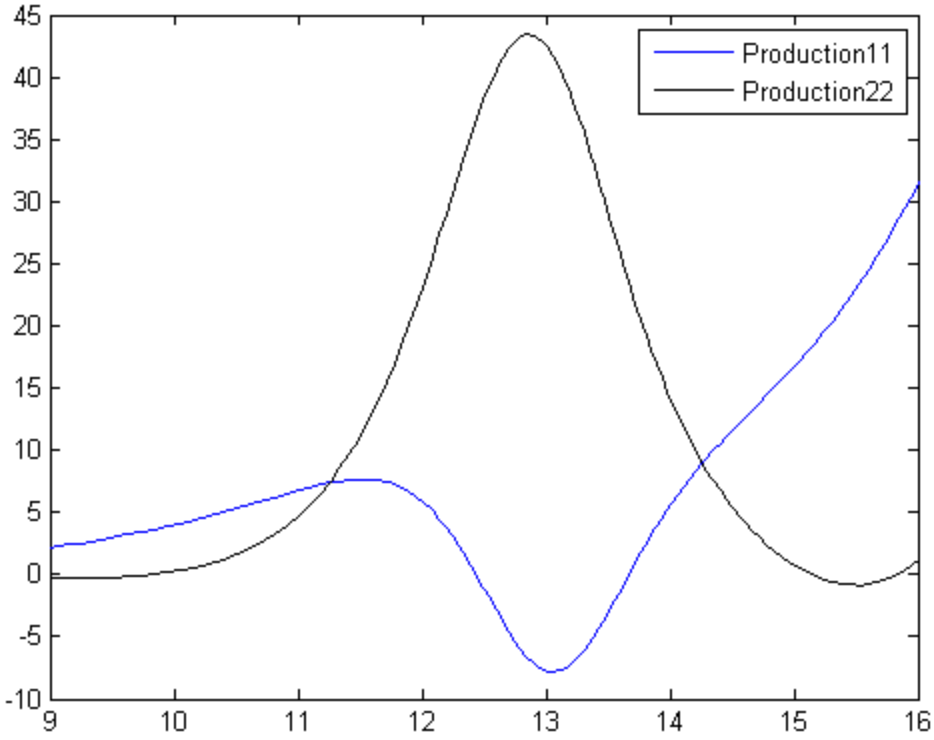

Figure 8 (c) Evolution of the production terms for the specific mode.

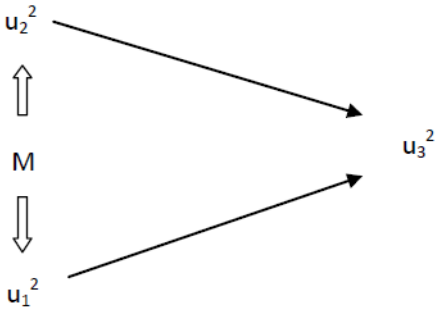

a) RDT-NS, hyperbolic flow.

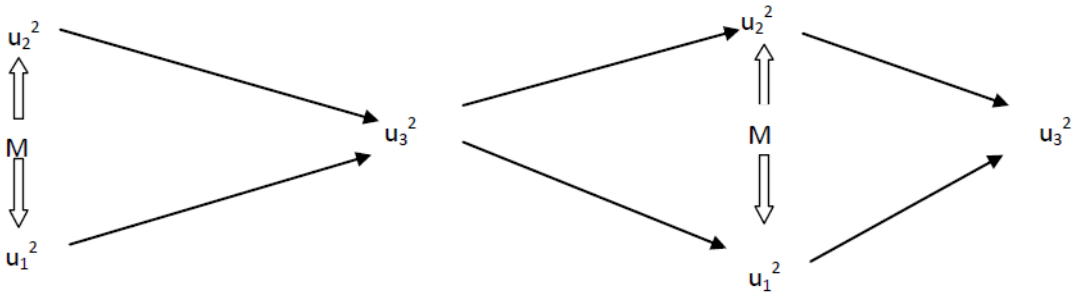

b) RDT-NS, elliptic flow.

c) RDT-Burgers, elliptic flow.

Figure 9 Schematic view of the Intercomponent Energy Transfer for different flows.

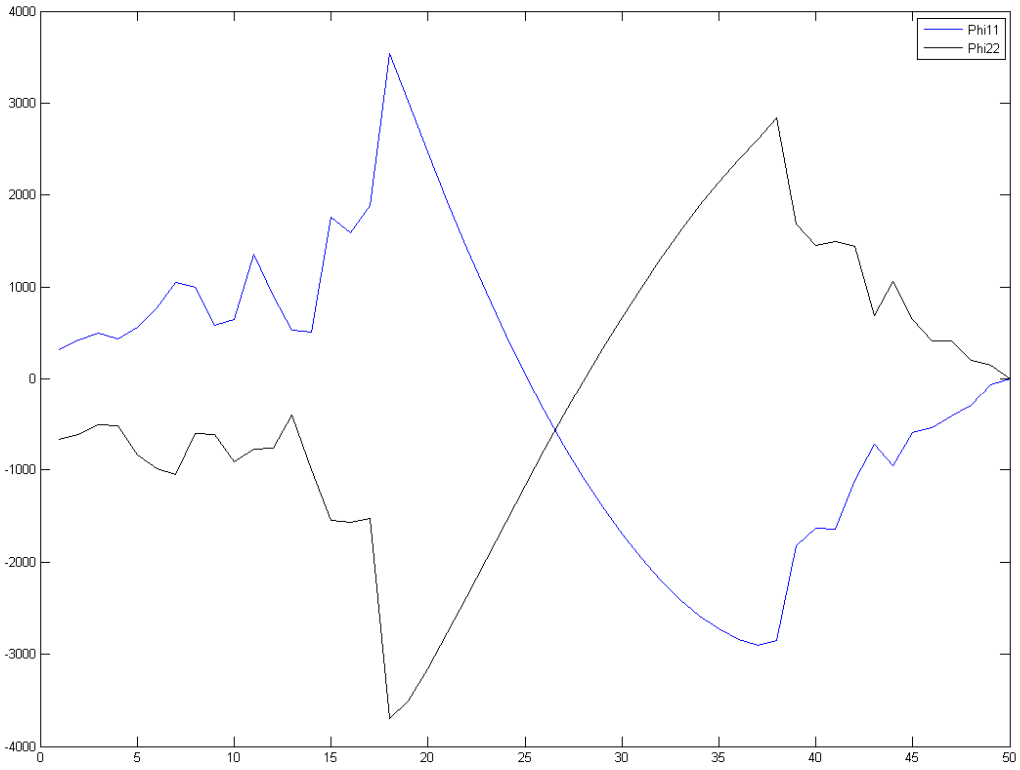

Figure 10 (a) Variation of the averaged value of the pressure strain correlation with azimuthal angle.

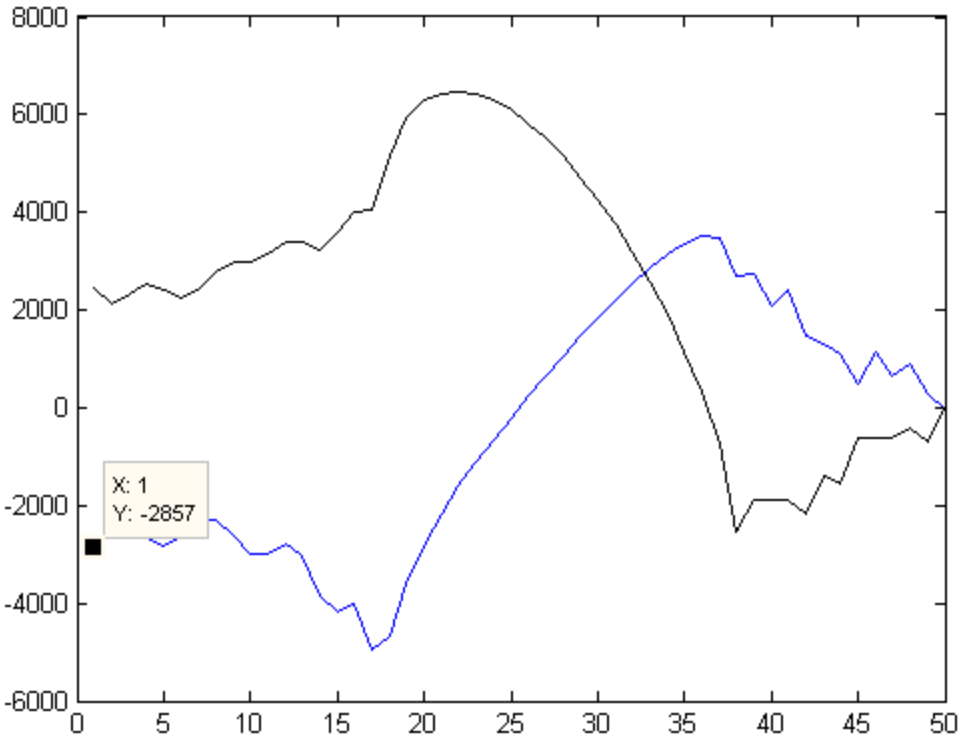

Figure 10 (b) Variation of the averaged value of production with azimuthal angle.

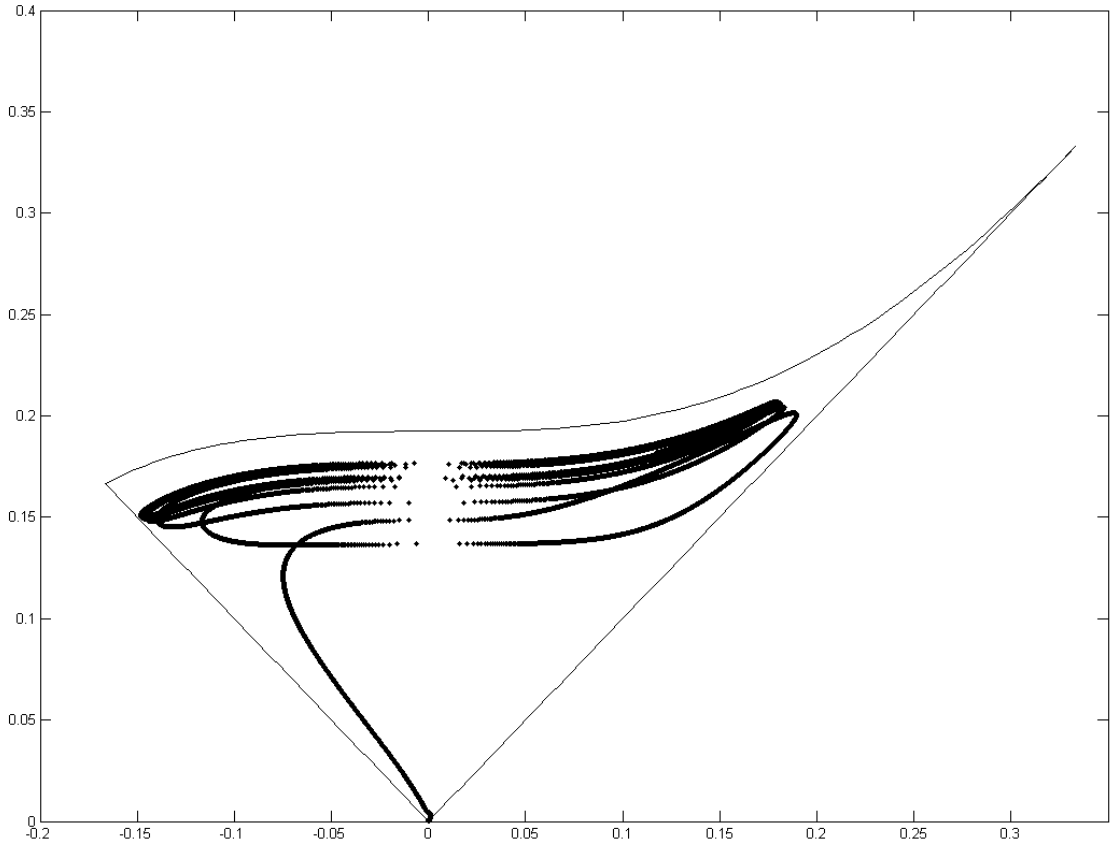

Figure 12 (a) Evolution of the Reynolds stress anisotropy invariants for a representative elliptic flow, RDT-NS

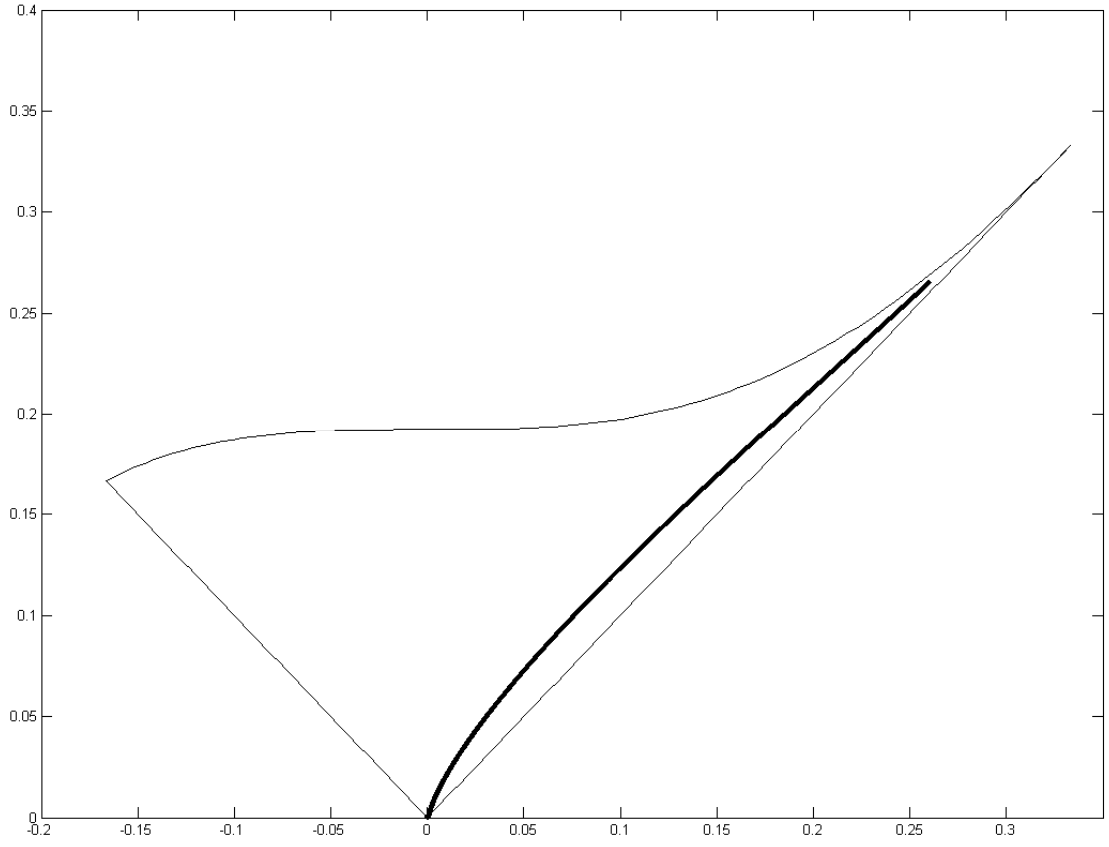

Figure 12 (b) Evolution of the Reynolds stress anisotropy invariants for a representative elliptic flow, RDT-B

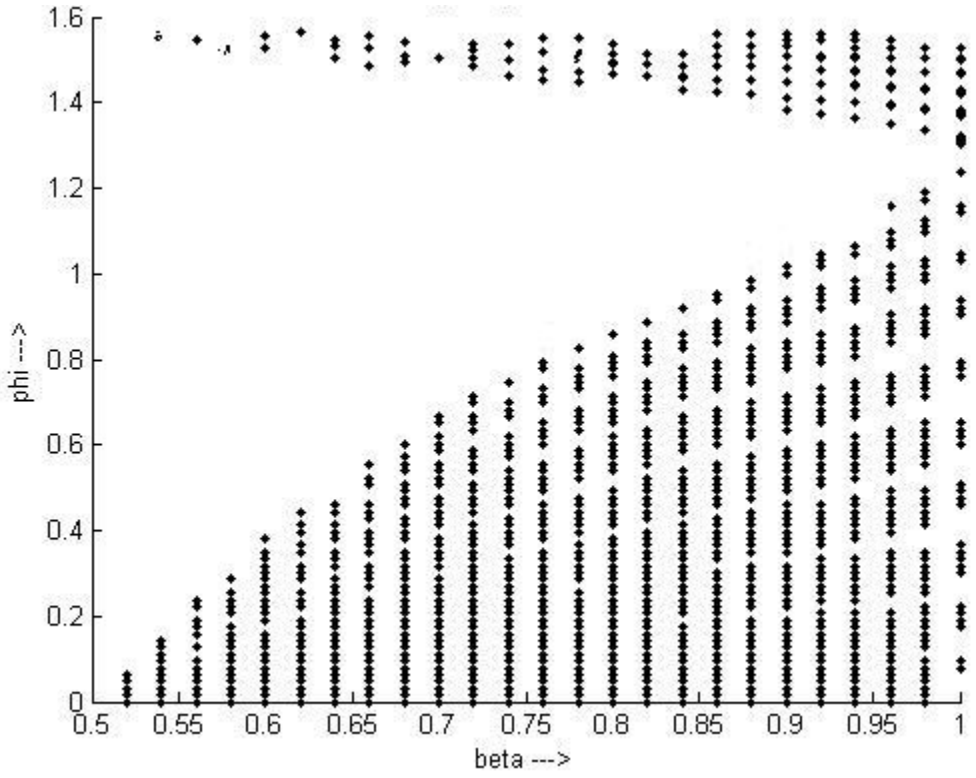

Figure 13 Floquet stability diagram for the elliptic flow regime.

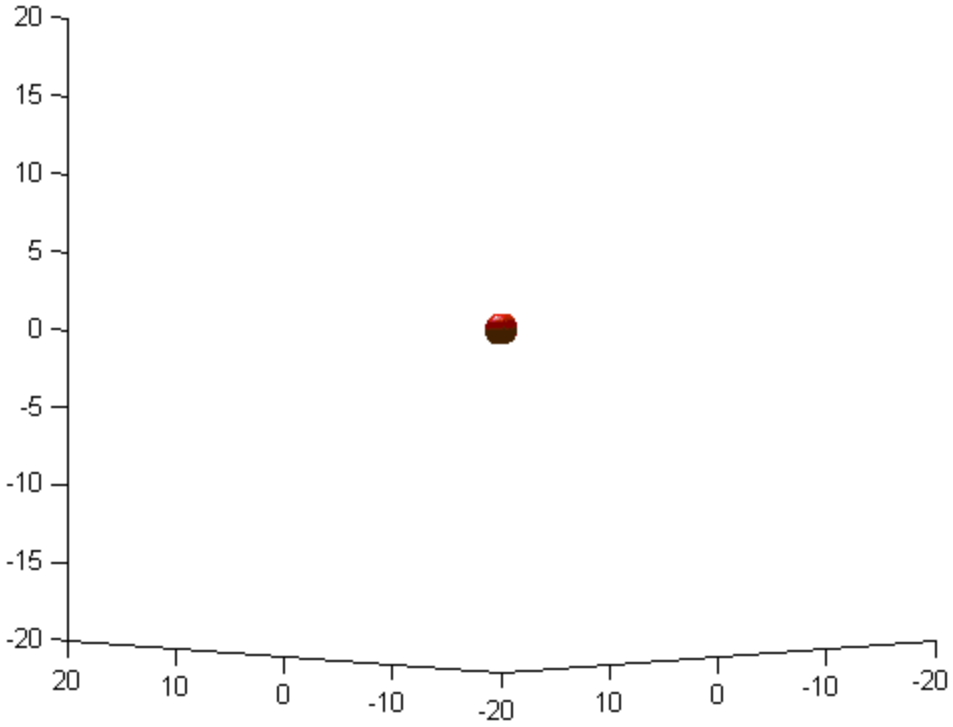

Figure 14 (a) Evolution of the phase volumes of hyperbolic flows, t=0.

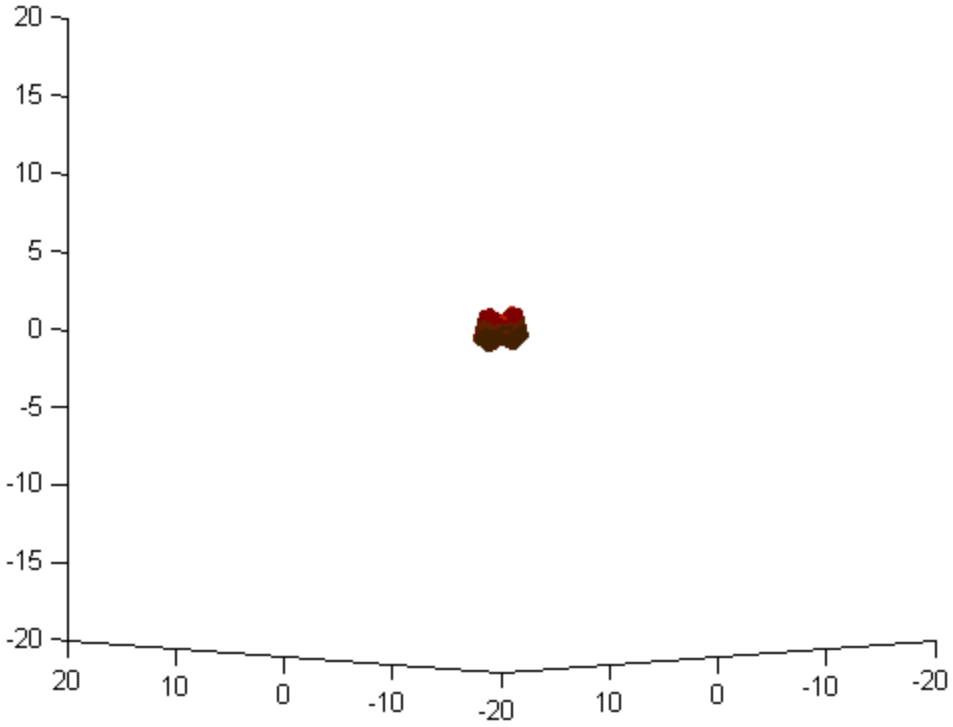

Figure 14 (b) Evolution of the phase volumes of hyperbolic flows, t=8.

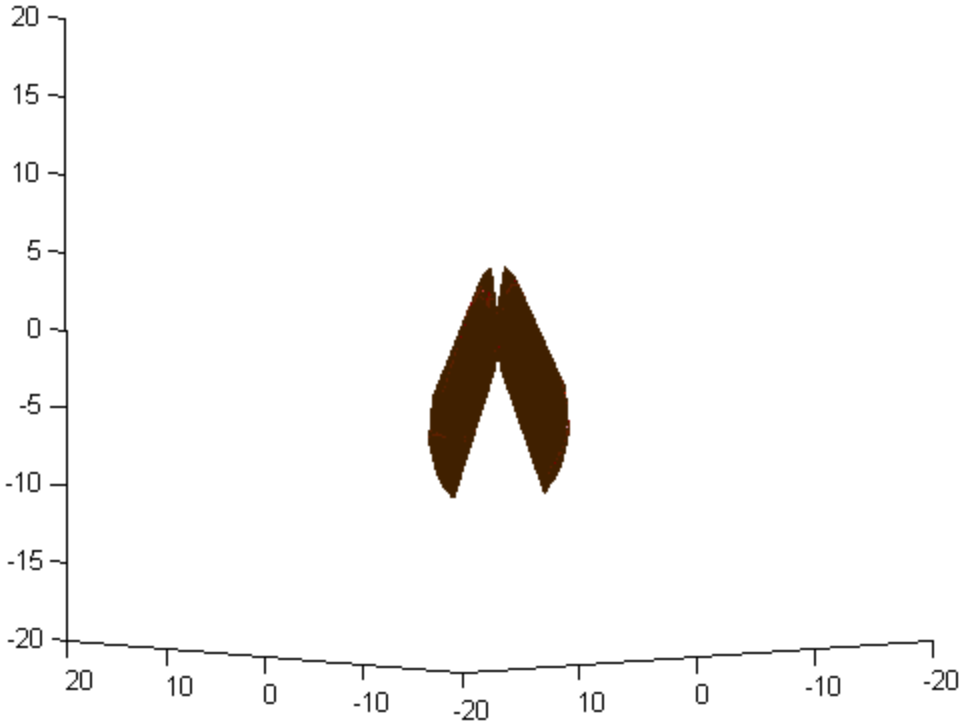

Figure 14 (c) Evolution of the phase volumes of hyperbolic flows, t=15.

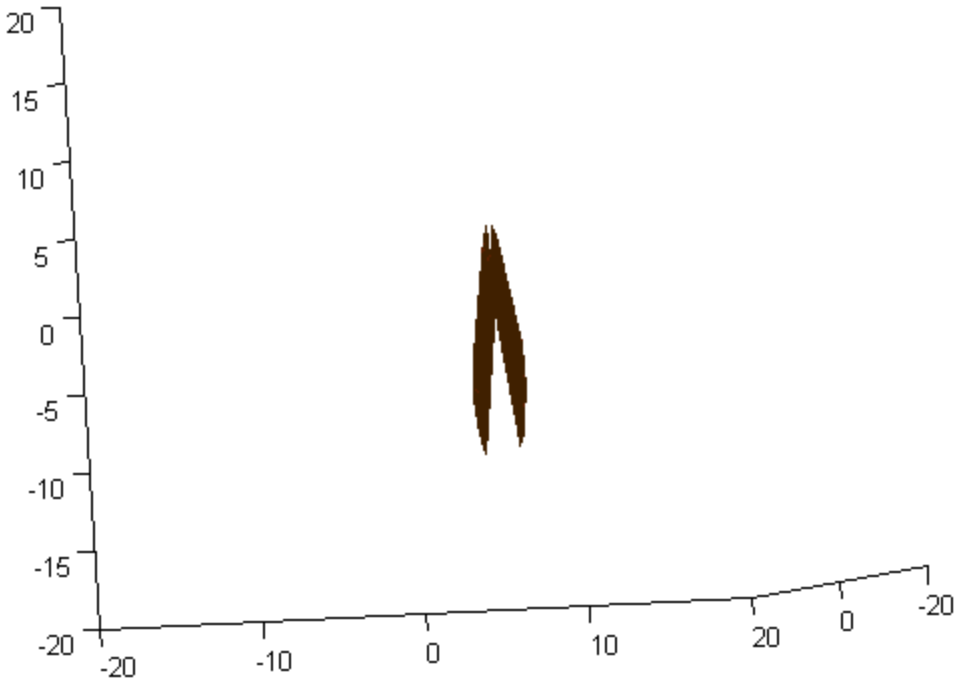

Figure 14 (d) Evolution of the phase volumes of hyperbolic flows, t=25.

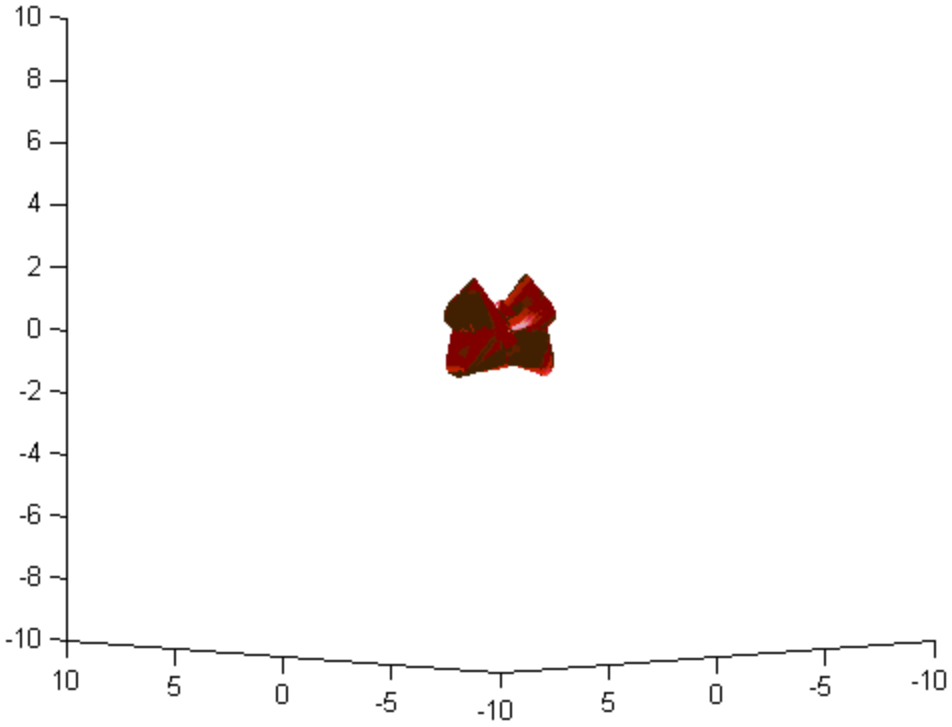

Figure 15 (a) Evolution of the phase volumes of elliptic flows, t=5.

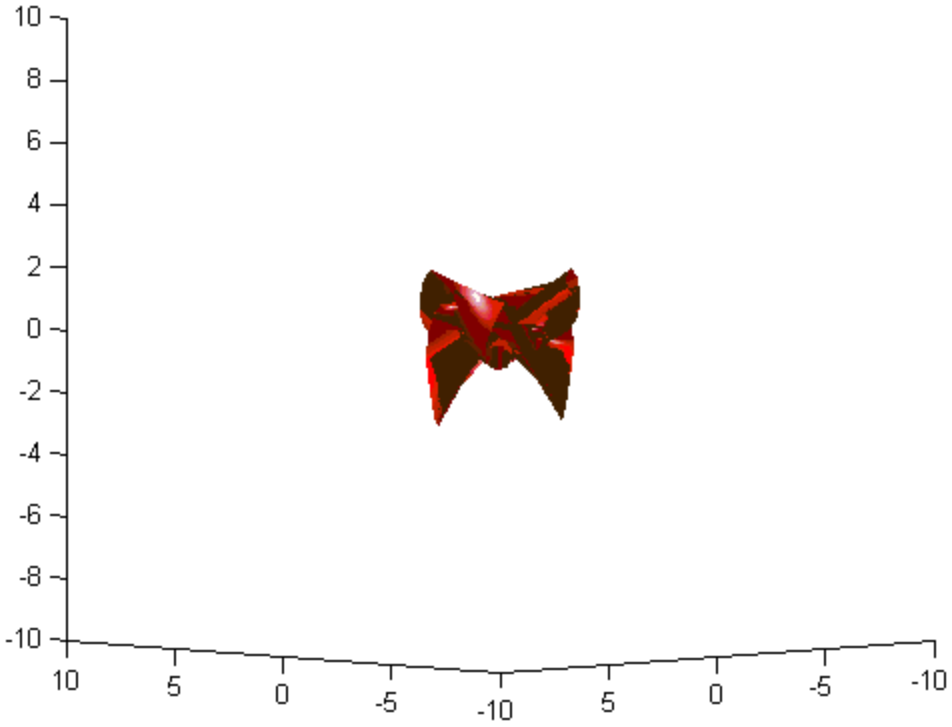

Figure 15 (b) Evolution of the phase volumes of elliptic flows, t=12.5.

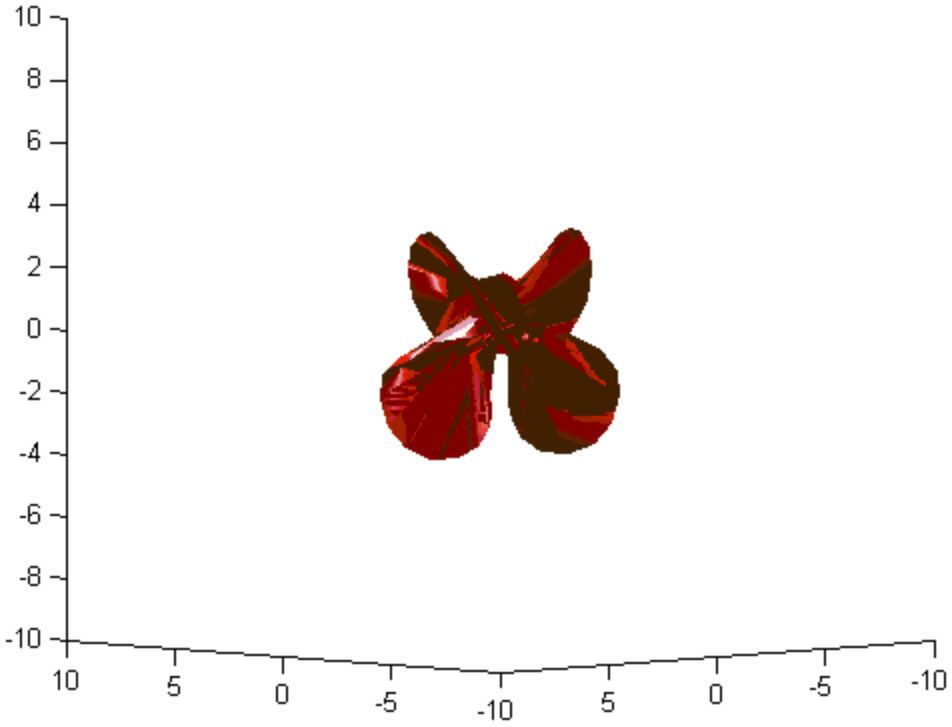

Figure 15 (c) Evolution of the phase volumes of elliptic flows, t=18.

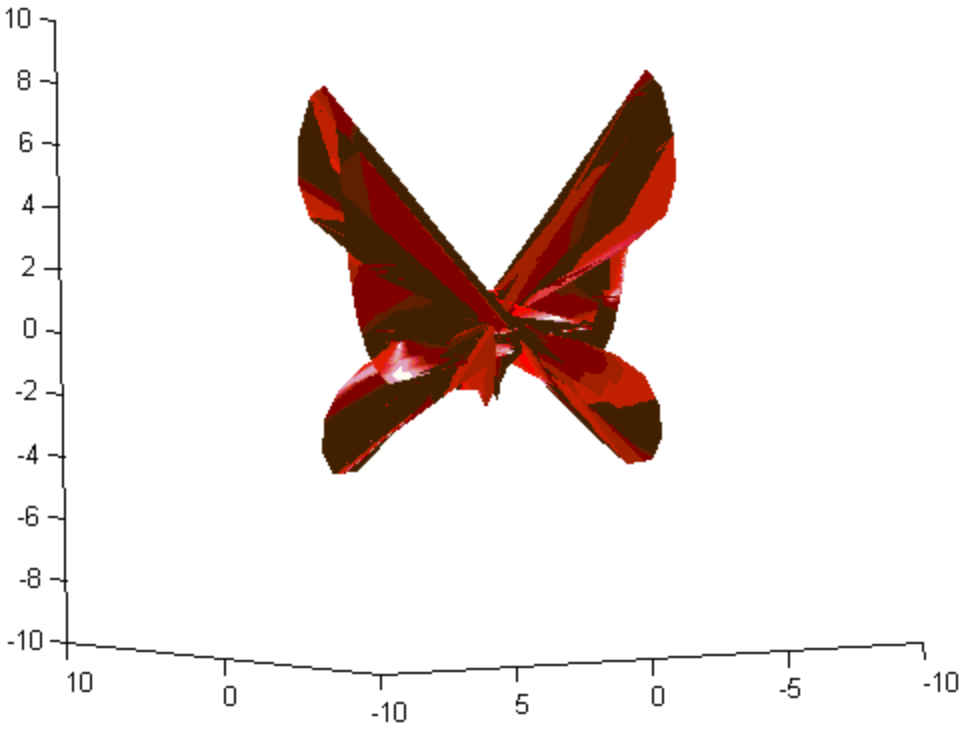

Figure 15 (d) Evolution of the phase volumes of elliptic flows, t=25.

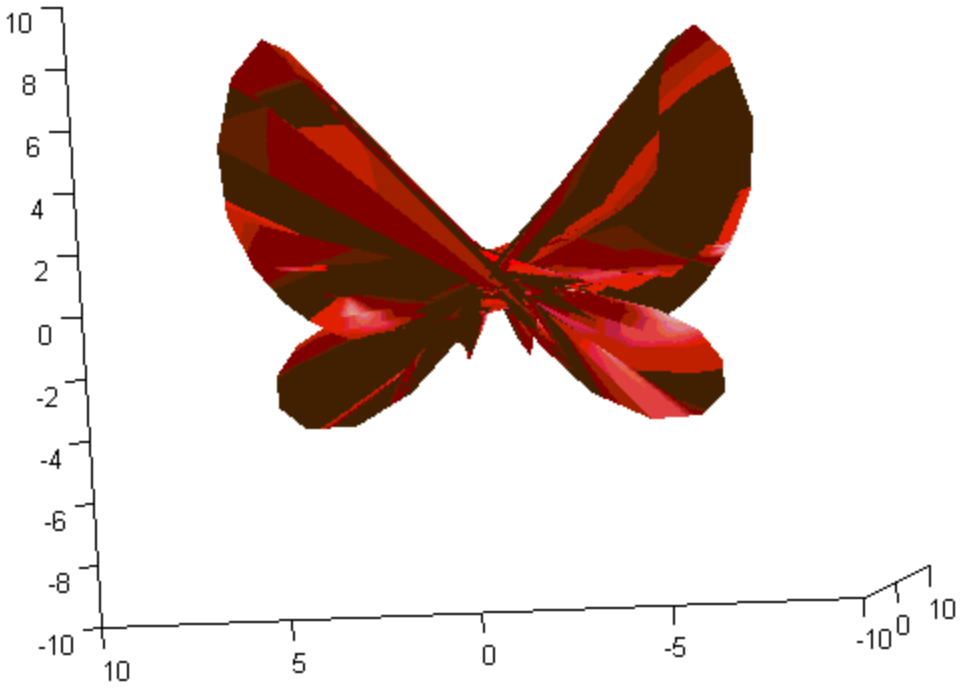

Figure 15 (e) Evolution of the phase volumes of elliptic flows, t=30.

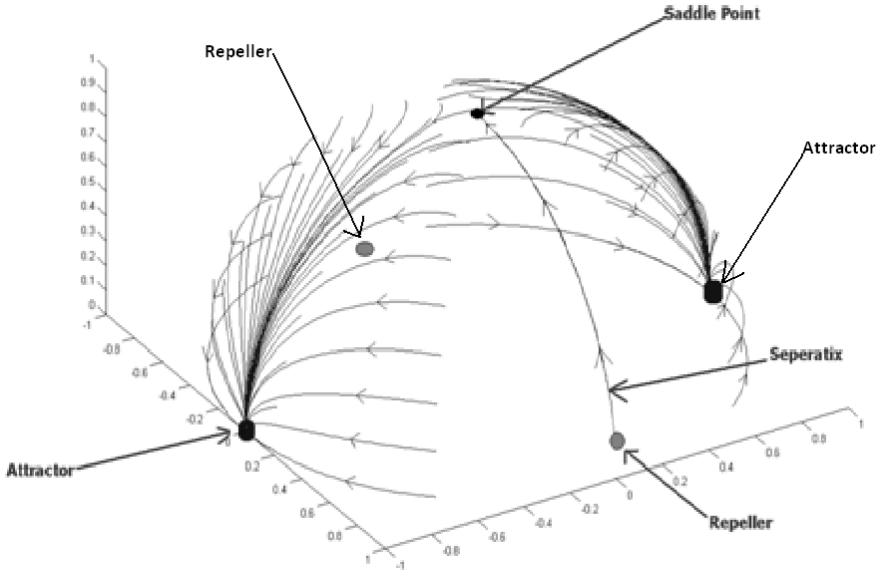

Figure 16 (a) Dynamics in unit wavenumber space for a representative hyperbolic flow.

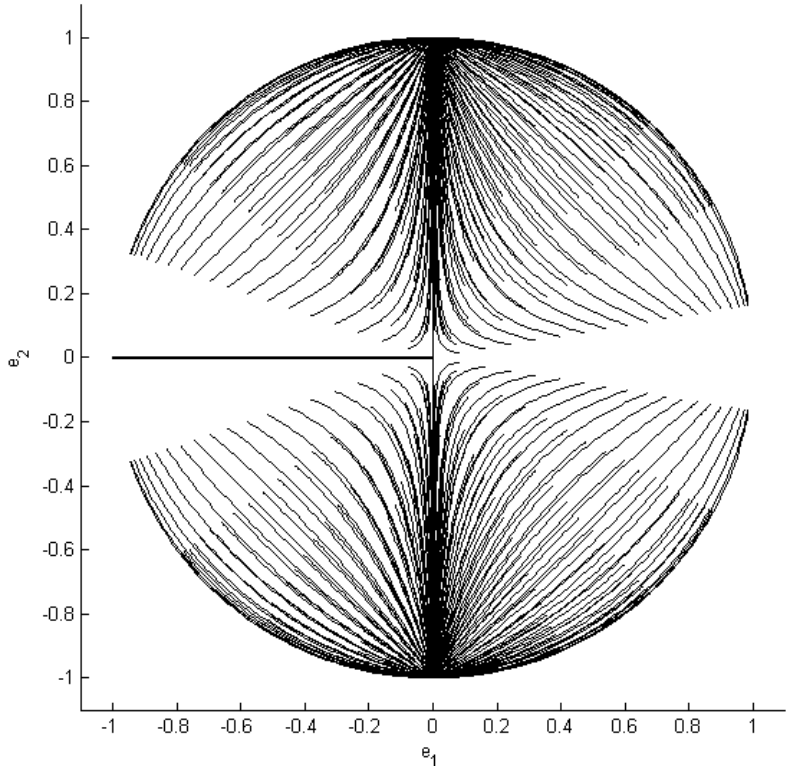

Figure 16 (b) Evolution of trajectories in unit wavenumber space for a host of initial conditions. (For the case of plane strain mean flow).

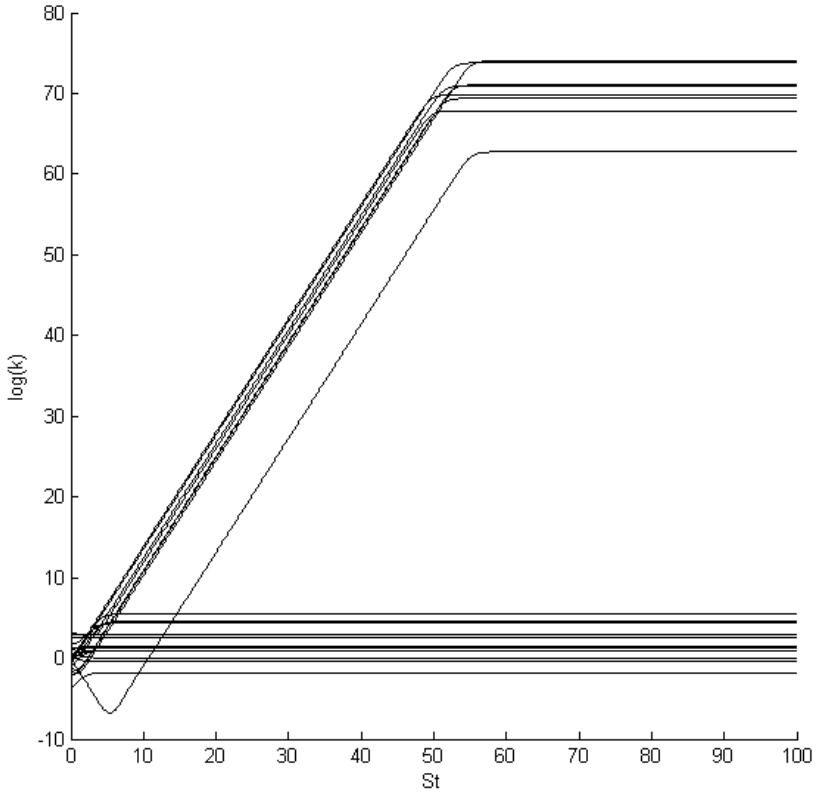

Figure 17 (a) Modal kinetic energy evolution for a generic set of initial conditions in a plane strain flow.

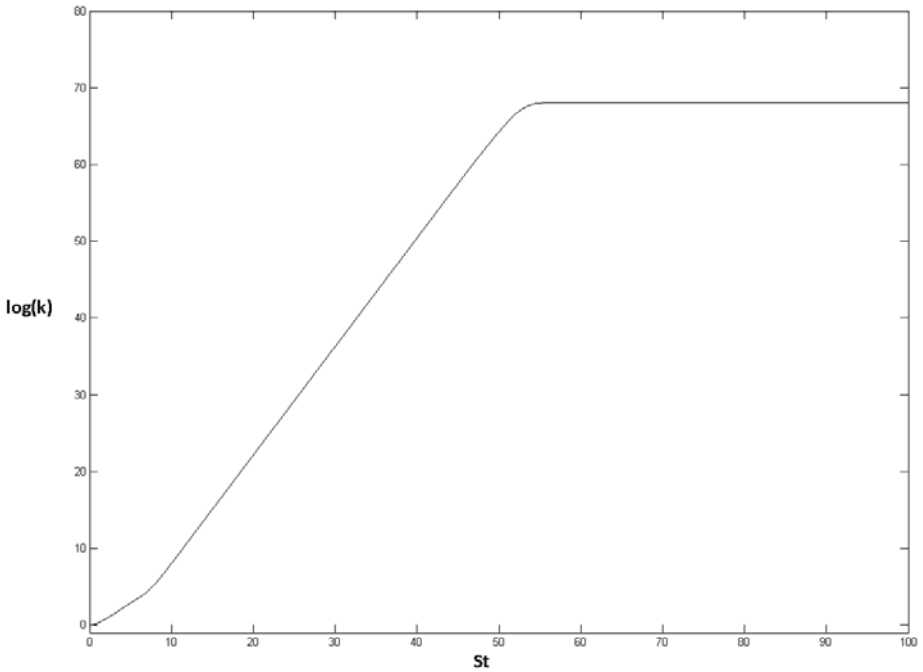

Figure 17 (b) Flow turbulent kinetic energy evolution for a plane strain flow.

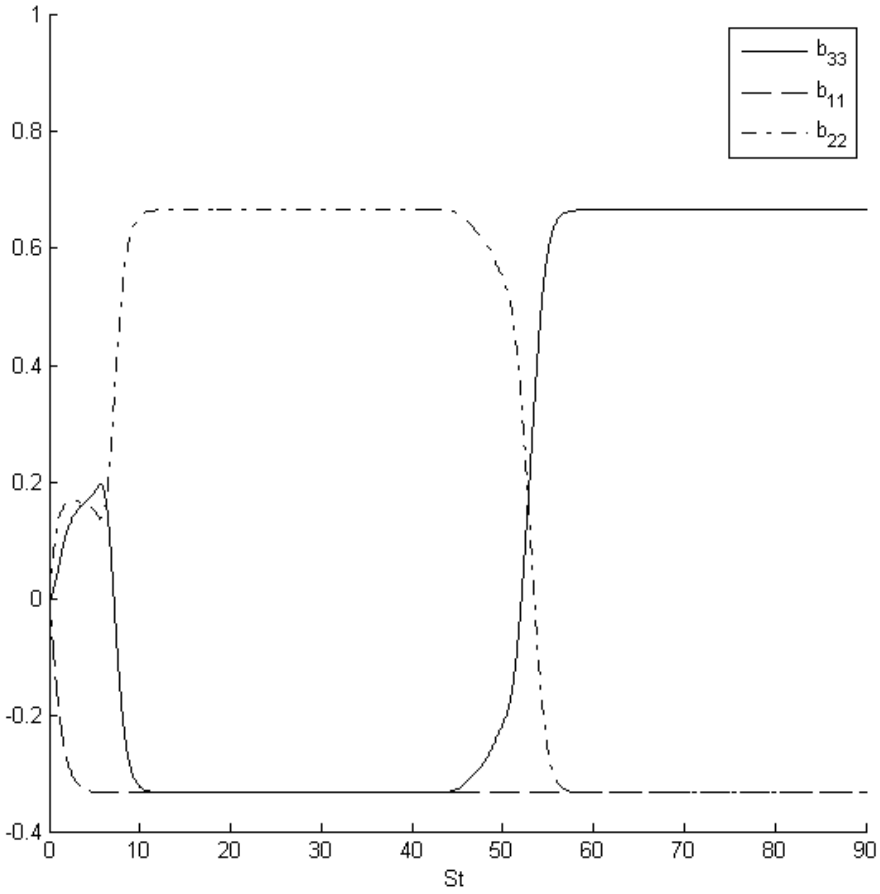

Figure 18 (a) Evolution of the Reynolds stress anisotropy tensor components for a representative hyperbolic flow.

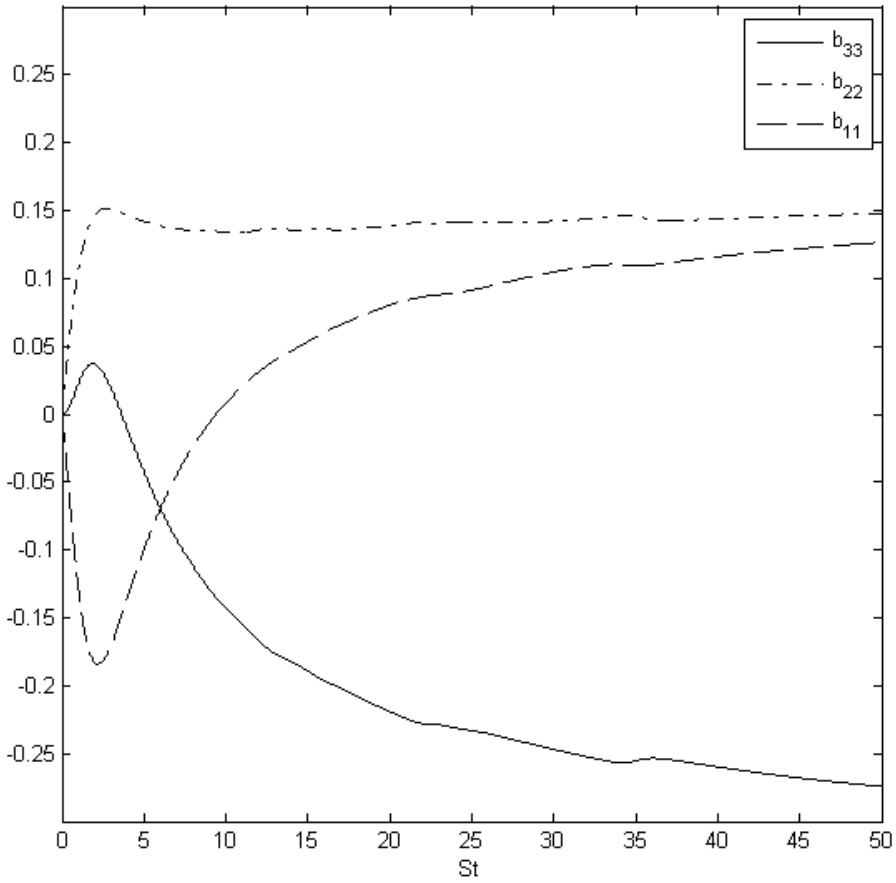

Figure 18 (b) Evolution of the Reynolds stress anisotropy tensor components for the homogeneous shear flow.

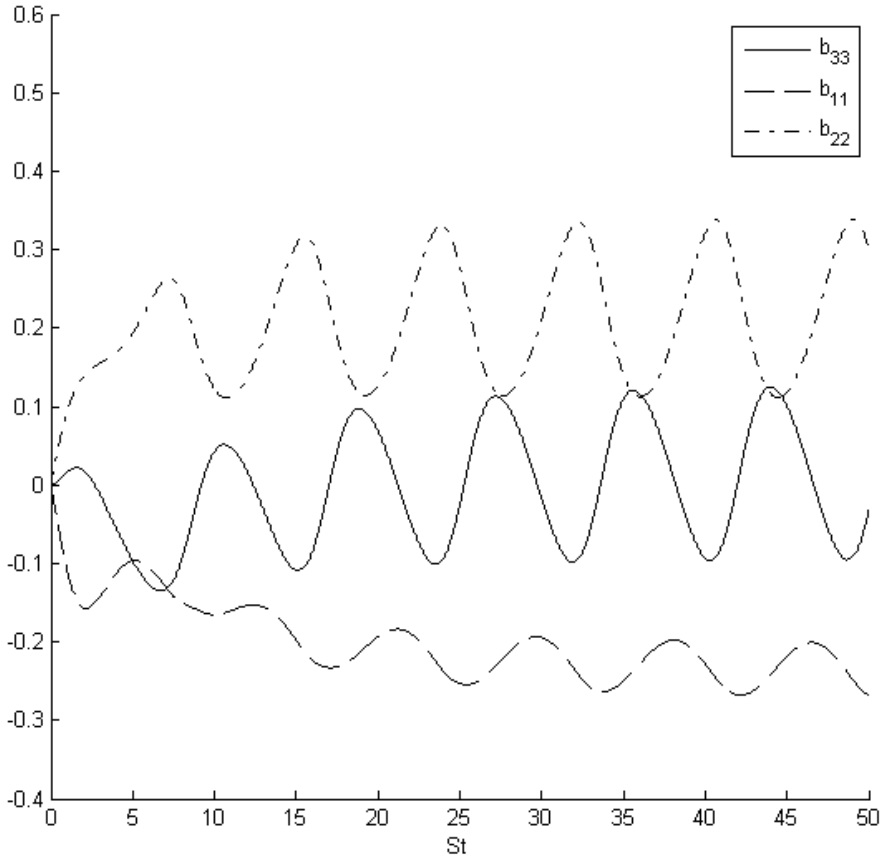

Figure 18 (c) Evolution of the Reynolds stress anisotropy tensor components for a representative elliptic flow.

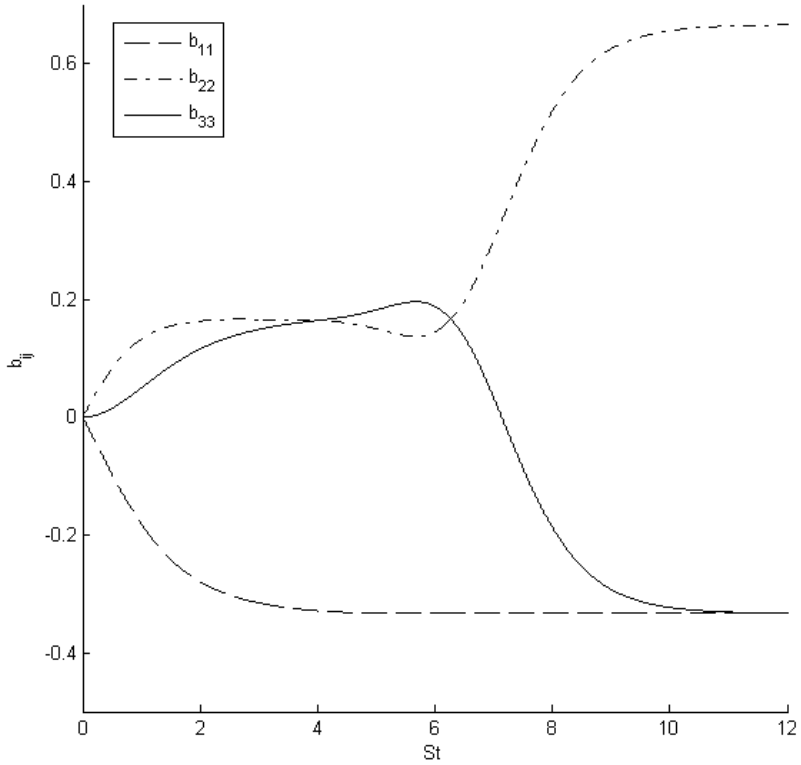

Figure 19 (a). Evolution of the Reynolds stress anisotropy tensor components for the case of plane strain flow, β=0.

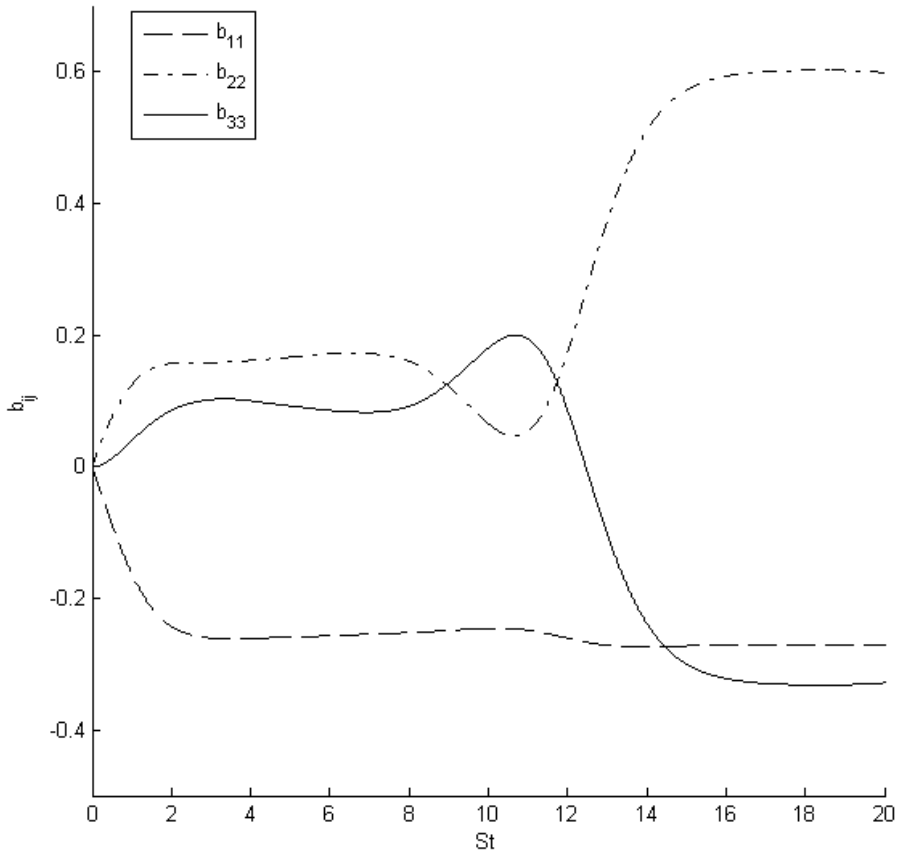

Figure 19 (b). Evolution of the Reynolds stress anisotropy tensor components for the case of β=0.19.

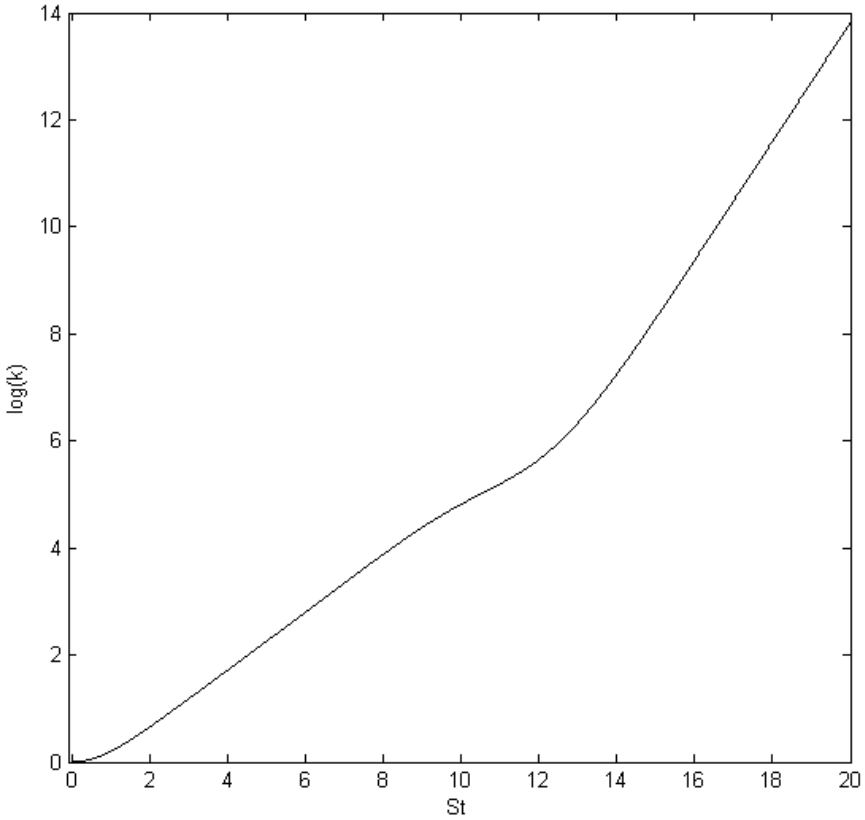

Figure 19 (c) Evolution of the turbulent kinetic energy of the flow for β=0.19.

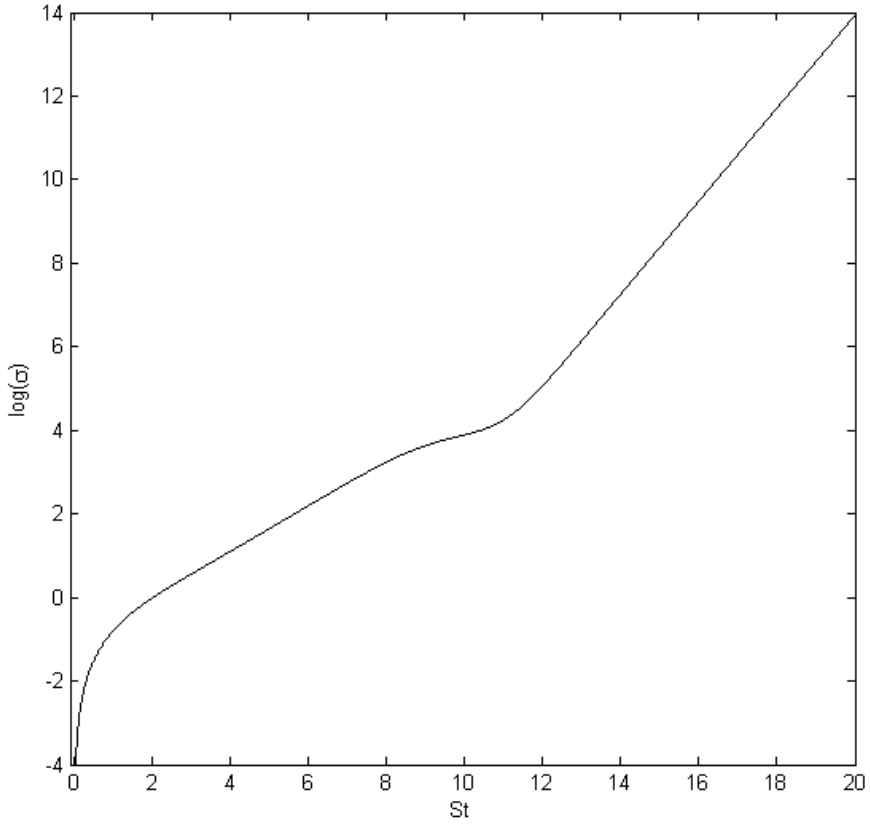

Figure 19 (d) Evolution of the temporal gradient turbulent kinetic energy of the flow (σ) for β=0.19.

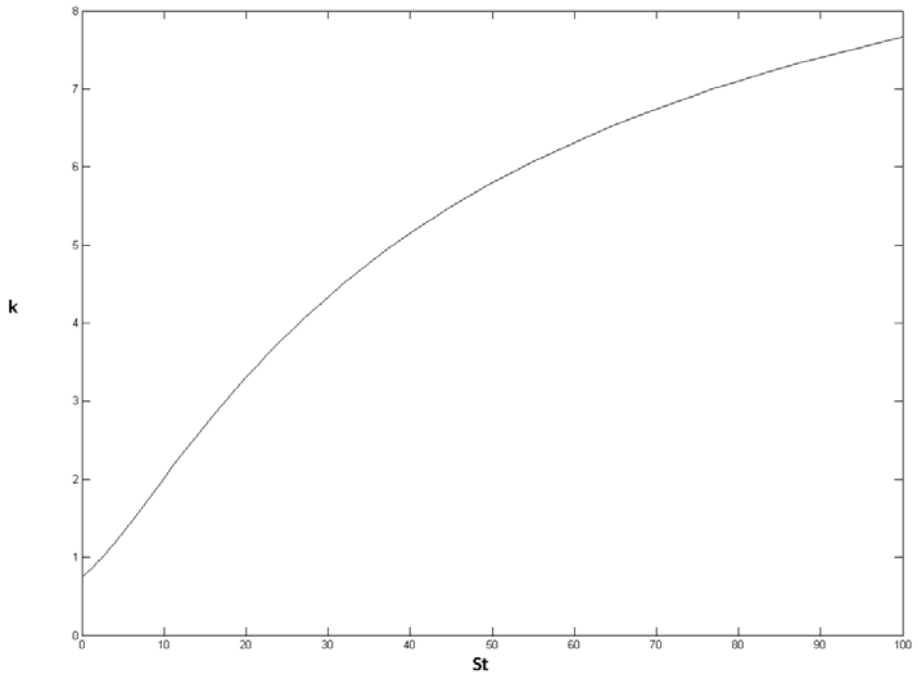

Figure 20 (a) Evolution of the modal kinetic energy for an eddy in the homogeneous shear flow.

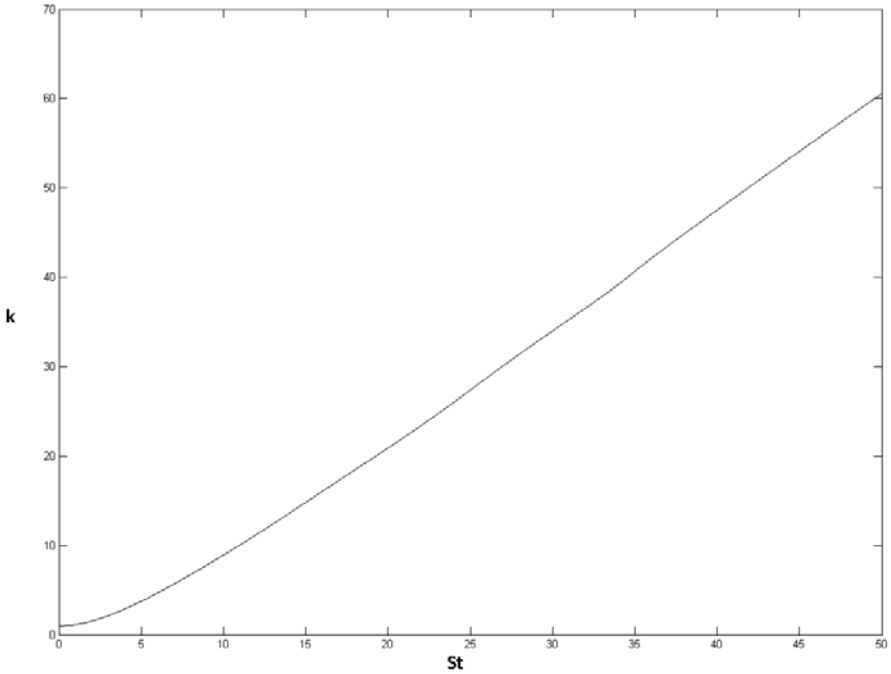

Figure 20 (b) Evolution of the turbulent kinetic energy for the homogeneous shear flow.

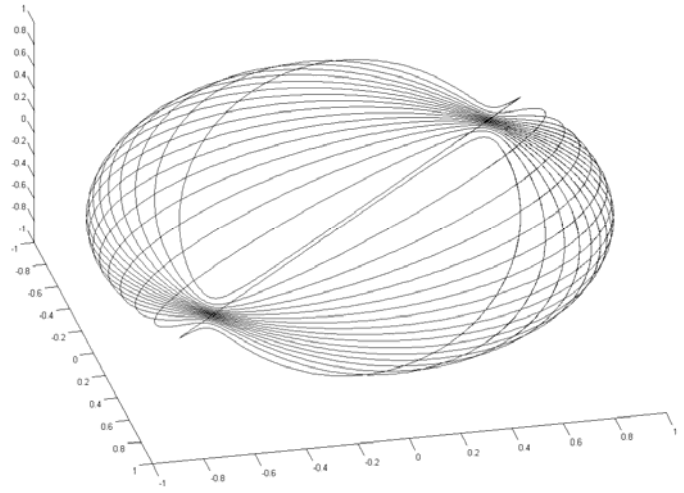

Figure 21 (a) Dynamics in unit wavenumber space for a representative elliptic flow, at a parameter value of β=0.51.

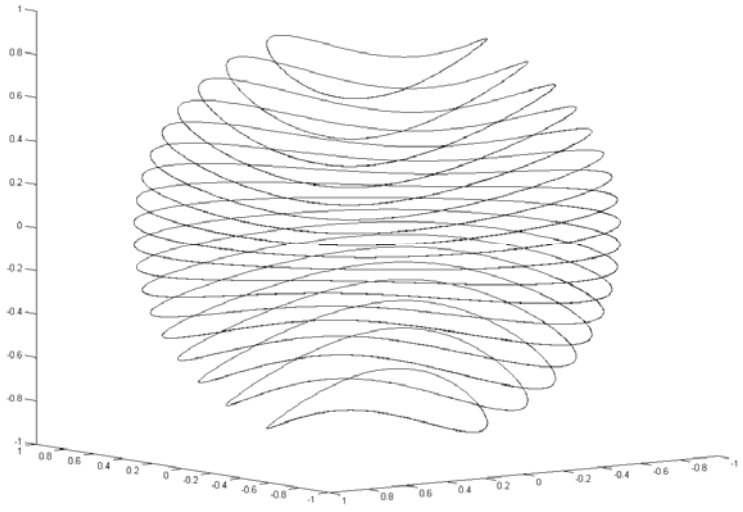

Figure 21 (b). Dynamics in unit wavenumber space for a representative elliptic flow, at a parameter value of β=0.75.

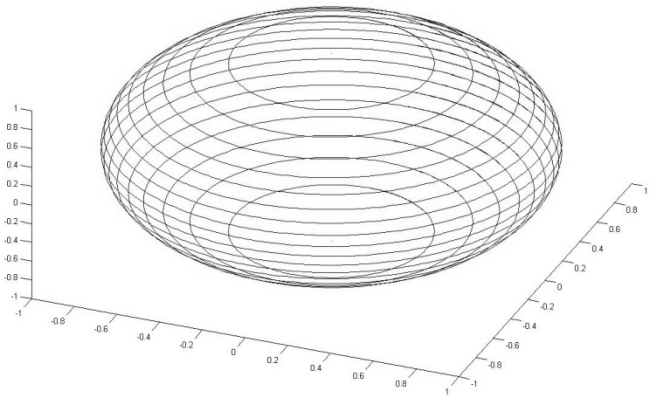

Figure 21 (c). Dynamics in unit wavenumber space for a representative elliptic flow, at a parameter value of β=1.0.

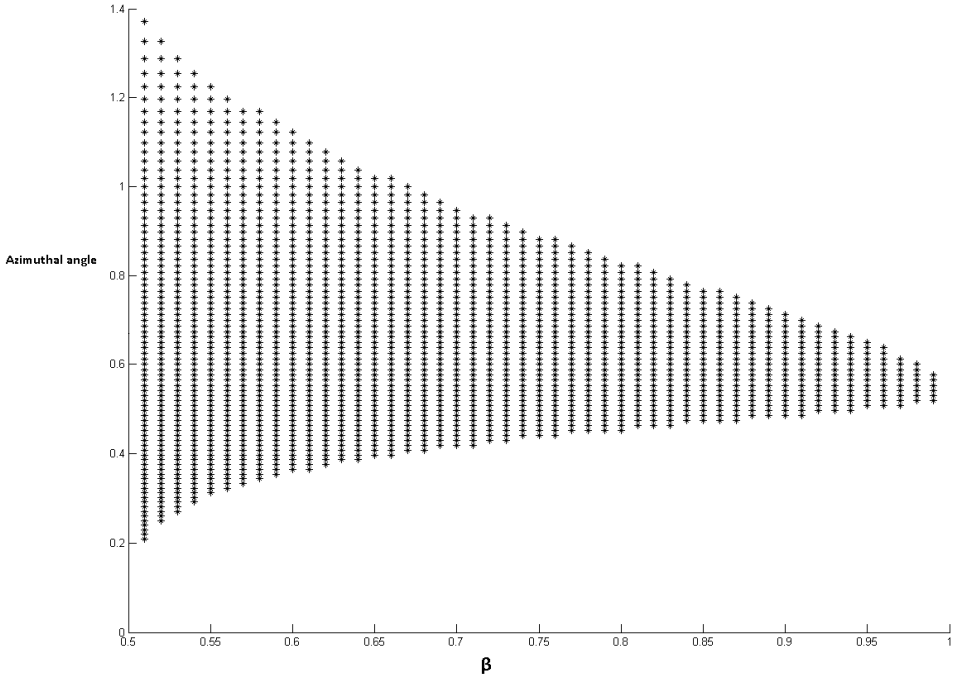

Figure22. Floquet stability diagram for the Elliptic instability.

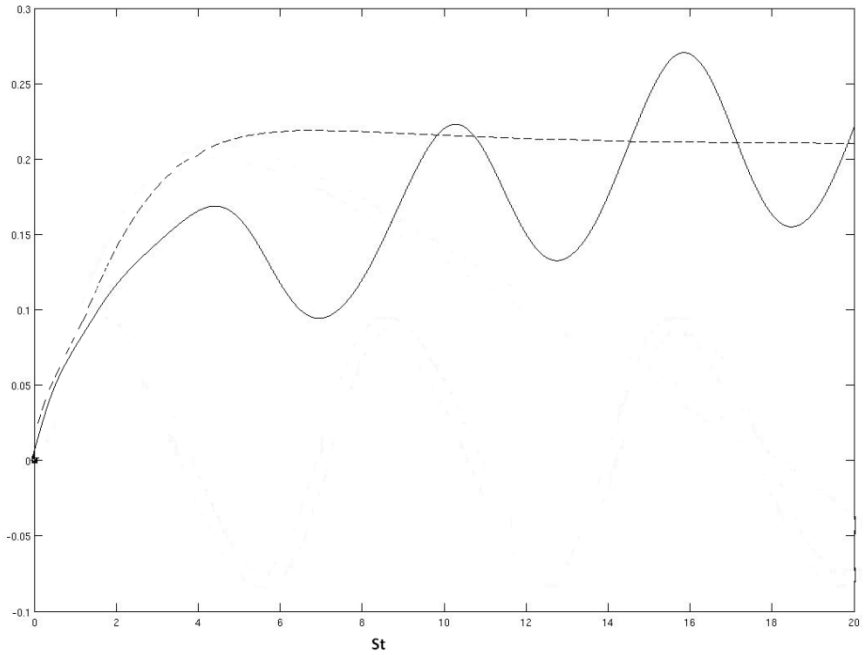

Figure 23. Schematic displaying the modeling methodology followed for elliptic flows.

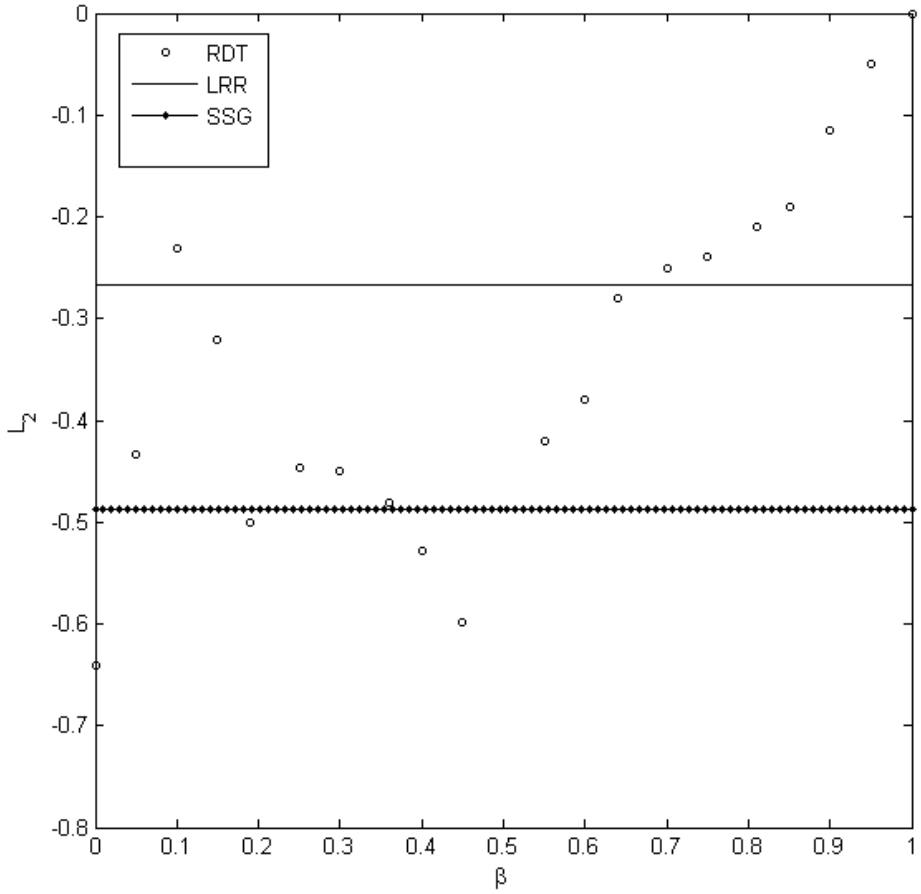

Figure 24 (a) Representative values of the L_2 coefficient, for the present investigation, compared to those of LRR and SSG.

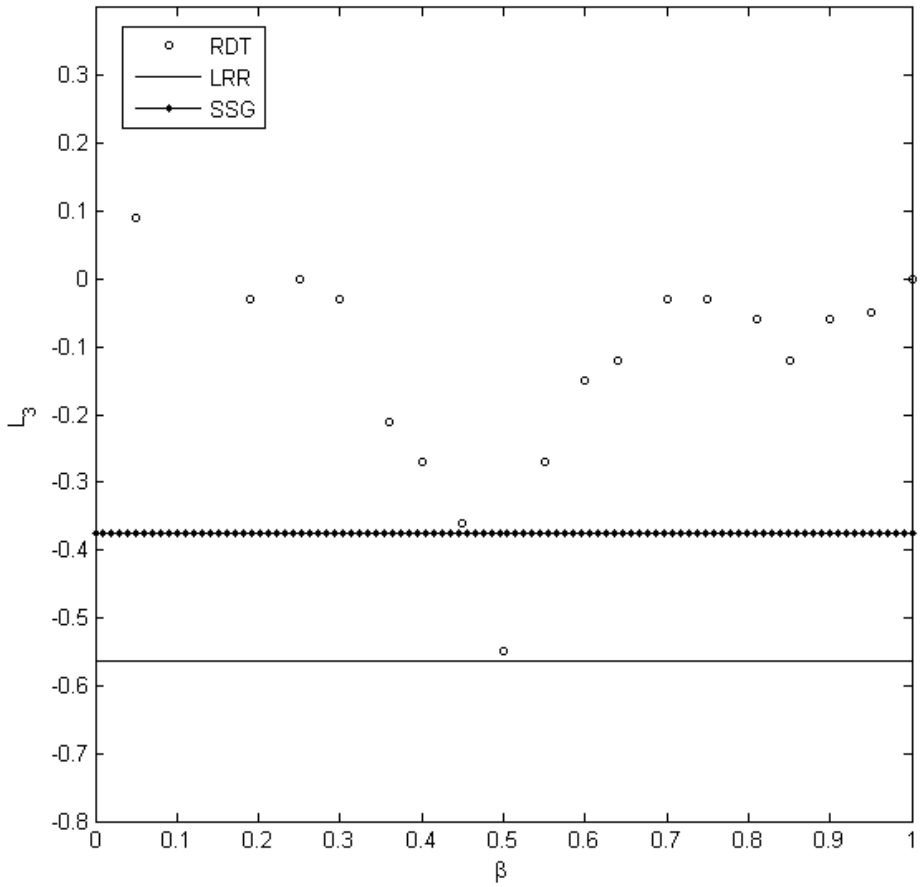

Figure 24 (b) Representative values of the L_3 coefficient, for the present investigation, compared to those of LRR and SSG.

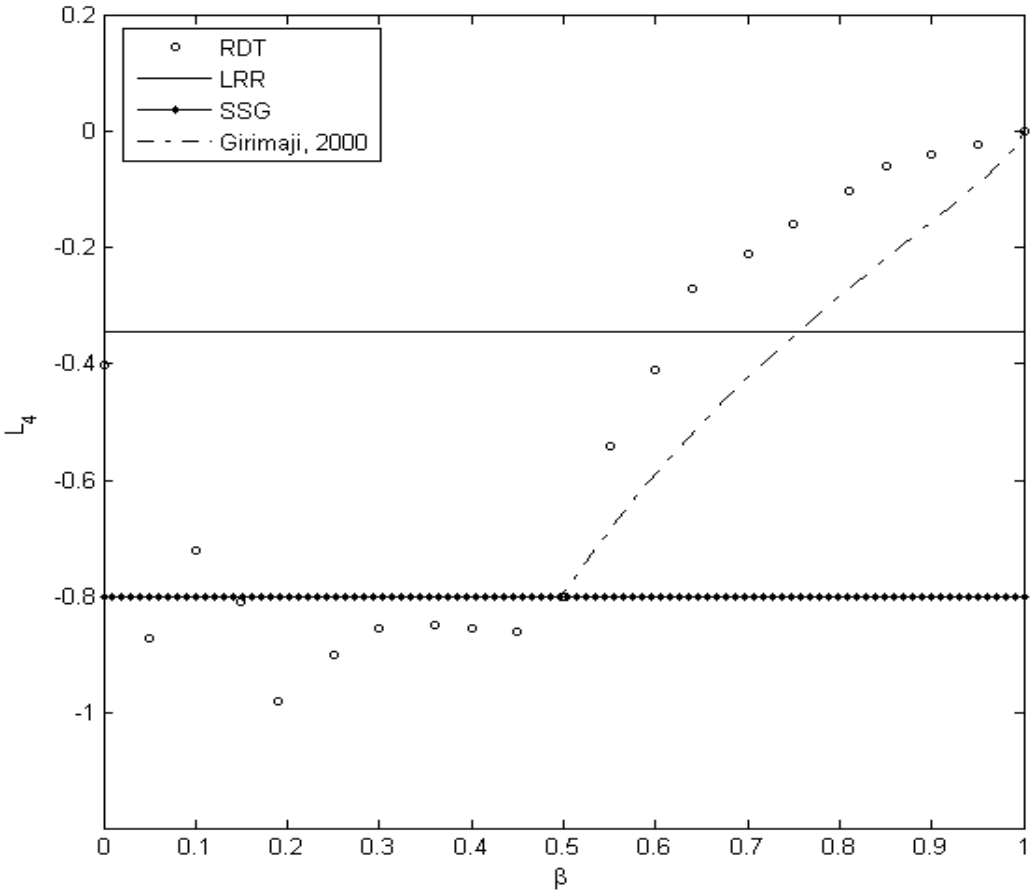

Figure 24 (c) Representative values of the L_4 coefficient, for the present investigation, compared to those of LRR, SSG and Girimaji (2000).

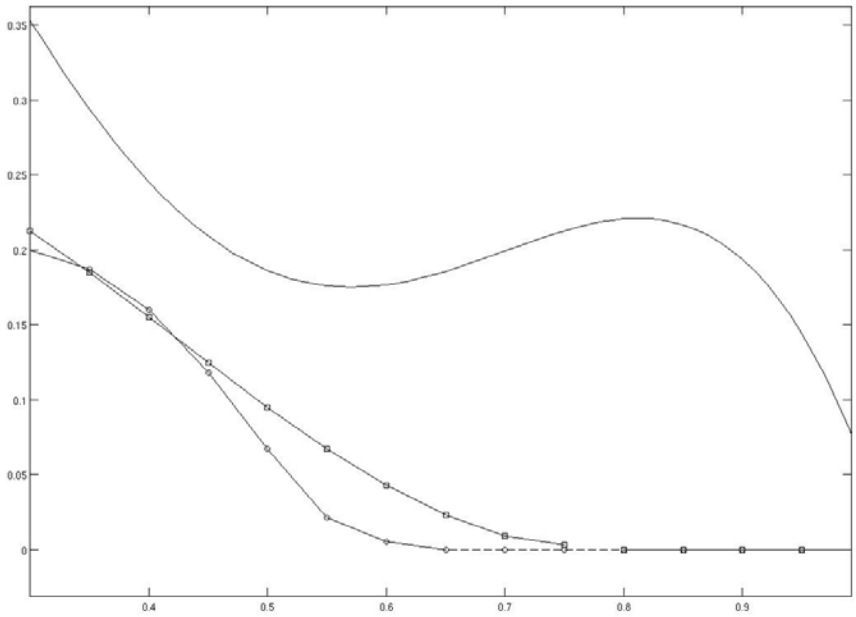

Figure 25. Bifurcation diagram exhibiting the behavior of the models. The present model is represented by a solid line. LRR and SSG are marked with squares and circles, respectively.

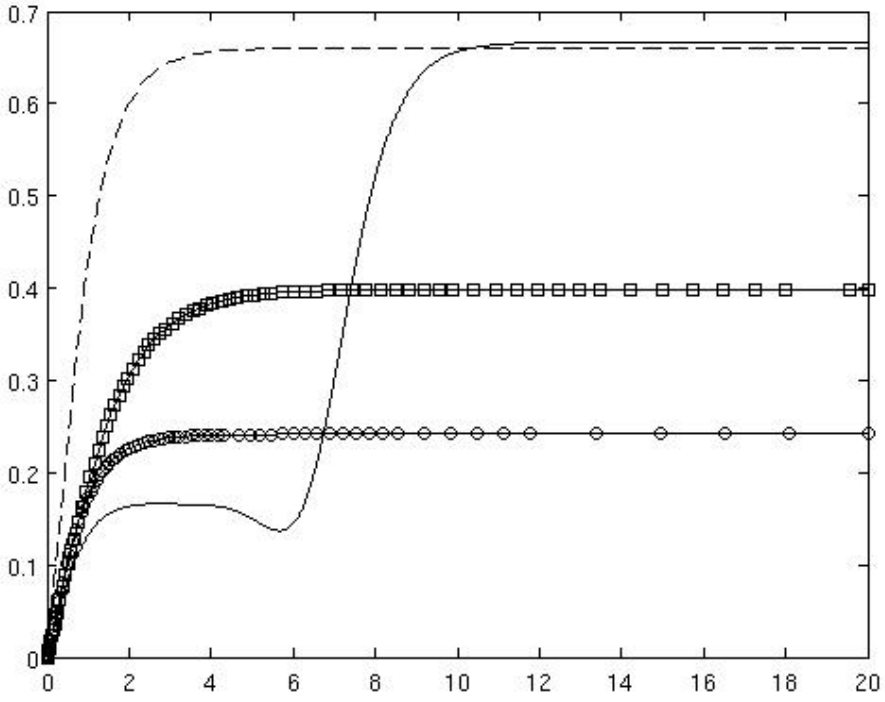

Figure 26. (a) Comparison of the model to RDT data and other models for the case of plane strain. The plotted values are for the b_{22} component. The solid line represents RDT data, the dashed line, the present model. LRR and SSG are marked with squares and circles, respectively.

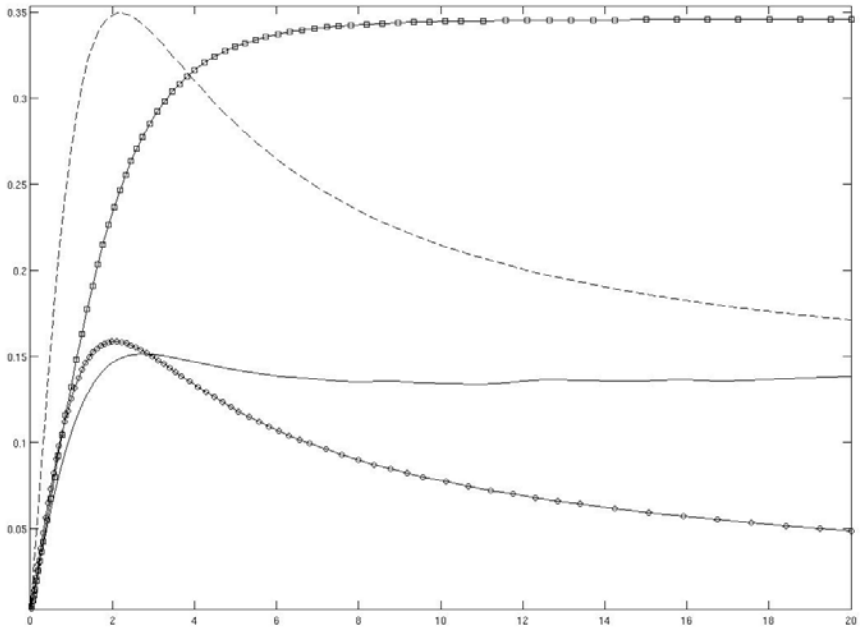

Figure 26. (b) Comparison of the model to RDT data and other models for the case of homogeneous shear. The plotted values are for the b_{22} component.

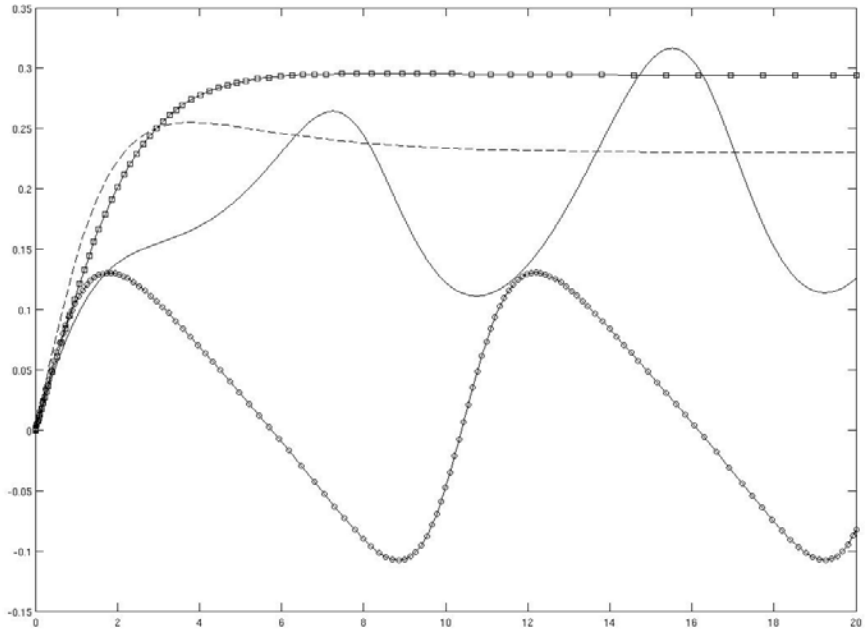

Figure 26. (c) Comparison of the model to RDT data and other models for a representative elliptic flow (β=0.64). The plotted values are for the b_{22} component.

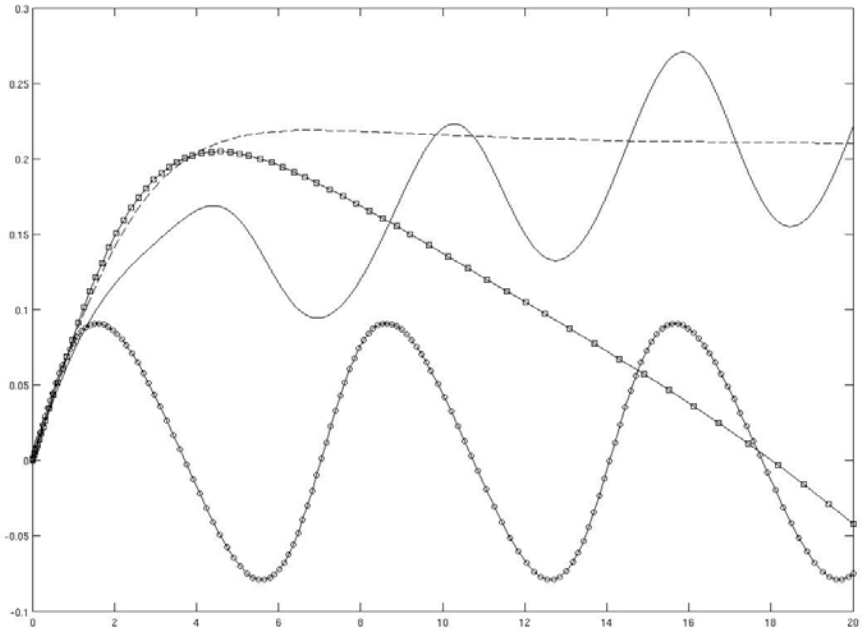

Figure 26. (d) Comparison of the model to RDT data and other models for a representative elliptic flow (β=0.81). The plotted values are for the b_{22} component.

VITA

Aashwin Ananda Mishra received his M.S. degree in Aerospace Engineering from Texas A&M University in 2010. He received a B.Tech. degree from the Indian Institute of Technology, Delhi in 2006. He can be contacted via:

Dr. Sharath Girimaji

Aerospace Engineering Department

Texas A&M University

College Station, TX 77843-3141.